NATIONAL CENTRE FOR COMPOSITIONAL CHARACTERISATION OF MATERIALS

A JOURNEY OVER 3 DECADES OF NCCCM

NCCCM COMMITTED TO EXCELLENCE IN ANALYTICAL MEASUREMENTS

YEARS OF NCCCM - BARC

Index

1. Production of Certified Reference Materials (CRMs) and development of traceable measurement methodologies for CRM production

Certified Reference Material (CRM) – are defined as homogenous and stable materials which are characterised by a metrologically valid procedure for one or more specified properties, accompanied by a certificate that provides the value of the specified property, its associated uncertainty and a statement of metrological traceability. CRMs are used for validation of analytical methods, calibration of instruments and to ensure accuracy of results. The use of CRMs is of utmost importance in analytical sciences as important decision in technology, trade and commerce are taken based on the accuracy of the results. Lack (Non-availability) of CRMs leads to difficulties in comparing the results from different laboratories or various methods and for quality control in routine analysis. A program was initiated at NCCCM-BARC, Hyderabad for the production of CRMs of national importance. With emphasis on production of CRMs a total of five CRMs were produced till now and many are in pipeline.

1.1 Alumina CRM (BARC – B1301) for six metallic impurities (Na_2O, CaO, Fe_2O_3, TiO_2, Ga_2O_3 and V_2O_5) in collaboration with NALCO

Quantification of metallic impurities in alumina is very important for various aluminum, refractory, ceramic, abrasive and chemical industries. The accurate and precise determination of these impurities necessitates a CRM of alumina. India is the second largest producer and exporter of alumina, however there is dearth of indigenous alumina CRM. Hence, National Centre for Compositional Characterisation of Materials (NCCCM) of Bhabha Atomic Research Centre (BARC) in collaboration with National Aluminum Company Limited Research and Technology Centre (NRTC) has initiated a project for the production of alumina CRM. Alumina powder (~20 kg) was supplied by NALCO refinery complex. After its physical processing, a batch of 154 bottles each containing 85 g of candidate alumina CRM material was packed. Homogeneity of the batch was established with respect to 11 property values. This CRM was certified for six metallic impurities (Na_2O, CaO, Fe_2O_3, TiO_2, Ga_2O_3 and V_2O_5) after inter laboratory comparison exercise (ILCE) and statistical evaluation of data. Further, five indicative values (MgO, ZnO, MnO, loss on ignition (LOI) and surface area) were also provided. This CRM was produced as per ISO 17034: 2016 and ISO guide 17035:2017 and the certified values are traceable to SI units. The alumina CRM, BARC- B1301, was released on 16.08.2024 at NRTC- NALCO Bhubaneswar by BARC and NALCO authorities.

1.2 Bauxite CRM (BARC-B1201) for nine property values (Al_2O_3, Fe_2O_3, SiO_2, TiO_2, V_2O_5, MnO, Cr_2O_3, MgO, and LOI): In collaboration with NALCO

NCCCM-BARC and NALCO, have produced an Indian origin bauxite certified reference material (CRM), referred as BARC-B1201, for the certification of major (Al_2O_3, Fe_2O_3, SiO_2, TiO_2, loss on ignition - LOI) and trace contents (V_2O_5, MnO, Cr_2O_3, MgO). Characterisation was undertaken by strict adherence to ISO Guides. A previously developed method comprising of single step for bauxite dissolution was validated in our laboratory. Subsequent to the dissolution, the quantitation (of Al_2O_3, Fe_2O_3, SiO_2, TiO_2, V_2O_5, MnO, Cr_2O_3 and MgO) by ICP-AES (SSBD ICP-AES was used for homogeneity studies and an inter-laboratory comparison exercise (ILCE) of the candidate CRM. LOI was determined by thermo-gravimetric analysis. Property values were assigned after an interlaboratory comparison exercise with participation from seventeen reputed government and private sector laboratories in India. The CRM was certified for nine property values; Al_2O_3, Fe_2O_3, SiO_2, TiO_2, V_2O_5, MnO, Cr_2O_3,

MgO and LOI which are traceable to SI units. Production of bauxite CRM (BARC- B1201) was assessed and accredited by NABL under ISO 17034:2016. Bauxite CRM (BARC – B1201) was released by BARC and NALCO authorities on 23.03.2023

Geostandards and Geoanalytical Research 47 (2023) 629

1.3 Dolomite CRM (BARC - B1101) for Al_2O_3, BaO, CaO, Fe_2O_3, MgO and SrO: in collaboration with AMDER

Dolomite is an anhydrous carbonate mineral composed of calcium magnesium carbonate ($CaMg(CO_3)_2$). Analysis of major and minor constituents in dolomite is very important for nuclear industry. Hence, NCCCM-BARC and AMDER jointly initiated the program for the certification of major and minor constituents in dolomite. Approximately ~10 kg of dolomite was collected from the uranium mines at Tummalapalle, YSR District, Andhra Pradesh. The raw material was crushed, milled and sieved to a powder of around 10-micron particle size. The sieved material was further homogenized thoroughly by a mechanical homogenizer. The above processes were carried out at AMDER, Hyderabad. The powder of 50 g aliquots was packed into 150 pre-cleaned high-density polyethylene (HDPE) bottles. The dolomite material was certified for the major and minor constituents (Al_2O_3, BaO, CaO, Fe_2O_3, MgO and SrO) by means of an inter laboratory comparison (ILC) exercise. Analytical technique used for the determination of major and minor constituents by the participant laboratories is ICP-AES. The CRM was produced as per ISO 17034:2016 and the assigned property values were established according to ISO Guide 35:2017. Production of Dolomite CRM (BARC B1101) was assessed and accredited by NABL under ISO 17034:2016.

1.4 Quartz CRM (BND 4101.01) for (Al, Ca, Fe, K, Mg, Na and Ti)

CRM for trace elements in quartz matrix is required to assess the performance of analytical methods in regards to their validation, calibration and for comparison of measurements between laboratories. Due to unavailability of matrix matched CRMs in our country, NCCCM/BARC, Hyderabad and CSIR-National Physical Laboratory (NPL), New Delhi have initiated a program for the production of a CRM of high purity quartz for the certification of critical trace elements. Preparation and certification of Indian Reference Material (BND 4101.01), quartz powder with certified mass fractions of seven trace impurities was carried out jointly by NCCCM and NPL; two national laboratories of Government of India. Sampling constant (Ks) were established before carrying out the within and between bottles homogeneity test. The homogeneity test was carried out by NCCCM. The certified values were assigned after Inter Laboratory Comparison Exercise (ILCE) between reputed National Laboratories in India as per ISO 17034 & ISO Guide 35. Analytical techniques like Inductively coupled plasma atomic emission spectrometry (ICP-AES), Flame atomic absorption spectrometry (FAAS) and Total reflection X-ray fluorescence analysis (TXRF) were used for the characterisation of property values. Production of Quartz (BND 4101.01) CRM was assessed and accredited by NABL under ISO 17034:2016

Microchemical Journal 172 (2022) 106926

1.5 Tea CRM (BARC-D3201) for K, Ca, P, Mg, Mn, Al, Fe, Ba, Zn, Cu, Sr, Pb, As, Cd & Hg

CRM for major and trace elements in black tea powder was produced. The study involved an acid assisted microwave digestion of tea powder followed by quantitation of K, Ca, P, Mg, Mn, Al, Fe, Ba, Zn, Cu and Sr by ICP-AES, Pb, Cd by GFAAS and As, Hg by AFS in the digests. The method was validated in terms of selectivity, linearity, limit of detection (LOD), limit of quantification (LOQ), trueness,

precision, traceability, ruggedness and combined uncertainty using a CRM of tea powder (NMIJ CRM - 7505a) and spike recovery studies. Precision (% RSD) of the method was found to be < 5% for all the analytes majorly present in tea (K, Ca, P, Mg, Mn, Al, Fe, Ba, Zn, Cu and Sr) and it was found to be maximum of6.5 % for As, at 95% confidence level. The validated method was used for characterisation of candidate tea CRM during homogeneity and stability studies. Candidate tea CRM (~3.6 Kg) was processed (which included spiking, drying grinding and sieving) and its homogeneity was assessed at various levels with respect to all 15 property values. A total of four techniques, ICP-MS, ICP-AES, GFAAS and AFS were used during ILCE. Property values were assigned for 14 elements (K, Ca, P, Mg, Mn, Al, Fe, Ba, Zn, Cu, Sr, Pb, Cd, and Hg) along with expanded uncertainties. Long-term stability studies suggested the produced tea CRM was stable at storage temperature in the last two years, whereas short-term stability studies (at temperatures 4, 25 and 40 °C) established its transportation stabilities at tested temperatures for a period of three weeks. Preparation and certification of tea CRM (BARC D3201) was assessed and accredited by NABL under ISO 17034:2016

Food Control 158 (2024) 110241

1.6 Noodles CRM (BARC - D3101) for lead

Food Safety and Standards Authority of India (FSSAI) has set maximum permissible level of lead in noodle at 2.5 mg/kg. The standardized lead measurement is of high priority in food matrix to obtain closer comparability of results during routine measurement procedures. For this purpose, certified reference material (CRM) for lead in noodle matrix is required to assess analytical methods performance with respect to their validation, calibration and of comparability of measurements between laboratories. Considering the unavailability of matrix-matched reference materials, BARC-NCCCM has initiated a program for the production of a noodle CRM for the certification of lead mass fraction. Various parameters for homogeneous spiking were optimized for the production of 2.35 kg of homogeneous noodle matrix. Parameters for sample digestion and minimum sample intake for analytical homogeneity (HE) were established before carrying out the homogeneity test between and within bottles. Homogeneity assessment and stability tests were carried out according to the ISO 17034 and Guide 35. The certified value was assigned after inter-laboratory comparison exercise where eight reputed laboratories from both government and private sector participated. Preparation and certification of noodle CRM (BARC- D3101) was assessed and accredited by NABL under ISO 17034:2016

Accreditation and Quality Assurance 24(2019) 173-180

1.7 Determination of trace and ultratrace impurities in gold candidate reference material

Sample pieces of candidate gold reference material were prepared at IGM-MINT, Mumbai. These samples were analysed by GFAAS and ICP-AES at NCCCM for their impurity levels. After the dissolution of the samples, the elements Cu, Fe, Ag, As, Bi, Cr, Cd, Ca, Co, Ir, Pb, Li, Mg, Mn, Na, Ni, Pd, Pt, Rh, Ru, Se, Si, Te, Tl, Zn were determined by GFAAS and the elements Cu, Fe, Ag were also determined by ICP-AES. For the final certification, inter-laboratory comparison was carried out on atleast three independent determinations on six separate sample portions to determine the mass fraction of the desired analytes. The mean values of the inter-laboratory comparison were taken for the computation of certified mass fractions using weighted average procedure. The certified uncertainties were calculated by taking into account the contribution from inter-laboratory comparison, in homogeneity of the material. A RM (Royal Canadian MINT, Gold Reference Material, NIST, RM-8059) was used as a quality control

sample and was also analysed for all its elements along with the gold reference standard. Gold CRM was released in 2017.

1.8 Development of reference methodologies for the accurate and precise analysis

Production of certified reference material necessitates development of reference methodologies for the accurate and precise determination of the analytes. In this context various reference and high-performance methodologies with very low expanded uncertainties were developed for the analysis of various analytes. Few important reference methods developed at NCCCM/BARC are described here:

1.8.1 DNA quantification via traceable phosphorus measurement through microwave-assisted UV digestion-ion chromatography

Accurate quantification of deoxyribonucleic acid (DNA) is critical for many analyses in molecular biology and genetic tests. A method in which the stoichiometrically existing phosphorus content in purified genomic DNA is quantitatively converted into orthophosphate ions by microwave assisted-UV digestion in the presence of microlitre quantities of dilute reagents (HCl, HNO_3, H_2O_2) is adopted. The tandem use of microwave energy and ultraviolet photons for DNA digestion in pressurized quartz vessels enables a maximum reaction temperature of 240 °C resulting in efficient and fast mineralization of high molecular weight DNA within 30 minutes. Compared to hot plate digestion, the digestion time is reduced by a factor of 32. The MW-UV sample preparation approach coupled with the ion chromatographic measurement of phosphate using a high performance (HP) methodology provides an accurate quantitation of phosphorus mass fractions as low as 0.3 mg g^{-1}, corresponding to a DNA mass of 25 mg. The relative expanded uncertainties (% U) expressed at 95% confidence for these analyses range from 0.2 to 0.6%. Critically, the matrix of the calibrant solution is also matched with respect to the digested matrix anions (chloride, nitrate), without which significant bias in IC performance is observed. The phosphorus content of the calf thymus DNA was also measured using high-performance inductively coupled plasma optical emission spectroscopy (HP-ICP-AES), which provided independent data for comparison with the MW-UV digestion-IC based approach. Ion chromatography requires smaller volume of materials to perform the analysis and could be useful for characterising primary calibration standards and certified reference materials with low uncertainties.

Analyst 137 (2012) 668

1.8.2 Traceable quantitation of cyanocobalamin (vitamin B_{12}) via measurement of cobalt and phosphorus: a comparative assessment using ICP-AES and IC

Traceable and precise quantitative measurements of cyanocobalamin (CN-Cbl) have been hampered by the lack of well characterised standards and pure materials of this bio-inorganic analyte that belongs to the water-soluble vitamins of the B-group known as vitamin B12. Measurement of cobalt and/or phosphorus content of vitamin B12 offer an approach for its quantitation that is traceable to the International System of Units (SI) with low measurement uncertainty. Cobalt and phosphorus measurements of CN-Cbl were carried out by Inductively Coupled Plasma-Atomic Emission Spectrometry (ICP-AES) and Ion Chromatography (IC). Use of a mixed bed ion exchange column coupled with post column reaction; IC provides a means to differentiate free cobalt from the cobalt complexed inside the corrin ring of the CN-Cbl molecule. In the case of ICP-AES and IC, a prerequisite

for quality measurement is the purity of the starting vitamin B12 material. The relative expanded uncertainties (% U) expressed at 95% confidence for these analyses range from 0.3 to 1%.

RSC Advances 6 (2016) 111090

1.8.3 Accurate quantitation standards of glutathione via traceable sulphur measurement by ICP-AES and IC

The quantitative analysis of glutathione (GSH) is important in different fields like medicine, biology, and biotechnology. Accurate quantitative measurements of this analyte have been hampered by the lack of well characterised reference standards. The proposed procedure is intended to provide an accurate and definitive method for the quantitation of GSH for reference measurements. Measurement of the stoichiometrically existing sulphur content in purified GSH offers an approach for its quantitation and calibration through an appropriate certified reference material (CRM) for sulphur would provide a methodology for the certification of GSH quantity, that is traceable to SI (International system of units). The inductively coupled plasma optical emission spectrometry (ICP-AES) approach negates the need for any sample digestion. The sulphur content of the purified GSH is quantitatively converted into sulfate ions by microwave-assisted UV digestion in the presence of hydrogen peroxide prior to ion chromatography (IC) measurements. The measurement of sulphur by ICP-AES and IC (as sulfate) using the ‘‘high performance’’ methodology could be useful for characterising primary calibration standards and certified reference materials with low uncertainties. The relative expanded uncertainties (% U) expressed at 95% confidence interval for ICP-AES analyses varied from 0.1% to 0.3%, while in the case of IC, they were between 0.2% and 1.2%. Apparently, the described methods are more suitable for characterising primary calibration standards and certified reference materials of GSH, than for routine measurements.

Journal of Pharmaceutical Analysis 3(2013)180

1.8.4 A single step acid assisted microwave digestion method for the complete dissolution of bauxite and quantitation of its composition (Al_2O_3, Fe_2O_3, SiO_2, TiO_2, Cr_2O_3, MgO, MnO and V_2O_5) by ICP-AES

An acid assisted microwave-based method for the complete dissolution of bauxite using mixture of H_2SO_4, H_3PO_4 and HF acids in a single step was developed for the determination of various analytes (Al_2O_3, Fe_2O_3, SiO_2, TiO_2, Cr_2O_3, MgO, MnO and V_2O_5) using ICP-AES. The method was validated with respect to ruggedness, linearity, trueness, precision, limit of detection (LOD), limit of quantification (LOQ), working range and measurement uncertainties by analysing a bauxite reference material (Alcan BXT-12) and four certified reference materials (IPT-131, BXBA-4, NIST SRM 600, NIST SRM 697). The expanded uncertainties obtained for Al_2O_3 (40.0%), Fe_2O_3 (17.0%), SiO_2 (20.3%), TiO_2 (1.31%), Cr_2O_3 (0.024%), MgO (0.05), MnO (0.013), and V_2O_5 (0.60%), were 0.80, 0.40, 0.50, 0.033, 0.0008, 0.002, 0.0007 and 0.002 respectively, which are fit for the intended use to characterise bauxite. The developed method was also evaluated through participation in an interlaboratory comparison exercise organised by the Jawaharlal Nehru Aluminium Research Development and Design Centre (JNARDDC), Nagpur, India, using bauxite sample (BXT-JNA), with satisfactory z-scores achieved.

Geostandards and Geoanalytical Research 47 (2023) 403

1.9 Certified Reference Materials under production / planned

i. Ferrocarbanotite CRM for rare earth elements in collaboration with Atomic Minerals Directorate for Exploration and Research (AMDER) Hyderabad.
ii. Production of High strength and low alloy steel CRM in collaboration with Defence Metallurgical Research Laboratory (DMRL), Hyderabad.
iii. Production of coal fly ash (CFA) - CRM for Li, Ga, Ge, and rare earth elements (REEs).
iv. Production of special steel for nuclear applications for our department.
v. Production of cast iron CRM – to be used in Locomotive brakes in Railways.
vi. Production of high purity Niobium CRM in collaboration with Nuclear Fuel Complex (NFC), Hyderabad.

vii.

2. Characterisation and Analysis of Nuclear Materials

2.1 Quality assurance of carbon dioxide gas by gas chromatography-mass spectrometry for nuclear applications

Carbon dioxide (CO_2) due to its low thermal conductivity and low chemical reactivity is used as an annulus gas in pressurized heavy water reactors (PHWR) for monitoring the leak of heavy water from pressure tube or calandria. CO_2, however, may contain impurities such as free chloride, vinyl chloride and sulphur compounds which can induce corrosion of the structural material. Therefore, it is desirable to determine the contents of these impurities with good precision and accuracy.

A gas chromatography-mass spectrometry (GC-MS) based methodology was developed for the sensitive and precise measurement of vinyl chloride in CO_2. The analysis consists of three steps in the following order: (a) pre-concentration by solid phase extraction, (b) quantitative elution and (c) determination by GC-MS. In this work, 2.52 L of CO_2 gas at NTP (300K) was passed through activated charcoal cartridge, where vinyl chloride was adsorbed. Then the analyte was extracted using 2 mL of methanol. 1µL of extracted eluent was then injected into GC for vinyl chloride analysis. The concentration of vinyl chloride was found to be in the range of; 0.005 to 0.092 µL/L in different samples of CO_2 gas analysed.

For the analysis of sulphur compounds using GC-MS, a column oven program was optimized using ZB-1 column to resolve 23 sulphur compounds from a standard mix. For the analysis of sulphur compounds in CO_2 gas, the gas was adsorbed on activated charcoal cartridge at 50 mL/min for 1hr. The adsorbed sulphur compounds were then eluted in toluene and analysed using GC-MS. Total of 9 CO_2 cylinders from NPCIL were analysed for the presence of sulphur compounds. The cylinders from KAPS have shown presence of Carbonyl sulphide and Di-methyl sulphide below quantification limit whereas cylinders from TAPS did not show presence of any sulphur compounds.

2.2 Determination of trace level of phosphorus in Zr-Nb and Zircaloy

Zirconium alloys are used as coolant and fuel cladding tubes in PHWR. Phosphorus in zirconium alloys affects the fracture toughness when its concentration exceeds 10 mg kg^{-1}. A spectrophotometric method was developed for the determination of traces of phosphorus in Zr–2.5Nb and Zircaloy. It is achieved by selective fluoride complexation controlled by boric acid. The samples were dissolved in HF and fluoro-complexes of the matrices were formed by maintaining the concentration of HF while the excess HF was controlled by boric acid. After the formation of phosphomolybdate, extracted into n-butyl acetate, ion-associated with crystal violet and the absorbance was measured at 582 nm. The results obtained by this procedure were compared with the values determined by Glow Discharge-Quadrupole Mass Spectrometry (GD-QMS). Potential interferences of F^-, Si, As, Nb, Ti and Ta etc., were removed. LOD was found to be 0.055 mg kg^{-1} with RSD of ~3%.

Talanta 76 (2008) 134

2.3 Determination of boron oxide in boron powder and traces of boron in uranium matrices

The determination of boron is important for its applications in nuclear energy, metallurgy, pharmacy and agriculture. Boron powder quickly oxidises and its surface becomes coated with boric acid

after manufacture. Thus, the determination of traces of boric acid is essential for quality control and specification testing of elemental boron. Solid sample/solution was placed inside a vessel containing curcumin and the distillation was carried out at room temperature/on a water bath. The borate ester collected in to the curcumin solution was measured using spectrophotometer. This developed method was applied for the determination of traces of boric acid in boron powder by the distillation of methyl borate at room temperature. For other matrixes (water, uranium oxide, uranyl nitrate, fluoride salt, etc.,) distillation of ethyl borate was carried out on the water bath. LOD (3σ) was 5 ng g^{-1} for water and 30 ng g^{-1} for solid samples.

Analytica Chimica Acta 502 (2004) 265

2.4 Determination of boron isotope ratios by Z-GFAAS

Boron is used to control the reactivity in nuclear power reactors. It is also used as shutdown rods in the form of ^{10}B enriched boron carbide. The ^{10}B isotope has a high neutron absorption cross section of 3800 barns, whereas the cross section for ^{11}B isotope is 0.005 barns. Thus, the determination of boron isotopic ratios in such samples is very important in nuclear technology. A new method for the determination of isotopic ratio of boron using Z-GFAAS is developed using conventional hollow cathode lamp. The isotope-shift Zeeman Effect at 208.9 nm is utilized for $^{10}/^{11}B$ isotopic ratio. The absorbances are recorded at the field strength of 1.0 Tesla. The isotope ratios measured by the proposed method were in good agreement with the results obtained by ICP-MS. The developed method was applied for ^{10}B enriched boric acid samples from HWP, Talcher.

Spectrochimica Acta Part B: Atomic Spectroscopy 61 (2006) 314

2.5 Determination of trace levels of boron in graphite powder using ICP-AES

High-purity graphite for a nuclear purpose requires strict control of boron due to its large neutron absorption cross section. A method was developed for the determination of traces of boron in graphite powder. The graphite powder was made into a paste using Na_2CO_3 solution (flux). The paste form of graphite powder was fused in a muffle furnace and was mixed in a glycerol solution. The flux was separated from the glycerol solution as a solid residue by heating over a water bath. Boron present in the glycerol solution was measured by ICP-AES. Compared to conventional Na_2CO_3 fusion, the amounts of flux and fusion time were reduced by a factor of 32 and 8, respectively. Due to the extraction of boron from the flux into glycerol solution, the preconcentration was increased by a factor of 200. The separation of flux was >92% with the recovery of analyte in the range of 92–96%. The detection limit was found to be 90 ng g^{-1}.

Analytical Methods 5 (2013) 5799

2.6 Determination of Boron in U-Al-Si and Si-Al-Ni (SILUMIN) alloys by ICP-AES

The corrosion behaviour of aluminium-clad fuels in light water reactor environments was improved by the use of SILUMIN. Another important material used in the nuclear industry is uranium-aluminium-silicon alloy, which is used in thermal reactors, test reactors, and nuclear submarines. Satisfactory power output and neutron flux distribution of the reactor requires control of both total boron content and boron distribution in the fuel. Hence, it is essential to develop an accurate and precise method for the determination of traces of boron in both of these alloys. A novel and simple matrix separation method was developed for the trace level determination of boron in the alloys using ICP-AES. The samples were digested by HF/HF-HNO_3 in the presence of mannitol. Sample solution was evaporated to

dryness on a water bath and treated with ethanol to selectively extract the boron-mannitol complex from the solid residue of the matrix. The ethanol fraction containing the boron-mannitol complex was separated, evaporated to dryness, taken in water, and measured by ICP-AES. The limit of detection was found to be 0.270 mg kg^{-1}. The matrix removal was around 99.5%, the recovery of boron for 80–450 ng was in the 93–96% range.

Atomic spectroscopy 33 (2012) 24

2.7 Determination of Uranium and Thorium in Ilmenite by ICP-AES

Titanium diboride (TiB_2) is one of the candidate materials for high temperature structural applications and also for control rod elements in high temperature nuclear reactors. Ilmenite contains a range of impurities and traces of radionuclides such as uranium (U) and thorium (Th). Hence, it is essential to determine uranium and thorium in ilmenite. Major problems in the ICP-AES determination of trace level uranium and thorium in ilmenite are that both the matrix elements (titanium and iron) have strong spectral interference on the uranium and thorium lines. A simple matrix separation procedure is adopted for the determination of trace levels of uranium and thorium in ilmenite ore using ICP-AES. The sample was digested by potassium bisulfate fusion. After reduction of uranium (VI to IV) by aluminum powder, the analytes were co-precipitated with $BaSO_4$. The precipitate was dissolved in ammoniacal EDTA solution and measured by ICP-AES. The analytical results of uranium were cross-validated after matrix separation by solvent extraction using a liquid anion-exchanger. The results of the matrix separation procedure were in good agreement with that of co-precipitation method. The limits of detection were 0.7 and 0.5 mg kg^{-1} for uranium and thorium, respectively. The recovery for both analytes was more than 92%.

Atomic spectroscopy 31 (2010) 92

2.8 Measurement of oxide layer thickness of autoclaved zircaloy coupons by proton elastic backscattering (EBS)

The formation of zirconium oxide films on the surfaces of zirconium-based alloys, particularly under the high-temperature aqueous corrosion conditions encountered within reactor operations, presents a formidable challenge in the overall performance of nuclear reactors. The measurement of oxygen pick up *in-situ* by zircaloy during reactor operation is difficult. An estimation of the composition and thickness of oxide films formed under suitable test conditions is, therefore, desirable. Bbackscattering spectrometry was employed for the non-destructive determination of composition and thickness of zirconium oxide layers on autoclaved zircaloy coupons. The measurements enabled to model the oxidation kinetics of zircaloy in order to project their behaviour during reactor operation. A EBS techniques, namely $^{16}O(p,p)^{16}O$ elastic scattering at 2.5 MeV, and 3.05 MeV $^{16}O(\alpha, \alpha)^{16}O$ resonance scattering were utilised for analyzing films of zirconium oxide on autoclaved zircaloy specimens from Nuclear Fuel Complex (NFC), Hyderabad. The thicknesses of these layers determined by backscattering spectrometry were compared with cross-sectional micrographs taken by scanning electron microscope (SEM).

Journal of Radioanaytical and Nuclear Chemistry 265(2005) 441

2.9 $^{10}B/^{11}B$ isotopic ratio and atomic composition of boron carbide

2.9.1 Determination by proton induced γ-ray emission (PIGE)

Boron can be non-destructively determined by proton induced γ-ray emission (PIGE), nuclear reaction analysis (NRA) techniques and p-EBS. PIGE has the ability to determine $^{10}B/^{11}B$ ratio through the measurement of 429 or 2124 keV γ-rays that are emitted from $^{10}B(p,\alpha\gamma)^{7}Be$ or $^{11}B(p,p'\gamma)^{11}B$ nuclear reactions respectively (Figure 1). The method has a detection sensitivity of 50 ppm for boron in the suitable matrices.

Boron carbide, a non-metallic material, possesses several unique physical and chemical properties such as high hardness (~30 GPa), low density (~2.52 g cm^{-3}), excellent chemical and thermal stability, and high thermal neutron absorption cross-section (~ 3800 barns). In view of these properties, ^{10}B enriched boron carbide, often in the form of sintered cylindrical pellets, is used in the manufacturing of control rods in nuclear reactors. Two ion beam analysis methods, one based on particle induced γ-ray emission (PIGE) and another involving elastic backscattering spectrometry (EBS) technique, were standardized for the determination of $^{10}B/^{11}B$ isotopic ratio and the atomic composition of boron carbide. The PIGE technique, performed using ~ 4.0 MeV proton energy, utilizes ^{10}B, ^{11}B and ^{13}C specific reactions that occur simultaneously in the target to determine $^{10}B/^{11}B$ and B/C ratios. The uncertainty in the determination of the $^{10}B/^{11}B$ ratio and the B/C atomic ratio is about 2% and about 5% respectively.

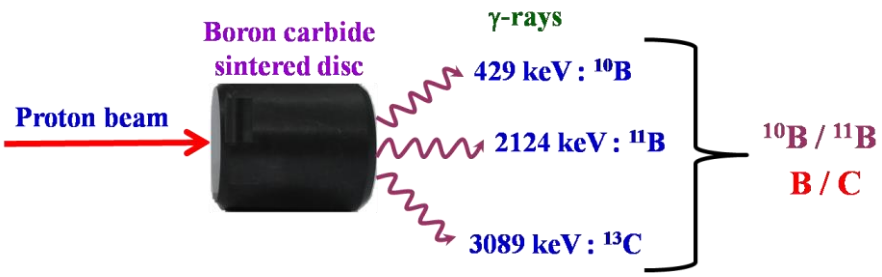

Figure 1: *Schematic of PIGE method for determination of boron*
Applied Radiation and Isotopes 128 (2017) 28

2.9.2 Proton elastic backscattering spectrometry (p-EBS)

The analysis by EBS, on the other hand, involves the $^{10}B(p,p)^{10}B$, $^{11}B(p,p)^{11}B$ and $^{12}C(p,p)^{12}C$ elastic scatterings at 2.0 MeV proton energy. Among the two methods, PIGE is the method of choice for bulk analysis while EBS is useful in discerning compositional variations on the surface regions. Hence, the examination of samples by the both methods is recommended for a comprehensive analysis. The important advantages of the methods are: (a) non-destructive and interference free analysis, (b) applicability to powder and sintered pellets, (c) possibility of the simultaneous detection of impurities, (d) qualitative comparison of the density of the sintered pellets and (e) rapid analysis. The methods, by virtue of these features, were used for the analysis of numerous boron carbide samples.

2.9.3 Determination of boron by Nuclear Reaction Analysis (NRA) method:

Nuclear reaction analysis based on $^{11}B(p,\alpha)2\alpha$ nuclear reaction is the method of choice for the trace level determination of B in materials, especially in elemental and alloy matrices. The method has been developed and standardized, and is in routine use for more than two decades. The reaction has a strong and wide resonance at 660 keV of proton energy. It involves the irradiation of the targets with ~750 keV protons and the detection of high energy α-particles with a surface barrier detector at ~ 1500 angle. Protons backscattered from the sample constituents, heavy or otherwise, are stopped in a stopper

foil and hence, the measurement is interference free. The method has a sensitivity to detect sub-ppm level of boron with ~10% precision in the suitable matrices. In this regard, the content of boron in several nuclear materials, determined using NRA technique is given in the following (Table 1).

Table 1: *Boron concentration in nuclear materials*

S. No.	Material	Content of Boron (ppm)
1	Zr-Nb alloy	1.4 ± 0.1
2	Al-clad	6 ± 0.4
3	SS	7.5 ± 0.5
4	Hf- shutter rod	0.5 ± 0.05
5	Zircaloy-4	2.4 ± 0.15

2.10 Elastic Recoil Detection Analysis (ERDA) and p-EBS measurements on Zr-2.5Nb samples

Due to the excellent neutronic and metallurgical properties, Zr-2.5 Nb is widely used in the manufacture of pressure tubes for pressurized heavy water reactors (PHWR). A pressure tube consists of an oxide layer, developed in the final stages of manufacturing, to minimize corrosion and hydrogen pickup during the course of reactor operation. The oxide layer, as result, plays an important role in governing the life expectancy of the pressure tubes. A systematic study on the behaviour of the oxide layers on Zr-2.5 Nb coupons prepared by autoclaving, in water and or steam environments at elevated temperatures was carried out in collaboration with PIE Division, BARC. The compositional analysis component of the study involved the determination of (a) Zr/O ratio and (b) hydrogen distribution in the oxide layers, and (c) thickness of oxide layers while structural, microstructural and chemical state analyses formed the other parts the investigation. The Zr/O ratio and the thickness of oxide layers were measured by proton elastic backscattering spectrometry (p-EBS) while H or and D were measured by elastic recoil detection analysis (ERDA). The study showed that depending on the nature and conditions of exposure, uniform/ localized oxide morphologies (nodular corrosion) are formed on the coupons. Some important observations arising from compositional analysis are (a) the thickness of the oxide ranged from 1.15 to 10 microns, (b) nodular regions bear hyper oxygen-stoichiometry and (c) the content of H/D varies from 2 to 10 at%. These results, in conjunction with other analytical measurements provide a detailed understanding of the response of autoclaved oxide layers to the aggressive water/steam environments.

3. Development of Analytical Methods

3.1 Determination of SO_4^{2-} and S^0 in ZnS by different liquid chromatography techniques

ZnS being a compound semiconductor has found many applications in various fields; such as phosphors, solar cells, and IR windows. Photoluminescence and IR transparency properties of these materials are extremely sensitive to trace impurities (trace metals, sulphate and elemental sulphur) and therefore close quality control in the production of zinc sulphide is mandatory. Distinction of elemental sulphur from sulphate in a solid sulphide matrix is a difficult analytical problem. A methodology for the determination of sulphate (SO_4^{2-}) and elemental sulphur (S^0) in zinc sulphide (ZnS) using ion-chromatography (IC) and reversed-phase HPLC was developed. Three sample pre-treatment approaches were employed with the aim of determining sulphate: (i) conventional water extraction of the analyte; (ii) solid–liquid aqueous extraction with an ultrasonic probe; and (iii) elimination of the zinc sulphide matrix via ion-exchange dissolution (IED). The separation of sulphate was carried out by an anion-exchange column (IonPac AS17), followed by suppressed conductivity detection. Elemental sulphur was extracted ultrasonically from the acid treated sample solution into chloroform and separated on a reversed phase HPLC column equipped with a diode array detector (DAD). The achievable solid detection limits for sulphate and sulphur were fund to be 35 and 10 μg g^{-1} respectively.

Analyst 130 (2005) 498

3.2 Development of microwave assisted-UV digestion using diluted reagents for the determination of total nitrogen in cereals by ion chromatography

A method based on a microwave assisted-ultraviolet (MW-UV) digestion in the presence of dilute HCl and H_2O_2 followed by ion chromatography (IC) measurements for the determination of total nitrogen in cereals was developed. This approach (MW-UV-IC) requires lesser time and does not need environmentally hazardous materials as used in Kjeldhal method. Further, the developed method requires only microliter quantities of dilute HCl and few millilitres of H_2O_2 for the matrix digestion and simultaneous conversion of nitrogen to its ionic species for the subsequent analysis by IC. At the optimized acid concentrations (200 μL of 0.1 mol L^{-1} HCl) and microwave power, the nitrogen in the cereals flours is converted to nitrate (NO_3), nitrite (NO_2) and ammonium (NH_4^+) ions. The nitrogen species were separated using IonPac AS-20 and IonPac CS-17 columns and then quantified using suppressed conductivity detection. The method was applied to estimate the total nitrogen in flours of various cereals like; wheat (*Triticum aestivum*), rice (*Oryza sativa*), finger millet (*Eleusine coracana*), jowar (*Sorghum*) and pearl millet (*Pennisetum glaucum*). The results obtained using proposed method, were in good agreement with that of Kjeldhal method. Moreover, the precision of the values obtained by developed method was on par with the Kjeldhal method for all the tested flours as verified by F-test (n =5 and 95% confidence limit). Additionally, greenness assessment tools like analytical Eco-scale and green analytical procedure index (GAPI) suggested the proposed MW-UV-IC method, for the determination of total nitrogen in cereal flours, to be excellently green and safe.

Current Research in Food Science 4 (2021) 421

3.3 Sample treatment approaches for trace level determination of cesium in Hepatitis B vaccine by suppressed ion chromatography

The hepatitis B surface antigen manufactured by recombinant DNA technology is extracted from the culture media by density gradient centrifugation using cesium salts. Cesium is considered to be toxic, because it affects active ion transport by blocking potassium channels. The residual trace levels of cesium in hepatitis B vaccine samples are determined by suppressed ion chromatography. Hepatitis B vaccines contain various buffer salts, aluminum-containing adjuvants, proteins and traces of iron. The polyvalent cations (Al^{3+}, Fe^{3+}) and proteins degrade the chromatographic performance in terms of decreased retention time and poor reproducibility. Different sample preparation approaches were evaluated with the aim of eliminating these foulants: (1) filtration, (2) digestion and (3) digestion-protein precipitation. Quantitative elimination of these foulants was achieved in the digestion-protein precipitation sample clean-up approach. Cesium was separated on the IonPac CS17 column with suppressed conductivity detection. The results of the ion chromatography (IC) method were compared with ICP-MS analysis. The precision of determination was better than 6.5% (% RSD) with a method detection limit of 45 ng mL^{-1}. The expanded uncertainty in the measurement at 95% confidence level (coverage factor 2) is better than 16.3%

Chromatographia 75 (2012) 17

3.4 Facile on-site quality monitoring of alcohol-based hand sanitizers by phase separation and colour development with butyl acetate-crystal violet mixture

Amidst the unprecedented demand for alcohol-based hand sanitizers in the wake of the continuing onslaught of COVID-19 pandemic, a simple and rapid method for identifying spurious or non-conforming products was required. Accordingly, a visual colourimetric method for the detection of methanol-based hand sanitizers and also for the semi-quantitative determination of ethanol or propanol in ethanol or propanol-based products was developed. Methanol based sanitizers pose a serious threat to human health while ethanol or propanol-based sanitizers containing <60% (v/v) alcohol are poor disinfectants. Taking cognizance of the fact that alcohol and water account for >95% volume of sanitizers, the method utilizes the alcohol dependent miscibility of alcohol-water binary mixtures in n-butyl acetate for analysis. The phase separations in the alcohol: water: n-butyl acetate ternary mixtures are quantitatively identified through colour contrast developed by the addition of crystal violet. The method was applied to several commercially available liquid and also gel type sanitizers. It works well for both colourless and coloured sanitizers.

Microchemical Journal 169 (2021) 106578

3.5 Overcoming the challenges to control sulphate blank from reagent (HF) used for matrix volatilization for the accurate determination of trace level of sulphur in quartz using ion-chromatography

A method was developed for the trace level quantitation of sulphur as sulphate in quartz samples using ion chromatography. The success of the method is based on the drastic reduction (1500 times) of sulphate blank in HF used for the digestion of quartz and release of sulphate from insoluble calcium sulphate precipitate using potassium oxalate solution. Instrument linear range for sulphate determination was found to be 1.0 – 10.0 mgL^{-1}. Limit of quantification at 10 σ was calculated to be 6 mg kg^{-1} (as sulphur). Analysis of Silicon 57A - CRM using the developed method resulted in 0.0031 ± 0.0003 % m/m of sulphur which is close agreement with the certified value of 0.003 ± 0.002 % m/m. This established the trueness of the developed method. The method has shown good repeatability and reproducibility. The developed method was successfully applied for the analysis of sulphur in quartz powders where the

concentration of sulphur varied from 10 - 60 mg kg^{-1}. The method was further utilized to analyse sulphur in other geological materials like basalt (BHVO-1, BIR-1) and granite (G2), the values of sulphur obtained by this method were in close agreement with the value published in literature as suggested by Student's t-test.

3.6 Analytical methods for the analysis of noble metals and their alloys

High precision stoichiometric determination of Platinum and Rhodium catalysts used in the feed stocks and also in the catalyst batches is of high importance, both due to their monetary value and the purity requirements. In addition, the determination of trace metallic impurities in Platinum-Rhodium catalyst is one of the major requirements in fertilizer industry. Optimized analytical procedures were developed to meet these requirements.

a) High Precision stoichiometric and trace analysis in Pt-Rh catalysts: After dissolution of the Pt-Rh catalyst in aqua- regia, rhodium is separated from platinum by oxidative hydrolysis using potassium bromate. After this step, platinum is determined by differential spectrophotometry and rhodium as Rh-$SnCl_2$ complex, whose λ_{max} lies at 480nm. The λ_{max} for Pt-$SnCl_2$ complex is found to be at 403nm. The typical RSD in this determination is 0.3%.

b) Determination of traces of gold in Pt-Rh catalysts: A spectrophotometric method for the determination of traces of gold in Pt-Rh catalyst was developed. The ion-associate of chloroaurate-crystal violet is extracted into a mixture of MIBK and benzene. Optimization of some other experimental parameters, enable the removal of common interfering ions like Ga(III), Fe(III), Indium and Silver. Thallium(III) interference was removed by Titriplex III.

3.7 Indigenous development of electrolyte cathode discharge atomic emission spectrometer (ELCAD-AES) technique

Low power direct current atmospheric pressure glow discharges are nowadays considered to be one of the most promising and alternative excitation sources against traditional plasmas, i.e., inductively coupled plasma and microwave induced plasma. These glow discharges are generated between metallic anodes and cathodes that are electrolyte solutions overflowing from inlet tubes or capillaries (electrolyte cathode discharge, ELCAD). An ELCAD source was designed and fabricated at NCCCM and coupled to emission spectrometer. It is an up-coming analytical technique and has several analytical advantages over conventional plasma sources. The source consumes little power (<75 W), does not require vacuum, operates in the ambient air, and therefore has very low operating cost. The detection limits (10s of ppb) are comparable to other techniques. This analytical technique was applied to various CRMs and samples of different matrix for their trace elemental content.

Analytical Chemistry 81 (2009) 8157

3.8 A sensitive vesicle mediated dispersive liquid-liquid microextraction of parts per quadrillion levels of beryllium from seawater samples prior to graphite furnace atomic absorption spectrometry determination

This work was carried out for beryllium plant, Vashi, Mumbai, to get environmental clearances for a proposed new Be processing plant at Pzayakal, Tamilnadu. Environmental safety agencies required a baseline data of Be in the surrounding environment of propose plant such as air, water and sea sediments. The levels of Be are at extremely low in seawater, hence a pre-concentration method was developed to

determine Be in different matrices using GFAAS. In this procedure, dioctylsulfosuccinate, an anionic vesicular surfactant and acetyl acetone are used as dispersing and chelating agents, respectively. At pH> 9.5, Be forms hydrophobic beryllium-acetylacetonate complex spontaneously at room temperature. This complex is selectively filled into the vesicular cavities of dioctylsulfosuccinate and is extracted into small chloroform phase from bulk aqueous phase. The Be present in the chloroform phase is back extracted with dilute nitric acid and analyzed by GFAAS. This method is applied to groundwater, seawater, coal fly ash, air filter and sea sludge samples. Limit of detection, limit of quantification and linear dynamic range are 10 fg mL^{-1}, 33 fg mL^{-1} and 40 – 500 fg mL^{-1} for seawater; 0.15 ng g^{-1}, 0.5 ng g^{-1} and 0.4 – 4 ng g^{-1} for air filter and 1.5 ng g^{-1}, 0.39 ng g^{-1} and 0.4 – 4 ng g^{-1} for coal fly ash, respectively. For 1 L seawater sample an enrichment factor of 954 is achieved. The relative standard deviations are 20%, 11%, 8% for ppq, ppt and ppb levels of Be, respectively. The accuracy of the procedure is verified by analyzing NIST SRMs 1640 and 1640a trace elements in natural water.

Analytica Chimica Acta 1191 (2022) 339313

3.9 Utility of permanent chemical modifiers in graphite furnace atomic absorption spectrometry

Permanent chemical modifiers (PCM) play a very important role in the analysis of complicated matrix by graphite furnace atomic absorption spectrometry (GFAAS). It replaces the conventional modifier Pd/Mg used during analysis. Usually, the refractory metals such as W, Zr, Ta and Nb are used alone or in combination with platinum group metals such as Pt, Rh and Ir to form stable and permanent deposit on the surface of graphite tube that can last for several hundred atomization cycles. These PCMs avoid the addition of modifier in each and every atomization cycle and improves the graphite tube atomizer life from 300 to 900 atomization cycles. These PCMs improve the sensitivity of the oxide forming analytes by reducing the oxygen partial pressure in the atomizer and hydride forming analytes by pre-concentrating them on the coated surface. They reduce the cost of analysis and also overcome the chloride interference encountered in the analysis of complicated matrices.

Journal of Analytical Atomic Spectrometry 61 (2001) 527
Journal of Analytical Atomic Spectrometry 17 (2002) 704
Journal of Analytical Atomic Spectrometry 20 (2005) 124
Spectrochimica Acta Part B: Atomic Spectroscopy 62 (2007) 504
Analytical Science 23 (2007) 351

3.10 Development of analytical methodology for the compositional characterisation of Ni-based superalloys by GD-QMS

Nickel based superalloys are the most important materials for development of gas turbine engine components. Advancements in the alloy compositions as well as manufacturing techniques have been attempted to improve the operating temperature and performance of the gas turbine engine. The present technology used for development of advanced gas turbine engine is the use of single crystal components made out of the super alloys. Single crystal blades, vanes and seals are commonly used in the latest generation turbine engines. Single crystal components offer better properties in terms of fatigue, oxidation and creep rupture in comparison to equiaxed or directionally solidified components. CMSX-4 is a second generation nickel base superalloy which is extensively used for the development of single crystal components for gas turbine components. The alloy is a constituent of more than 50 elements with varying concentrations ranging from percentage to parts per billion (ppb) range. Chemical characterization plays a very crucial role as the material is used for aeroengine components and the airworthiness certification for

the materials is very stringent. Therefore, a GDQMS method was developed to quantify trace and ultratrace impurities in the Ni-based superalloys. The relative sensitivity factors for all the analytes were generated using internal standards and applied to different Ni-based superalloys. The GDQMS results were validated with the corresponding ICPMS, GFAAS and ICPOES results.

3.11 Development of analytical methodology for the measurement of thickness of Cr-N film on SS by GD-QMS

Thin films of carbides and nitrides of transition elements on surfaces of various metals and alloys have found extensive tribological applications in many industries. These films have excellent wear, hardness, fatigue and corrosion resistance characteristics compared with the substrate materials. Such films can be prepared by several techniques such as magnetron sputtering, chemical vapour deposition and ion beam-assisted methods. Thin films of chromium nitride, prepared using ion beam-assisted deposition on stainless steel, were characterized for their composition and thickness by backscattering spectrometry and glow discharge mass spectrometry GDQMS. The composition and thickness of the films estimated by the GDMS method are consistent with backscattering measurements.

Thin Solid Films 388 (2001) 195

3.12 Chromium (VI) detection kit for drinking, tap, lake, river and ground water

Chromium is widely used in various industries like steel, chromo plating, paint manufacturing, leather treatment and as corrosion inhibitor. It exists in the environment primarily in two valence states, trivalent chromium, Cr(III) and hexavalent chromium, Cr(VI). Cr(III) is biological important element and needed for glucose and lipid metabolism. Cr(VI) however is considered toxic and carcinogenic to humans. Cr(VI) is known to cause lung and nasal cancer as well as other health related problems. Environmental protection agency (EPA) has established Maximum Concentration Limit for chromium as 100 µg L^{-1}, by assuming that the total chromium is present as Cr(VI). Indian standard has set its limit to 50 µg L^{-1}. For the detection of such a low levels, very sophisticated instrumentation such as HPLC-ICPMS is necessary. For accurate analysis, the samples can be sent to the laboratory; however, for initial screening, a field method for detection of Cr(VI) is required for onsite estimation. The exiting methods for field application are not sensitive enough to detect Cr(VI) at prescribed level of < 50 µg L^{-1}. A quick, easy and affordable kit was developed for onsite determination of Cr(VI) that meets EPA criteria. Cr(VI) detection kit is a simple, user-friendly and highly cost-effective kit for estimation of chromium (VI) in drinking, tap, lake, river and ground water in comparison to the currently available techniques. The procedure is as simple as adding a specified amount of reagents to the water sample to be analysed and identifying the colour developed. The colour develops within 5 minutes and the distinction can be made with the naked eye. For ease of comparison a colour chart is provided with the kit. Water samples can be immediately categorized as being safe or toxic for drinking from chromium (VI) point of view.

Technology transferred (2016)

3.13 Development of Iron detection kit for boiler coolant water using Smartphone / Spectrophotometer

The method involves the mixing of the four reagents (1, 2, 3 and 4) in a standard volumetric flask, at room temperature. A pink colour develops depending on the concentration of iron in the sample. The Smartphone based software ‘Colorimetry App’ is an interactive GUI app which captures image of sample solution using phone camera and analyzes the intensity of the colour to determine the ppb level of

iron. A spectrophotometer can also be used for detection in laboratory. The product is a kit designed at NCCCM along with Smartphone based colorimetry app software developed by Electronic Division, BARC. The kit includes a chamber where in sample is kept in standard flask after chemical processing, and a slot to keep the Smartphone which runs the colorimetric app. Total iron, Fe (II+III) in 10-80 ppb range can be determined that meets the specification of boiler coolant water. For 1-80 ppb range, the spectrophotometer can be used.

Technology transferred (2019)

3.14 Determination of parts per billion levels of total iron (Fe^{2+}+Fe^{3+}) in secondary coolants of nuclear reactors

A visual method was developed for the determination of total iron i.e. both the species Fe^{2+} and Fe^{3+} without using any oxidizing or reducing agents in nuclear reactor coolants and also in nuclear submarines. The required levels of determination are around 1 to 20 ng mL^{-1}. This method is useful for the interpretation of corrosion levels of coolant pipes of nuclear reactors and reactor systems. The determination of iron is also important in industries like thermal power plants, steam generator systems, and all other industries which involve heating and cooling of reactor systems in their usage. The main objective is to develop a simple and fast, low cost visual detection method for the determination of total iron (5 to 100 ng mL^{-1}) at the (natural) pH levels of the coolant waters (pH 9-10). The method is robust and applicable at sampling site with capability to overcome the interferences caused by the additives in the coolants.

Indian Patent No. 351799, dated 08-03-2019

3.15 Development of an analytical method to determine parts per billion levels of ammonia in water with emphasis on boiler coolant water.

A novel surfactant sensitized chemical methodology was developed for the determination of ultra-trace levels of ammonia in boiler coolant waters using spectrophotometer. In these waters, ammonia is monitored regularly in the range of 10 to 500 ng mL^{-1} to prevent stress corrosion cracking that commonly occurs in copper-based alloys generally used in the cooling systems. Accurate quantification of ammonia in boiler water is useful for the interpretation of early stages of brittle fracture of brass condenser tubes. It facilitates to take early stage preventative action to increase the life time of condenser tubes. The determination of ammonia at these levels is important in industries like power plants, steam generators, cooling towers and various other industries that use the heating and cooling systems. The method has to have low detection limits of 10-1000 ppb in the basic pH of coolant and boiler waters. The method is simple and cost effective, applicable for onsite determination. It takes around 30-60 minutes at lower levels and 5-10 minutes at higher levels to get accurate results. The sample prepared is not turbid and viscous for analysis. There is no sample pretreatment required for the analysis. No pre-concentration required just simple rotation for 30-60 minutes. Very less amount of sample is required approximately 5 ml. The method is robust and applicable at sampling site with capability to overcome the interferences caused by the additives of the boiler waters.

Indian Patent no. 463966, 2023

3.16 Stoichiometric determination of Ba and Ti in $BaTiO_3$

$BaTiO_3$ is an advanced ceramic material with many electronic applications. The stoichiometry determination of Ba and Ti in $BaTiO_3$ is necessary as the above applications are dependent on

stoichiometry. The sample was decomposed by treating with HF and $HClO_4$, and after removing HF, Ti was determined by spectrophotometric method by forming a peroxy complex in $HClO_4$ medium and Ba was determined by gravimetric method as $BaSO_4$

3.17 Methodology for hydrogen determination and depth profiling using resonance in $^{1}H(^{19}F,\alpha\gamma)^{16}O$ nuclear reaction

Hydrogen embrittlement is of concern in nuclear materials. It is responsible for fracture start and subcritical crack growth in material and subsequent loss in mechanical properties. Similarly nitriding at higher temperatures resulting in the embrittlement of the structural components is also of serious concern in nuclear materials. The determination of concentration profiles of low Z elements such as hydrogen, nitrogen, oxygen etc., is vital to control the manufacturing process and also in failure analysis to establish the mechanism of degradation. At NCCCM we have developed IBA methodology for non-destructive depth profiling of hydrogen using 6.4 MeV resonance in $^{1}H(^{19}F,\alpha\gamma)^{16}O$ nuclear reaction.

Nuclear Instruments and Methods in Physics Research B 142 (1998) 549

Hydrogen determination experiments were carried out at the vicinity of electron beam welded joints in Ti-Al-Sn alloys received from VSSC, Trivandrum. The depth profiling of hydrogen was carried using 6.4 MeV resonance in $^{1}H(^{19}F,\alpha\gamma)^{16}O$ nuclear reaction. The measurements showed that at the welds and the base regions of the samples, hydrogen was largely confined in the surface region ~50 nm. Its content decreased from about 16 *at.%* in the top surface regions to about 4 *at.%* at depths beyond 250 nm. However, in the Ti-Al-Sn alloys that were vacuum annealed, the hydrogen content was below 8 *at.%* at the surface regions and it dropped to below 1 *at%* above 50 nm depth.

Further, depth profile of hydrogen was also carried out in a silicon nitride film using resonance in $^{1}H(^{19}F,\alpha\gamma)^{16}O$ nuclear reaction.

3.18 Determination of nitrogen by alpha induced γ-spectroscopy

Nitrogen plays a vital role as a major constituent in semiconductor technology, development of wear resistant bulk materials and surface coatings. The presence of nitrogen as an impurity, particularly in certain semiconductor materials, even at trace quantities is undesirable. It can affect the electronic properties, such as increased leakage current, decreased electron mobility, and increased electrical resistivity. Also, nitrogen as an impurity in steel can lead to its embrittlement. Therefore, it is essential to determine nitrogen in order to control its level during the processing of the materials.

A methodology based on $^{14}N(\alpha,p\gamma)^{17}O$ nuclear reaction for the determination of nitrogen in materials was standardised. The determination is based on the detection of the 871 keV prompt γ-rays, characteristic of the reaction, by high resolution γ-ray spectrometry. The limit of quantification of the method for nitrogen in carbon and stainless steel matrix is ~290 ppm. The superior sensitivity, in comparison to $^{14}N(p, p'\gamma)^{14}N$ and $^{15}N(p, \alpha\gamma)^{12}C$ proton induced nuclear reaction analysis and $^{14}N(p, p)^{14}N$, $^{14}N(\alpha,\alpha)^{14}N$ elastic backscattering, is due to the low background and absence of any competing reactions when α particle is being used as a projectile. The method is simple, non-destructive, rapid and provides quantification with a precision of 7%.

Nuclear Instruments and Methods in Physics Research B 548(2024)165260

Austenitic stainless steel wires used to hold catalyst in an ammonia converter vessel of a heavy water plant had cracked after being in use for five years. Depth profiles of H and N in the corroded wires

received and unused wires were measured in order to investigate the factors that led to their cracking. For the determination and depth profiling of nitrogen the resonance at 429 keV in $^{15}N(p,\alpha\gamma)^{12}C$ nuclear reaction was used. Analysis of several specimens suggests that the depth distribution of nitrogen in each wire specimen varies. It was found that diffusion of nitrogen inside stainless steel wires at the operating temperatures of a heavy water plant promoted nitriding of stainless steel leading to the formation of brittle nitride phases.

Nuclear Instruments and Methods in Physics Research B 240 (2005) 704

3.19 Lithium Isotopic abundance determination by NRA

Determination of overall lithium content in lithium bearing minerals such as spodumene, mica pegmatite etc., is important as these are major sources of Li. Apart from overall content, determination of lithium isotopic abundance is also important in the fields of nuclear technology, geochemistry, astrophysics, biomedicine, and environmental research. Due to large relative mass difference (16.7%) the fractionation occurs by way of diffusion, preferential partition into aqueous fluids etc.

Lithium analysis is generally performed using a 1–4 MeV proton beam and involves the measurement of the 478 keV prompt γ-rays, from $^{7}Li(p,p\gamma)^{7}Li$ nuclear reaction. However, there has been no work reported for the Li isotopic abundance determination by using IBA techniques. A carbon induced γ-ray emission spectroscopy methodology was standardized for the determination of ^{6}Li and ^{7}Li isotopic abundance. The nuclear reactions utilized are $^{7}Li(^{12}C, \alpha\gamma)^{15}N$ (Q= 12.38 MeV) which emits γ-rays of E_γ=5.27 MeV and $^{6}Li(^{12}C, \alpha\gamma)^{14}N$;(Q= 8.79 MeV) ; $^{7}Li(^{12}C, \alpha n\gamma)^{14}N$ (Q= 1.55 MeV) which emits E_γ=2.3 MeV γ-rays. A 6.0 MeV carbon beam was used in these experiments. The Li_2CO_3 enriched in ^{6}Li were used as standards. Both standards and samples were irradiated under identical experimental conditions. A mathematical formulation was developed to determine the isotopic abundance of ^{6}Li, ^{7}Li and overall Li content from the 5.2 MeV and 2.3 MeV γ-ray yields. The methodology was applied to geological (spodumene) samples to determine the ^{6}Li and ^{7}Li isotopic abundance.

3.20 Indirect determination of Li via $^{74}Ge(n,\gamma)^{75m}Ge$ activation reaction

An indirect PIGE methodology was developed to determine Li by $^{74}Ge(n,\gamma)^{75m}Ge$ activation reaction induced in a high purity Ge (detector) crystal by neutrons from the $^{7}Li(p,n)^{7}Be$ reaction. Experiments were carried with proton beams of energies in excess of 1.88 MeV, the threshold energy (E_{th}) of the $^{7}Li(p,n)^{7}Be$ reaction. The determination involves the activity measurement of ^{75m}Ge isotope that has a half-life of 47.7 s and decays with the emission of 139 keV γ-rays. Rapidity, selectivity and sensitivity down to ppm levels are the attractive features of the method. It is a suitable alternative to $^{7}Li(p,p\gamma)^{7}Li$ reaction based PIGE technique for the analysis of matrices that contain light elements such as Be, B, F, Na and Al in significant proportions.

3.21 Oxygen determination in materials by $^{18}O(p,\alpha\gamma)^{15}N$ and $^{18}O(p,p'\gamma)^{18}O$ nuclear reactions

The determination of oxygen in thin films or bulk compounds is a complex and challenging task. In these materials, oxygen is present either as a major constituent or as an impurity element. In this regard, proton induced γ-ray emission methods based on $^{18}O(p,\alpha\gamma)^{15}N$ and $^{18}O(p,p'\gamma)^{18}O$ nuclear reactions were developed and standardised for the determination of bulk oxygen in materials.

The determination of oxygen by $^{18}O(p,\alpha\gamma)^{15}N$ involves the measurement of 5.27 MeV γ-rays emitted following the de-excitation of ^{15}N nuclei. The experiments were performed at ~ 4.0 MeV energy

and the γ-ray were measured with a high purity germanium detector (HPGe) or a bismuth germanate detector (BGO) at 0° or 90° angles. The limit of detection of the method is about 1.3 *at.%* while its probing depth is several tens of microns. Interferences can arise from fluorine due to the occurrence of $^{19}F(p,\alpha\gamma)^{16}O$ reaction that emits 6-7 MeV γ-rays.

The determination of oxygen by $^{18}O(p,p'\gamma)^{18}O$ (E_γ= 1982 keV) nuclear reaction involves the bombardment of the targets with 4.0-4.2 MeV protons and the measurement of the 1982 keV prompt γ-rays. It has a limit of detection ~2 *at%* in heavy matrices and ~ 15 *at%* in light matrices, and has a probing depth of more than 30 μm at 4.2 MeV of proton energy. High precision measurement of oxygen (~ 2 %) in mid and high Z matrices is one of the important features of the method.

These methodologies were successfully employed in the analysis of several binary oxides (e.g., titanium oxide, manganese oxide, iron oxide), ternary oxides (e.g., lithium carbonate, lithium titanate, lithium iron phosphate) and also in non-oxide materials such as tungsten and copper powders.

Nuclear Instruments and Methods in Physics Research B 378 (2016) 38
Journal of Radioanalytical and Nuclear Chemistry 314 (2017) 1803-1812
Nuclear Instruments and Methods in Physics Research B 274 (2012) 154–161

3.22 Determination and depth profiling of Fluorine

Determination of fluorine is an important in the development of glasses for the immobilization of nuclear waste from advanced heavy water reactor (AHWR). The limitations of chemical analytical techniques in the determination of fluorine in materials in general and glass in particular are well known. Particle induced γ-ray emission (PIGE), is the technique of choice for the analysis of fluorine. It is sensitive, rapid and non-destructive which obviates the problems of contamination and formation of volatile fluoride species generally encountered during analysis by chemical methods.

Fluorine content was determined in glasses used for nuclear waste immobilization by $^{19}F(p,p'\gamma)^{19}F$ reaction using 110 keV and 197 keV characteristic γ-rays of the reaction. As an alternate approach, we have also examined $^{19}F(p,\alpha\gamma)^{16}O$ and $^{19}F(\alpha,\alpha\gamma)^{19}F$ nuclear reactions which emanate 6-7 MeV and 1278 keV γ-rays, respectively for this application. The fluorine concentration ranged from 0.5 to 2.85 wt%.

A thin coating of Teflon was applied on the wedge-shaped edge of the surgical blades for safety considerations. Thickness of Teflon $(C_2F_4)_n$ coatings on knife edges of the surgical blades, from Hindustan Surgical Company, was determined. To determine the exact thickness of the coating, $^{19}F(p,p'\gamma)^{19}F$ nuclear resonance reaction that exhibits a sharp resonance (FWHM = 400 eV) at 1088 keV was utilised. This resonance width corresponds to a 200 Å depth resolution in Teflon. The thickness of the coatings on two different types of blades was estimated to be 440 Å and 420 Å.

3.23 Magnesium depth profiling using a resonance in $^{24}Mg(p, p'\gamma)^{24}Mg$ nuclear reaction

Mg-based thin films, compounds and alloys find applications in hydrogen storage, optical devices and superconductors. Atomic composition and depth distribution of the constituents of the films provide vital information on their functionality. However, unlike other low Z elements, very few ion beam analysis (IBA) methodologies are available for depth profiling Mg. A methodology based on 2010 keV resonance in $^{24}Mg(p,p'\gamma)^{24}Mg$ nuclear reaction for depth profiling of Mg in thin films was developed. The resonance reaction, based on the detection of characteristic 1368 keV γ-rays, enables interference free measurement of Mg down to 2×10^{20} atoms/cm^3 and has a probing depth of about 20 μm. The width of the resonance extracted from excitation curves for thick (>180 nm) thermally grown elemental Mg films,

is about 350 ± 50 eV. The reaction was used to depth profile Mg in a Mg/Ti/Mg/Si film which provides information on interfacial mixing involving Ti layer and the underlying Mg layer.

Nuclear Instruments and Methods in Physics Research B, 266 (2008) 3281

3.24 ^{28}Si(p,p′γ)^{28}Si nuclear reaction in the detection and depth profiling of Si in materials

Si is the most important elemental semiconductor and is a major constituent of some compound dielectrics/ceramics such as silicon carbide, silicon nitride and silicon oxide. Amongst the ceramics, silicon carbide is a candidate material for fuel cladding applications in nuclear power reactors. Depth profiling of silicon is important for investigating compositional variations and interfacial reactions, occurring particularly at high temperatures. A proton induced γ-ray emission method for depth profiling Si in the surface regions of materials was developed and standardized. The method utilizes the resonance at 3098 keV in ^{28}Si(p,p′γ)^{28}Si nuclear reaction and involves the measurement of 1778 keV γ-rays emitted from the reaction. The resonance has a width of ~12 keV and, therefore, the depth resolution of the method is rather poor (~ 600 nm in Si). However, it is compensated by a fairly large probing depth, about 11 μm in Si, which is dictated by another resonance, albeit weaker, at 3337 keV in the yield curve. The method is free from any spectral interference and has a detection sensitivity of ~0.7 *at.%*. Depth profiling of Si in silicon carbide crystals and films of silicon nitride on gallium arsenide with <10% combined uncertainty establishes that this method is well suited for probing Si in the deep surface regions of bulk materials and thick films.

Nuclear Instruments and Methods in Physics Research B 527 (2022) 12

3.25 Measurement of resonances and cross-sections in ^{32}S(p,p′γ)^{32}S nuclear reaction

Sulphur, is a major constituent of chalcogenide semiconductors (e.g., CdS, $CuInS_2$, etc.,) while, on the other hand, it is an undesirable species in many metallurgical applications as it deteriorates the mechanical properties of metals and alloys by inducing corrosion. The possibility of the occurrence of such a corrosion process or sulphur poisoning is quite prominent. This is known from the fact that sulphur bearing species are amongst the most abundant contaminants in gases, particularly in organic gases and are also formed as by-products in several chemical processes. Apart from materials of different kinds, the determination of sulphur is also important in biological and environmental studies.

To determine and depth profile sulphur, the widths and differential cross-sections of resonances at 3.089, 3.379 and 3.717 MeV in the ^{32}S(p,p′γ)^{32}S nuclear reaction were measured. The cross-sections are computed at 0º and 90º angles (relative to the beam direction) from thick target excitation curves constructed by measuring 2230 keV γ-rays, characteristic of the reaction. The differential cross-sections of resonances are about 18, 64 and 70 mb/sr respectively at 0º angle and decrease by a factor of 2 at around an angle of 90º. These resonances can be effectively utilised for sensitive and high resolution depth profile measurements of sulphur in films and materials surfaces.

Nuclear Instruments and Methods in Physics Research B 269 (2011) 2557

3.26 Depth profiling of titanium using a resonance in ^{48}Ti(p,γ)^{49}V nuclear reaction

Titanium is a constituent of several technologically important materials. Its depth profile in the surface regions is desirable for standardizing the manufacturing process and assessment of functionality of the materials. The resonance at 1362 keV in ^{48}Ti(p,γ)^{49}V nuclear reaction (E_γ = 7.9 MeV) was used for depth profiling of Ti in Ti based films. The γ-rays are measured by a bismuth germanate detector. The method has a detection sensitivity of about 5.1×10^{20} at.cm^{-3} and can provide determinations with a depth

resolution of about 24 nm up to a depth of about 800 nm in Si matrix. Selectivity is another important feature of this non-destructive method of depth profiling.

Journal of Radioanalytical and Nuclear Chemistry 302 (2014) 1455

3.27 Chromium depth profiling in surface layers by $^{52}Cr(p,\gamma)^{53}Mn$ nuclear resonance reaction

Chromium is an important constituent of several structural materials and functional coatings. Its determination and depth distribution in the surface and near surface regions are of interest from the point of view of investigating corrosion, interfacial reactions and composition-property correlations. A methodology for depth profiling chromium in the surface and near surface regions of materials using the resonance at 1005 keV in $^{52}Cr(p,\gamma)^{53}Mn$ nuclear reaction is developed. The detection sensitivity, depth resolution and probing depth of the resonance in Si are determined to be about 3 *at.%*, 25 nm and 2.5 μm, respectively.

Journal of Radioanalytical and Nuclear Chemistry 302 (2014) 1399

3.28 Methodology for nickel depth profiling

Nickel is an important alloying element in materials for high-technological applications such as molten salt reactors (MSR), nuclear micro-reactors (MR). Nickel, as an implanted ion, plays a crucial role in the modification of physical properties in structural materials for nuclear applications. Also, nickel and its oxide films find applications in sensors, semiconductors etc. In all these studies, the determination of composition, film thickness and depth profiles of nickel is of prime importance for understanding the physical processes. A methodology was developed for high resolution depth profiling of nickel using a resonance at 1424 keV in $^{58}Ni(p, \gamma)^{59}Cu$ nuclear reaction. The reaction emits 491 keV, 4330 keV and 4820 keV characteristic γ-rays. The characteristic γ-rays were detected using HPGe, BGO and NaI(Tl) detectors. The γ-ray yield at 90°, with respect to beam direction, is higher by 25% relative to the 0° direction. The yield/cross-section curves of the reaction were constructed in bulk Ni, thin film Ni targets and also in Ni implanted Si substrates. Interferences were also studied. The reaction has sensitivity < 0.1% for Ni. The depth resolution of the resonance is 20 nm in Si substrates. Probing depth of the reaction is 5 μm.

3.29 Investigations on the applicability of proton induced γ-ray emission in the determination of lanthanides and heavy metals

Particle induced γ-ray emission (PIGE), an ion beam analysis (IBA) technique, is widely used for the determination of low Z elements such as Li, B, N, F, and Na, in materials. It has also been employed for the determination of mid-Z elements, for example, Ti, Cr, Mn, Fe and As, on several occasions. However, the instances of its application to high Z elements are very few. In an attempt to probe the analytical potential of PIGE for high Z elements, we have performed measurements on lanthanides (La, Gd, Dy and Nd) and on other elements such as Pt-group elements, coinage group elements, Hf and W. The exercise involves the bombardment of targets, oxides of lanthanides and thick foils of metals, with 1.0 - 4.2 MeV protons and the measurement of the prompt γ-rays spectra with a high purity Ge (HPGe) detector. The objectives of the experiments were to (a) identify the transitions and the relevant γ-rays for the interference free detection of the elements and (b) to assess the suitability of the γ-rays for the analytical purposes.

Nuclear reactions such as $^{139}La(p,n\gamma)^{139}Ce$ and $^{174}Hf(p,p'\gamma)^{174}Hf$ emitting 760 keV and 208 keV γ-rays were utilized for the construction of thick target yields of La and Hf respectively. As the Coulomb barrier for lanthanides is >10 MeV, the excitation of nuclear states is predominantly through inelastic Coulomb scattering. PIGE for high Z elements, with 4.2 MeV protons lacks the sensitivity observed for low Z elements or even mid Z elements and is suitable for estimating them only at percentage or sub-percentage levels. The suitability was established by analysing O/M (M= Dy, Gd etc.,) ratio in the respective oxides with < 3 % uncertainty. Incidentally, oxygen in the compounds was determined through $^{18}O(p, p'\gamma)^{18}O$ nuclear reaction (E_γ= 1982 keV) that occurs simultaneously.

3.30 Oxidative pyrolysis combined with microwave-assisted extraction method for the multi-elemental analysis of boron carbide powders by inductively coupled plasma optical emission spectrometry (ICP-AES)

The ability of boron carbide to absorb neutrons without forming long lived radionuclides makes it attractive as an absorbent for neutron radiation arising in nuclear power plants. Boron carbide containing boron enriched in the ^{10}B isotope is used in the control rods of the fast breeder reactors to control neutron flux, as shielding material and as neutron detector in nuclear reactors. However, nuclear properties of boron carbide are strongly influenced by the presence of impurities even at low concentrations. Therefore, determination of metallic impurities in boron carbide powders in production control and quality assurance is of great importance.

It is difficult to chemically treat the B_4C sample and bring the impurities into solution due to its refractory and chemically resistant nature; hence extreme sample treatments are required for the quantitative determination of impurities. A method based on oxidative pyrolysis (OP) using in-house quartz chamber in combination with microwave-assisted extraction (MAE) was developed as a new sample preparation approach for the determination of metallic impurities (W, Si, Pb, Ni, Fe, Ca, Mg, Ti and Al) in boron carbide powders. Initially, quartz boat containing known amount of boron carbide powder (100-400 mg) was inserted in the pyrolysis chamber. The chamber was then heated to ~500^0C using a Bunsen burner, in the presence of a continuous oxygen stream. After a few minutes (1-2 min), the sample gets burned and extinguished. After this pyrolysis step, followed by cooling, a MAE was applied with an extractant mixture of 10 mL of 30%HNO_3+10%HCl+5% HF. After completion of the extraction process, the supernatant was separated from the undissolved residues by centrifugation for 4 min at 5000 rpm. The supernatant was analysed for W, Si, Pb, Ni, Fe, Ca, Mg, Ti and Al by ICP-AES. The results of the developed method were in good agreement with values obtained by sodium carbonate fusion method. The average recoveries for most of the selected elements were in the range of 97-104%. The method was successfully applied to the analysis of boron carbide samples of different composition.

Analytical Methods 5 (2013) 1515

3.31 Development of microwave-assisted extraction method for the rapid determination of chloride and fluoride in nuclear-grade boron carbide powders

Presence of F^- and Cl^- in boron carbide as impurities even at trace level accelerates the corrosion of metallic components of the system. The specification limits, for chloride and fluoride in boron carbide has been prescribed as 75 µg g^{-1} and 25 µg g^{-1} respectively. Hence determination of chemical purity of boron carbide is very important towards quality control of boron carbide.

A simple and efficient microwave-assisted extraction (MAE) method for the rapid determination of chloride and fluoride in nuclear-grade boron carbide powders was developed using a closed

microwave-vessel (G30, Anton Parr) and domestic microwave oven. The optimized MAE conditions for quantitative recovery of chloride and fluoride were obtained by irradiating ~0.5 g of sample in 10 mL of 10% HNO_3 for about 30 sec at a microwave power of 480W. After completion of the extraction process, the sample mixture was centrifuged and the supernatant was subsequently analysed for of Cl and F using ion-selective electrode (ISE). Pyro-hydrolysis method was applied for validation of the results of the proposed MAE method with average recoveries for both chloride and fluoride were in the range of 98-101%. The LOD values for chloride and fluoride in conjunction with the proposed MAE were found to be 1.9 µg g^{-1} and 1.2 µg g^{-1} respectively while the relative standard deviation (RSD) was less than 10% in most of the cases. Under optimal conditions, the proposed MAE method was successfully applied to the analysis of boron carbide samples of different composition.

Analytical Methods 6 (2014) 261

3.32 Development of Oxidative Pyrolysis Method for the Rapid Determination of Boron in Graphite Powders by Inductively Coupled Plasma Optical Emission Spectrometry (ICP-AES)

Graphite is a base material for the preparation of mixed carbide fuels (e.g., (U, Pu)C) for the fast breeder reactors (FBR). The content of boron in nuclear-grade graphite is of particular concern among the other impurities due to its high neutron absorption cross section. Hence, high-purity graphite for nuclear purposes necessitates a strict control of boron whose specification limit has been set as 5 µg g^{-1}.

For the analysis of graphite, microwave decomposition and fusion using Na_2CO_3/$NaHCO_3$ or $Ba(OH)_2$ are the two standard sample preparation methods used for the determination of boron. However, due to need of large quantities of flux employed in decomposing the sample, a large number of steps and long sample preparation time (~3 h per sample) limit its application for routine analysis. Hence a new sample preparation method based on oxidative pyrolysis (OP) was developed for this purpose.

A known amount of graphite powder (~0.2 g) was mixed with carbon powder (1:0.75) along with 5 mg of Na_2CO_3 (250 µL of 20 mg mL^{-1} solution) and an appropriate amount of polyvinyl alcohol (binder). After drying under the IR lamp, the sample mixture was pressed into a pellet and introduced into the in-house pyrolysis chamber. The chamber was then heated using a Bunsen burner in the presence of an oxygen stream. The pyrolysis process commenced when the temperature reached ~400 ^{0}C and was completed in 5 minutes. After allowing the chamber to cool down to room temperature, a mixture of 0.2 mL of 1% mannitol, 0.5 mL of HNO_3 and 0.1 mL HF was added to the boat for treating the sample residue and was analysed by ICP-AES. The detection limit of boron was 0.05 µg/g and the relative standard deviation (RSD), was about 4%. The recoveries for the spike tests were obtained ranging from 98-102%. A fusion method was adopted for validation of the developed method. The developed method was applied to the analysis of graphite powder samples in which the concentrations of boron ranged from 3 to 60 ppm.

Atomic Spectroscopy 35 (2014) 109

3.33 An integrated approach based on oxidative pyrolysis and microwave-assisted digestion for the multi-elemental analysis of coal samples by ICP-based techniques

Concern over release of various trace elements to the environment as a result of coal utilization (mainly in thermal power plants) has made the determination of these elements an increasingly important aspect of coal analysis. The reported methods are associated with major limitations which include use of excessive amount of reagents for sample treatment process and long sample preparation time.

As an alternative to tedious traditional sample preparation methods, a simple and robust method for the multi-elemental (major to ultra-trace) analysis in carbon sample is developed. In this method, sample is sequentially subjected to oxidative pyrolysis (OP) in an in-house pyrolysis set-up and microwave-assisted digestion (MWD) of the pyrolysed coal residue is developed. The coal samples were initially subjected to OP in a pyrolysis chamber by heating it to ~500^{o}C in the presence of an oxygen stream. The pyrolysis process was complete in ~3 min when ~0.25 g of coal sample was used. Subsequently MWD was applied to the pyrolysed coal residue with an acid mixture of 8 mL of 20%HNO_3+5%HF+5%H_2O_2 or 20%HNO_3+0.4%NH_4HF_2 +5%H_2O_2 using the optimized microwave program. After completion of the digestion process, the obtained clear sample digests were diluted to required volume for subsequent analyses by ICP-MS (Be, V, Cr, Mn, Co, Ni, Cu, Zn, As, Rb, Sr, Mo, Cd, Sb, Cs, Ba, W, Tl, Pb, Th, U and REEs) and ICP-AES (Na, K, Ca, Mg, Fe, Al, Sc, Ti). Critical experimental parameters such as oxygen gas flow rate and sample mass (related to OP), acid composition, digestion temperature and time (related to MWD) were optimized through the analysis of two standard reference materials (SRMs) NIST-1632d and NIST-2685b to get the quantitative recovery of the target elements. The results obtained by the developed method agreed well with the certified values with recovery of the chosen elements between 95-106%. The optimized method was subsequently applied to Indian coal samples collected from different coal mines.

Fuel 158 (2015) 770

3.34 Development of a simple and robust microwave-assisted decomposition method for the determination of rare earth elements in coal fly ash by ICP-AES

A simple and reliable two-step method for the total decomposition of coal fly ash (CFA) material for the quantitative determination of rare earth elements (REE) by inductively coupled plasma optical emission spectrometry (ICP-AES) was developed. In the first step, coal fly ash samples were heated at ~200^{o}C on a hot plate for about an hour in the presence of 2 mL of sulphuric acid followed by the addition of 0.5 mL of HF. After completion of the hotplate treatment (HT) process, the sample mixture was further subjected to microwave-assisted decomposition (MWD) after adding 8 mL of 20% HCl (v/v) for its total decomposition. The final sample digests were analysed for REEs by ICP-AES (La, Ce, Pr, Nd, Sm, Eu, Gd, Tb, Dy, Ho, Er, Tm, Yb, Lu, Y and Sc). Critical experimental parameters related to first step of hotplate decomposition and second step of MWD processes were optimized for achieving quantitative recovery of REEs (>95%) through the analysis of a standard reference material (SRM) CFA NIST-1633b. The optimized two-step approach was subsequently applied to two Indian coal fly ash samples collected from different thermal power stations. The proposed two-step method in conjunction with ICP-AES can be utilized for the quantitative determination of REEs in CFA materials.

Analytical Methods 9 (2017) 2031

3.35 Development of a simple and efficient two-step microwave-assisted digestion method for the determination of REEs, HFSEs and other elements in granite samples by ICP-AES

An efficient two-step microwave digestion (MWD) method for the complete decomposition of granite material for the quantitative determination of rare earth and high field strength elements was developed. In the first step, granite sample was mixed with 2 mL each of HF, HCl and HNO_3 and subjected to microwave-assisted decomposition (MWD). After completion of first step MWD process, the sample mixture was transferred to PFA vial and heated on hot plate to incipient dryness for the removal of

silica matrix. The residual sample matrix was further subjected to second step of MWD after adding 6 mL of mixture of 50% HCl+HNO_3 (v/v) for its total decomposition. The final sample digests were analyzed for REEs by ICP-AES (La, Ce, Pr, Nd, Sm, Eu, Gd, Tb, Dy, Ho, Er, Tm, Yb, Lu, Y and Sc). Critical experimental parameters related to first and second step of MWD processes were optimized for achieving quantitative recovery of REEs (>95%) through the analysis of two certified reference materials SARM 1 and NCSDS. The concentrations of REEs La, Ce and Nd were found to be > 25 mg/kg, while Sm, Sc and Y ranged between 5-15 mg/kg and the rest of the REEs were less than 2 mg/kg. Trace elements such as Ba, Sr, Zn, Nb, Zr, U, Th and major elements like Al, Fe, Mg, Ca, Ti and Mn were also determined by ICP-AES. The method was validated using two granite CRMs. The % recovery of the above elements including REEs was in the range of 90-99%. The proposed two-step MWD approach in conjunction with ICP-AES has a great potential for the quantitative determination of REEs in granite materials.

Journal of Analytical Atomic Spectrometry 39 (2024) 2116

3.36 A Novel Digestion Method Utilizing In-house PTFE Digestor for the Rapid and Reliable Determination of Technology-Critical Elements (TCEs) in Granite Samples by ICP-AES: A New Development in Hotplate Digestion Approach

A new and high performance polytetrafluoroethylene (PTFE) digestor was designed and fabricated in-house for the total dissolution of granite samples for the quantitative determination of technology-critical elements (TCEs) by ICP-AES. A test portion of the granite sample (~250 mg) was weighed into the PTFE vessel and added 8 mL of 20%(v/v) HF + 40%(v/v) HCl + 10%(v/v) HNO_3 acid mixture. After closing, the PTFE vessel was heated on a hotplate at ~250^{o}C for about 2 h. Subsequently, the sample mixture was transferred to a graphite-bottom Teflon beaker for evaporation on hotplate at ~180^{0}C to incipient dryness for the removal of silica matrix and excess fluoride (evaporation step (ES)). The sample residue was re-dissolved in 3 mL of 60% (v/v) aqua regia and ES was carried out. This process was repeated once again for the complete transformation of highly insoluble metal-fluoride complexes to soluble chloride/nitrate complexes which produces stable solutions for analysis (aqua regia treatment step (ATS)). After ATS, the sample residue was reconstituted in 3 mL of 60% (v/v) aqua regia and made up to 50 mL. The final sample digests were very clear with no apparently visible fluoride precipitates indicating complete decomposition of different phases present in the granite matrix. The clear sample digests were analysed for REEs (La, Ce, Pr, Nd, Sm, Eu, Gd, Tb, Dy, Ho, Er, Tm, Yb, Sc and Y), high field strength elements HFSEs (Ta, Ti, Zr, Nb, Hf and Th) by ICP-AES. The key experimental parameters related to the proposed digestion protocol were optimized for achieving quantitative recovery (>95%). This procedure was validated through the analysis of granite based reference materials viz., JG-2, SARM-1 and NCSDC-73376. The developed method was applied to wide variety of granite samples of different geological origin for their economic viability with respect to TCEs. Taking into account the high cost of commercial digestion vessels, the in-house PTFE vessel design is simple, very efficient, cost effective and suitable for rapid digestion of complex geological matrices for the determination of wide variety of elements of highly technological relevance.

Communicated to ACS Journal Analytical Chemistry

3.37 Determination of trace elements in the Pb–Bi eutectic system by inductively coupled plasma quadrupole mass spectrometry after sequential removal of the matrix by precipitation

Lead and the lead–bismuth eutectic (LBE) system, an alloy of lead (~ 44.5%) and bismuth (~ 55.5%), are used as spallation targets in an accelerator driven system (ADS), in which the neutrons produced can be used either in sub-critical power reactor systems or in the long-lived actinide transmutation systems. The LBE system in general has Ti, Fe, Cu, Mo, Ag, Cd and Tl as impurities, which can lead to the formation of radiotoxic nuclides and results in difficulties during the operation of the reactor. Likewise, steels used as structural materials coming into contact with the coolant comprise the transition elements, V, Cr, Mn, Fe, Ni, Cu, Nb and Mo, the common alloying elements in high alloy steels, which may cause corrosion. It is thus essential to determine these elemental contents for the suitability of the LBE system. A simple method was developed for the separation of trace element impurities in the lead–bismuth eutectic (LBE) system followed by their determination using ICPQMS. The matrix components, Pb and Bi, were separated by sequential precipitation after sample dissolution in nitric acid. Pb was precipitated as lead(II) chloride followed by Bi as bismuth(III) phosphate. The separation of both the matrix elements (Pb and Bi) was found to be >99%. The concentration of 14 elements (Rb, Te, Ba, Li, As, Cd, Zn, Ag, Cu, Mg, Co, Ni, Be and Mn) in LBE sample, present in the supernatant, could be determined with quantitative recoveries ranging between 85–100%. The developed method was applied to three lead–bismuth alloy samples and validated independently by a FI-ICPMS method.

Journal of Analytical Atomic Spectrometry 29 (2014) 1720

4. Trace Elemental Characterisation of High Purity Materials

4.1 Development of analytical methodology for trace and ultratrace characterisation of ultrapure germanium

A wet chemical method was developed to characterize ultrapure germanium of 9N (99.9999999%) purity. In this method, matrix germanium is separated from all its impurities with matrix volatilization procedure. In this procedure, chlorine gas is generated in-situ and reacts with germanium solid material directly at the temperature of 230 ± 5 ^{o}C and separates Ge matrix as volatile $GeCl_4$ from all its impurities. Further modifications were done to the matrix volatilization setup earlier used for 8N pure Ge to further control the contamination of atmospheric gases to the 9N pure Ge sample during different stages of matrix volatilization procedure. After modifications, the method provides sub parts per billion and parts per trillion levels of process blanks and extremely low limits of detections. More than 60 elements were examined for their separation from Ge matrix using the method and found to be quantitatively separated. Determination of impurity concentrations was done by inductively coupled plasma quadrupole mass spectrometer (ICP-QMS) and high resolution continuum source graphite furnace atomic absorption spectrometer (HR-CS-GFAAS). In the absence of certified reference materials for ultrapure germanium, accuracy of the present method is established by spike recovery tests. Precision of this method is between 4 to 10% for impurity concentrations from 0.28 to 0.011 ng g^{-1}. Limits of detection (LOD) are found to be between 4.6 – 0.005 ng mL^{-1} or 1.4 – 0.002 ng g^{-1} for the target analytes with this method. The wet chemical method was found to be useful for the characterization of ultrapure germanium material of 9N purity.

Different analytical methodologies for the determination of impurities in different high purity materials such as 6N pure Gallium, 7N pure Tellurium, 6N pure GaAs, 4-5N pure Antimony were also done.

Atomic Spectroscopy 40 (2019) 1
Talanta 159 (2016) 14
Talanta 146 (2016) 259
Atomic Spectroscopy 34 (2013) 119

4.2 Determination of impurities in semiconductor grade chemicals

The high purity chemicals are utilized as precursors for thin film deposition in semiconductor industry. In the fabrication of microelectronic devices, current thin-film fabrication techniques require ultra-high purity precursors for depositing specific films. As device densities increase and critical dimensions decrease, electrical requirements of constituent thin- films become increasingly critical. Dielectric films used to insulate gate and multi-level interconnect structures are commonly formed of silicon dioxide (SiO_2) and must possess specific electrical properties. To reliably and reproducibly achieve such electrical properties, the precursors used to deposit the corresponding silicon dioxide thin-films must be of ultra-high purity. Hence high purity chemicals are produced for electronic industry. Therefore, it is very essential to characterize these chemicals for their ultratrace level impurities for their utility in final applications in semiconductory industry. Since the impurity levels are present at ppb and sub-ppb levels, very sensitive analytical instruments are required for their characterization. Hence, GF-AAS is a sensitive analytical instrument for determination of analytes at ppb and sub-ppb levels. The

indigenously prepared high purity chemicals such as Hydrochloric acid, Methanol, Hydrogen peroxide, Ammonium hydroxide, Isopropyl alcohol (IPA), Phosphoric acid, Sulphuric acid, Ethylene glycol, Alkaline water, Tetraethylorthosilicate (TEOS), Tetramethylammonium hydroxide (TMAH), Choline hydroxide, etc., were analysed by GFAAS for their critical impurities (around 20 elements in each sample) after optimising the instrumental parameters for each sample. Right from the raw chemicals to 12^{th} batch of indigenously produced chemicals were analysed by GFAAS.

Spectrochimica Acta Part B: Atomic Spectroscopy 180 (2021) 106184

4.3 Development of analytical methodology for the determination of trace and ultratrace impurities in high purity silicon carbide single crystals by GDQMS

Single crystal silicon carbide (SiC) is a strategic electronic material mostly used in the semiconductor industry. Moreover, it is highly chemical resistance and can also be used under extreme temperature conditions. The properties of single crystal SiC is greatly affected by the presence of various impurity elements. Therefore, there is a need for suitable analytical methods for quantitative determination of trace impurities for SiC single crystal technology. SiC being a refractory and highly chemical resistant material necessitates extreme chemical treatment for complete decomposition. The introduction of high alkali metal salt contents significantly limits its applications, especially for high purity materials (5N and above) and trace elemental analysis. Therefore, solid sample analytical technique such as Glow Discharge Quadruple Mass Spectrometry (GD-QMS) is preferred for trace element analysis for single crystals SiC. Therefore a GD-QMS method was developed for the quantification of trace and ultratrace impurities using secondary cathode method. A high pure copper plate (oxygen free copper) was used as secondary cathode for generating the glow discharge plasma as well as ionizing the silicon carbide sample. The RSFs of the analytes were generated using known values of constituents of a nickel based superalloy and used for the quantification of impurities in single crystal SiC.

4.4 Development of i*n-situ* vapour phase matrix/analyte volatilization system

For high-purity analysis, major source of contamination is caused by the reagents used for the dissolution of matrix. Existing vapour phase digestion (VPD) methods have certain disadvantages due to complicated set-up and special heating apparatus. NCCCM developed simple VPD systems operated at room temperature/on a water bath using commercially available vessels for analysis of various matrices. This VPD system ensured the reduction of reagent blank by up to 500 times, thus obviate the need of costly supra-pure grade reagents for sample digestion.

4.5 Room temperature isopiestic distillation of arsenic as $AsCl_3$ for analysis of As_2O_3

As_2O_3 is used as a precursor for the manufacture of semiconductor grade arsenic. Hence, it is essential to determine trace level impurities in As_2O_3, for which matrix separation with minimum contamination is desirable. Among the separation methods, matrix volatilization is commonly used due to retention of large number of impurities with lower blanks. Volatilization of arsenic as As_2O_3 or $AsCl_3$ from acid solution or acid vapours is reported at elevated temperatures. Major disadvantages of these procedures are the use of a complicated volatilization setup, loss of volatile elements, and higher blanks due to the use of large quantities of acids or its vapours generated externally. A method was developed for room-temperature *in-situ* vapour phase matrix separation followed by determination of impurities (22 elements) in the residual sample solution using ICP-AES. The vapour pressures of HCl and $AsCl_3$ were utilized for the removal of As_2O_3 by isopiestic distillation.

Analytical Chemistry 74 (2002) 6102

4.6 *In-situ* volatilization of borate ester for analysis of high purity H_3BO_3 and B_2O_3

Nuclear industries use boric acid in primary water systems of pressurised water reactors (PWRs), and the impurities present in H_3BO_3 affect reactor components. Boric acid is also a precursor for B_2O_3, which is being used as a network former in optical wave-guide, where stringent purity levels are required. In this method, H_3BO_3/B_2O_3 sample was placed in an inner vessel; while this container as a whole was placed in a closed outer vessel containing glycerol-methanol mixture. The set-up was heated over a water bath, methanol volatilized and reacts with H_3BO_3/B_2O_3 forming trimethyl borate. It is hydrolysed as boric acid by glycerol present in the outer vessel and the process is continued till complete volatilization of matrix. Methanol and glycerol function as carrier and sink respectively. Impurities present in the residual sample solution were determined by ion-chromatography for acetate, oxalate, sulphate, phosphate, Li, Na, K, Mg and Ca. The method detection limit is ranged from 0.3 to 8 ng g^{-1}. This matrix removal procedure allows determination of Al, Cd, Cr, Cu, Fe, Mg, Mn, Ni, Sb, Sn and Zn in B_2O_3 using GFAAS with fast furnace analysis (without an ashing step and modifier). The method detection limits for the impurities are in the range of 0.5 (Ni) and 2.9 (Al) ng g^{-1}.

Journal of Chromatogaphy A 1002 (2003) 137
Analytica Chimica Acta 546 (2005) 229

4.7 Multichannel Vapor Phase Digestion (MCVPD) of High Purity Quartz Powder

Since the past three decades, NCCCM is analysing raw and high-purity quartz samples (purification developed at NCCCM) for Gimpex Ltd Chennai. Supra-pure HF is very expensive and AR/GR grade could not be used due to the presence of impurities. We have developed a Multichannel Vapor Phase Digestion **(**MCVPD) set-up for simultaneous digestion of 21 samples in a closed chamber and achieved ~500 times reduction in blank values from AR grade HF. The accuracy of the results was validated by conventional dissolution with suprapur grade HF.

Atomic spectroscopy 24 (2003) 143

4.8 Determination of trace metallic impurities in high-purity quartz by ion chromatography (IC)

High-purity quartz is widely used to produce optical wave-guide, high performance lens, prisms, photovoltaic materials and for frequency control applications. Any trace impurities (Fe, Cu, Ni, etc.,) in this material strongly influences the quality of the final products. A method was developed for the determination of relevant trace impurities (alkali, alkaline and transition metals) in high purity quartz by ion-chromatography. *In-situ* reagent (HF) purification and simultaneous sample dissolution was achieved in a multichannel vapour phase digestion assembly. In the vapour phase digestion method, the blank level of NH_4+ reduced drastically by 250 times, thereby enabling the determination of trace level of impurities in high purity quartz. After volatilisation of the matrix, the clear water leached solutions were injected into an ion-chromatograph equipped with conductivity detector for the determination of alkali and alkaline earth metals. The transition metals separated on a mixed bed analytical column (IonPac CS5) was determined spectrophotometrically, after post column derivatisation using 4-(2-pyridylazo) resorcinol (PAR).

Journal of Chromatography A 1022 (2004) 25

4.9 Phosphorus determination in quartz and silicon

High-purity quartz is the basic materials for the manufacture of semiconductor-grade silicon, in which boron and phosphorus affect the semiconducting property. *In-situ* reagent purification, matrix digestion and oxidation of phosphorus to orthophosphate ion were carried out simultaneously in the VPD assembly using a mixture of HF, HNO_3 and H_2O_2. A drastic reduction (475 times) in phosphate blank from reagents (HF/H_2O_2) was achieved. The sample residues after the volatilisation of silica consisting of insoluble phosphate/fluoride salts of divalent and trivalent cations were solubilised by ion-exchange dissolution followed by PO_4^{3-} determination by IC. Accuracy was evaluated by analysing a CRM (silicon, NIST 57a). The method detection limit was 0.05 µg g^{-1}.

Journal of Chromatography A 1036 (2004) 223

SiO_2/Si sample was placed inside a polypropylene vessel containing 1:1 mixture of HF: HNO3. The closed vessel was heated on a water bath for sample digestion. The sample residue was treated with H_2SO_4 and $HClO_4$ followed by molybdate solution which results in formation of 12-molybdophosphoric acid (12-MPA). The ion-pair of 12-MPA with crystal violet was extracted into n-butyl acetate. Then organic layer in acetone is measured at 596 nm using spectrophotometer. No interferences due to F^-, Si and As up to 10^3 times the content of phosphorus is observed. LOD was found to be 0.066 µg g^{-1} and method was validated using a CRM (Si, NIST 57a).

Talanta 55 (2001) 501

4.10 Analysis of high-purity water, HCl, HF, HNO_3 and $H_2O_2$for ionic impurities by Ion Chromatography (IC)

The purity of reagents used in the wafer cleaning operation in semiconductor industries has a direct impact on device reliability. IC separation is a suitable analytical technique for the determination of various ionic species but suffer from high ionic matrices. *In-situ* matrix evaporation of high-purity acids based on isothermal distillation was achieved to avoid contamination from the laboratory environment. The solubility of water and acid vapours in glycerol due to co-association was utilized to achieve complete evaporation. A 50-fold pre-concentration with >99.9% matrix removal was achieved for the analysis of HCl, HF, HNO_3 and H_2O_2. The non-volatile ions NH_4^+, Li^+, Na^+, K^+, Mg^{2+}, Ca^{2+}, SO_4^{2-} and PO_4^{3-}were determined by IC. The detection limits were 6–130 ng/L.

Journal of Chromatography A 1050 (2004) 223
Chromatographia 66 (2007) 819

4.11 Determination of traces of low melting elements in high-purity Nickel

Nickel based super alloys, by virtue of their excellent high temperature properties coupled with corrosion resistance, have been widely used in jet engine, gas turbine engine components where high strength at high temperature is needed. Among the impurities in nickel based alloys, low melting elements such as B, As, Se, Te, Pb etc., are detrimental to the strength of high temperature alloys even when present at very low concentrations. Therefore, it is essential to determine traces of these low melting elements in nickel matrix. Hydride generation – AAS/ICP-AES are among the most sensitive techniques for the determination of traces of As, Se and Te. However, due to the strong interference of nickel in hydride generation process, it is difficult to analyze nickel matrices for low melting elements. A method

was developed for the determination of traces of As, B, Bi, Ga, Ge, P, Pb, Sb, Se, Si and Te in nickel matrix. The sample was dissolved in $HClO_4$ (150°C) and nickel was settled as crystalline nickel perchlorate [$Ni(ClO_4)_2$] on cooling. The $Ni(ClO_4)_2$ crystals were ultrasonicated and after the separation of [$Ni(ClO_4)_2$], analytes of interest were determined in the supernatant using ICP-AES.

Talanta 131 (2015) 505

4.12 Determination of Indium in high purity Antimony by GFAAS using H_3BO_3as modifier

The determination of traces of indium in high purity antimony is important in the microelectronics industry as it has detrimental effects on the performance characteristics of the end product. It was found that the negative influence of HF used for the digestion could not be eliminated by using stabilized temperature platform furnace (STPF) alone. Due to the high dissociation energy (D_0 = 506 kJ mol^{-1}) of indium fluoride, it is difficult to dissociate in the gas phase and hence is lost. In presence of HF, the universal Pd–Mg modifier also does not work satisfactorily. Additionally, rising corrosion and reduced tube lifetime were observed when the acid digested (HF-HNO_3) antimony solution was injected in to the platform. Improvement in platform life and elimination of interferences were achieved by the addition of boric acid as a chemical modifier together with ruthenium coating of the platform. A characteristic mass of 36 pg and LOD of 0.04 µg g^{-1} are obtained in the developed method. The developed method was applied to the determination of indium in real samples. The data obtained by this method were in good agreement with those obtained by ICP-MS.

Talanta 70 (2006) 602

5. Characterisation of materials by Ion Beam Analysis (IBA)

Ion beam analysis (IBA) is a class of non-destructive surface analytical technique, which is extensively used for compositional analysis of materials and is applied in the fields of materials science, environmental science, biology etc. The primary techniques encompassing IBA are (a) Rutherford Backscattering Spectrometry (RBS), (b) Elastic Recoil Detection Analysis (ERDA), (c) Nuclear Resonance Reaction Analysis (NRRA), (d) Particle Induced X-ray emission (PIXE) and (e) Particle induced γ-ray emission (PIGE). Energetic ion beams such as protons, α-particles and other heavy ions are employed as projectiles in these techniques. The requisite projectiles are generated by means of a charged particle accelerator.

The 3MV tandem accelerator along with experimental ports at NCCCM-BARC, Hyderabad, installed in the year 1995, is shown in figure 2 and a typical ion-matter interaction is schematically depicted in figure 3.

Figure 2: *3 MV Tandem Accelerator facility at NCCCM-BARC, Hyderabad*

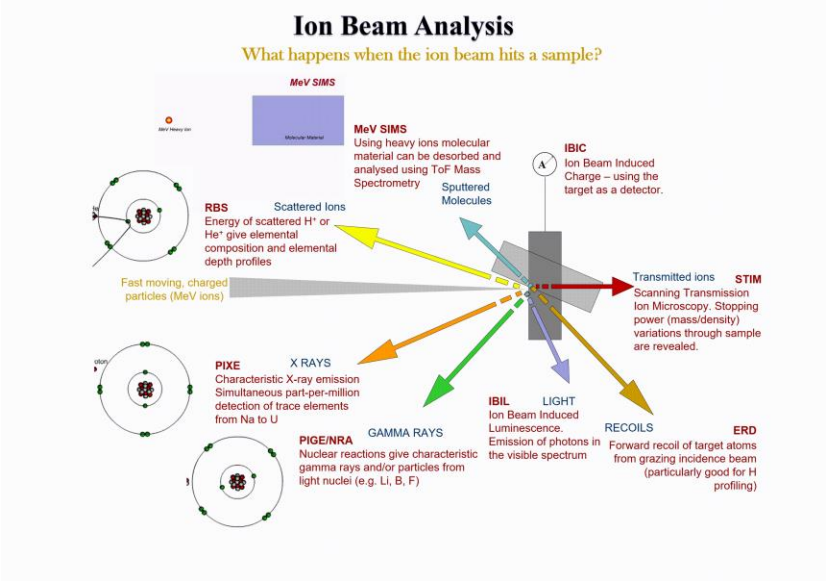

Figure 3: *Schematic of ion-matter interaction*

5.1 Characterisation of Optical Multi-layer Coatings

In a collaborative programme, we have characterised, using RBS, multi-layered optical coatings developed by Optics and Instrumentation Section, Spectroscopy Division, BARC, which find applications in high power laser systems and synchrotron beam lines. Characterisation of the coatings in terms of composition and thickness of individual layers, interfacial reaction or diffusion, presence of contaminants etc., was carried out. This analysis provides an exhaustive insight into their performance, which is useful in failure analysis and more importantly serves to optimize deposition parameters so as to prepare films with tailor-made properties. In the current work a 21-layer all-dielectric interference Fabry–Perot narrow bandpass filter was reverse engineered with the help of Rutherford backscattering spectrometry (RBS). The detailed geometries of the TiO_2 and SiO_2 layers, and their positions, thickness and substrate information can be very well observed in figure 4. Apart from investigating this 21 layered film, RBS experiments were also conducted to analyse a 41 and 43 layered HfO_2 and TiO_2 multilayer coatings from BARC.

Applied Optics 52 (2013) 2102

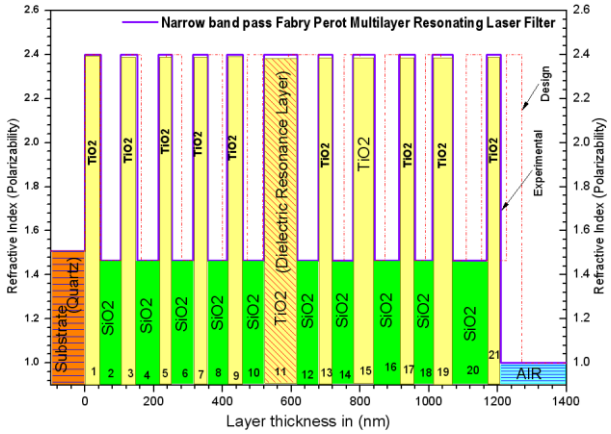

Figure 4: *Schematic depiction of the determined SiO_2/TiO_2 multilayer coating on SiO_2 substrate*

5.2 Multilayer coatings for space applications

Thickness determination of metallic multilayer coatings from M/s. Astra Microwave Products Limited was carried out by RBS. These coatings find applications in space technology. The measurements were carried out using 3.2 MeV proton backscattering spectrometry to determine the thickness of individual layers in multi-layered (Au/Cu/Au) coatings on Al_2O_3 and Ni substrates.

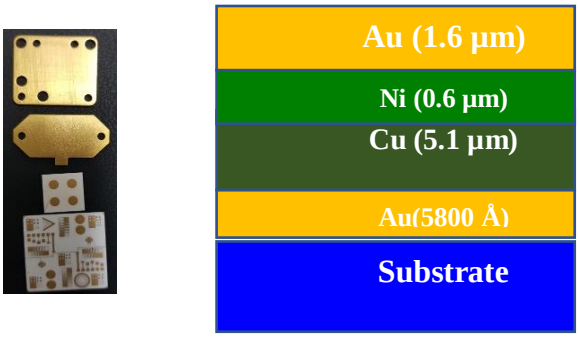

Figure 5: *Layer structure of metallic coatings on Al_2O_3*

The samples consisting patterns of multi-layered structures were analysed by directing a beam of 0.5 mm diameter onto the patterns. The experimental data was fitted with SIMNRA to obtain thickness profiles. The figure 5 shows the patterned multi-layered coatings and the corresponding experimentally determined layer structure.

5.3 Determination of thickness of gold coatings on contactors of micro-switches

Backscattering spectrometry experiments were carried out on the contactors of micro-switches. The micro switches consist of gold coated contacts of 2.0 mm diameter (Figure 6). The gold coating was applied on the contactors for the effective electrical contact. The quality check of the micro-switches was ascertained by carrying out the thickness determination of the gold coatings. To determine the thickness of gold coating a proton beam of 0.3 mm diameter was precisely directed on the 2.0 mm contacts. The backscattered protons were detected using silicon surface barrier detector at 170°. The experimental data was fitted using SIMNRA to obtain thickness of the layers. The thickness of few of the gold coatings is below the specified value of 0.10 µm.

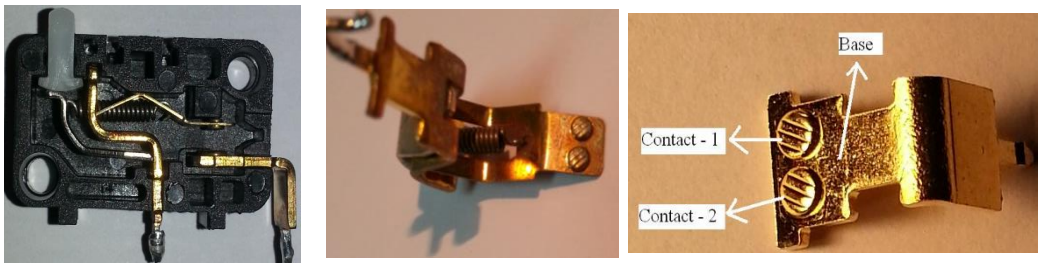

Figure 6: *Gold coated contactors in micro switches*

5.4 Multi-layered Antireflection Coating

Antireflecting (AR) coatings are used to improve the transmittance of visible and infrared radiations by reducing their reflection. Refractive index and thickness of an AR coating are two important considerations for obtaining improved transmittance of a radiation of desired wavelength. AR coatings can be single layered or multi-layered.

AR coatings are extensively used in military armaments. In one of the applications, these are integrated with devices in guided missiles to track the trajectory of enemy planes or missiles. AR coatings facilitate efficient transmission of infrared radiations emanated by the enemy planes, which is used in ascertaining their presence as well as location. In view of such sensitive applications, the exact nature of AR coatings is not discussed in open literature. ARCI, Hyderabad has approached NCCCM for the analysis of such AR coatings of anonymous nature. Except for the composition of the substrate (ZnS), no *a priori* information on the nature of coating was available.

A systematic approach was adopted to unravel the layer structure of the antireflection coating by utilizing the specific features of different IBA techniques. Examination of the specimen by PIGE technique revealed that F is one the major constituents of the coating. Composition analysis was carried out by PIXE. The studies revealed the presence of Ti as one of the constituents, however no other information could be discerned due to a high background resulting from the elements comprising the substrate i.e. Zn and S. In view of the crucial information provided by PIGE about the presence of large content of F in the coating, depth profile measurements of F were carried out in an attempt to ascertain its

distribution across the layer. These measurements were accomplished by nuclear resonance reaction analysis (NRRA) involving $^{19}F(p,\alpha\gamma)^{16}O$ reaction.

Since, RBS is eminently suitable for the analysis of single or multi-layered coatings in terms of their composition and individual or overall thicknesses; this technique was also adopted for the characterisation of AR coatings on ZnS. From RBS measurements the presence of Hf was inferred and the same was confirmed by PIXE measurements on scraped powder of the AR coatings. To establish the position of different layers in the specimen, 3.6 MeVα-RBS spectra of the same was recorded at different tilt angles. Tilting of the specimen results in increased thickness of the layers, as seen by the beam, by a factor of *1/cos (tilt angle)*. Consequently the variation in the measured energy of a peak at a particular tilt angle with respect to zero tilt (normal incidence) is expected to be in accordance with the position of corresponding layer in the coating. In other words, there would be no difference in the energies pertaining to surface layer while it would be the maximum for the most buried layer. Based on the RBS experiments at two different tilt angles, the positions and the thickness of the layers were determined. By means of extensive IBA analysis involving PIGE, PIXE, NRRA and RBS the following (Figure 7) layer structure was proposed.

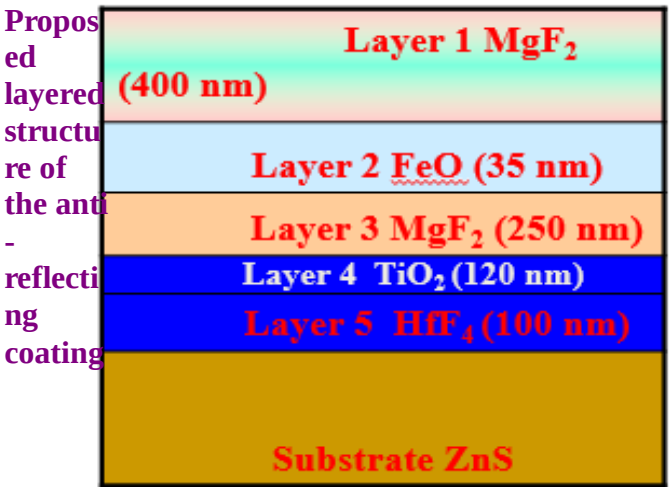

Figure 7: *The proposed layer structure using by IBA measurements*

5.5 Simultaneous determination of ^{14}N and ^{15}N isotopes in opium by particle induced γ-ray emission

The determination of the isotopic ratio of ^{14}N and ^{15}N, and $\delta^{15}N$ in turn, is useful in tracing and assigning the geographical provenance of bio-materials. A proton induced γ-ray emission (PIGE) method was standardized to determine $^{14}N/^{15}N$ isotopic ratio non-destructively in plants and subsequently extended to opium contrabands (powders) supplied by CFSL. The method involves the irradiation of the samples with 3.5 MeV protons and the measurement of 2.313 and 4.4 MeV prompt γ-rays emitted simultaneously from $^{14}N(p,p\gamma)^{14}N$ and $^{15}N(p,\alpha\gamma)^{12}C$ nuclear reactions respectively. The $\delta^{15}N$ values in the samples ranged negative to positive, suggesting that the contrabands had different provenance. The methodology provides an easy, rapid and solid-state approach to determine the isotopic ratio of ^{14}N and ^{15}N and has been used for the first time in the analysis of opium. An improvement in the precision of the

measurement, which currently is about 8%, and analysis in conjunction with $^{12}C/^{13}C$ isotopic ratio would facilitate better data interpretation and rather unambiguous provenance.

Journal of Radioanalytical and Nuclear Chemistry 294 (2012) 127

5.6 Depth profiling of Li in electrode materials of lithium ion battery by $^{7}Li(p,\gamma)^{8}Be$ and $^{7}Li(p,\alpha)^{4}He$ nuclear reactions

Lithium ion battery (LIB) is one of the most widely used portable energy devices. It is a kind of electrochemical cell. Knowledge of the depth distribution of Li in the anode as well as the cathode of a LIB is essential for a comprehensive understanding of the working of the device. The studies also assist in devising strategies for improving its energy density and life expectancy. A proton induced γ-ray emission technique based on $^{7}Li(p,\gamma)^{8}Be$ proton capture reaction and a nuclear reaction analysis method involving $^{7}Li(p,\alpha)^{4}He$ reaction were developed and standardized for depth profiling Li. Depth profiling by $^{7}Li(p,\gamma)^{8}Be$ reaction is accomplished by the resonance at 441 keV and involves the detection of 14.6 and 17.6 MeV γ-rays, characteristic of the reaction, by a NaI(Tl) detector. The method has a detection sensitivity of ~0.2 *at.%* and enables profiling up to a depth ≥20 μm with a resolution of ~ 150 nm. Interferences from fluorine and aluminium are limitation of this depth profiling methodology. The depth profile measurement by $^{7}Li(p,\alpha)^{4}He$ reaction, on the other hand, utilises 2-3 MeV protons and entails the detection of α-particles at 90° or 150° angles. The reaction exhibits inverse kinematics at 150°. This method also suffers interference from fluorine due to the simultaneous occurrence of $^{19}F(p,\alpha)^{16}O$ reaction. The method is endowed with a detection sensitivity of ~ 0.1 *at.%*, a depth resolution of ~ 100 nm. While it can respectively probe a depth of ~ 30 μm and 5-8 μm in the absence and presence of fluorine in the material. Both methods yield comparable depth profiles of Li in the cathode (lithium cobalt oxide) and the anode (graphite) of a Li-ion battery. The method(s) is a suitable alternative to neutron depth profiling (NDP).

Nuclear Instruments and Methods in Physics Research B 400 (2017) 22

5.7 Analysis of samples by Proton Induced X-ray Emission spectroscopy (PIXE)

Proton Induced X-ray Emission spectroscopy measurements were carried out on medicinal plants, blood serum, kidney stones, plant samples, environmental particulate matter etc. The solid samples loaded into the scattering chamber were irradiated with 2.0-2.5 MeV protons and the characteristic X-rays emitted were detected using Si(Li) detector.

Nuclear Instruments and Methods in Physics Research B 343 (2015) 163

6. Development of Materials

6.1 Inter-diffusion and stability studies in W/Cr and W/Fe films

Plasma facing components in fusion reactors are subjected to high energy neutron flux and intense thermal loads. Under these conditions, constant sputtering at the surface and the out diffusion of light elements takes place. To investigate these competing processes bi-layer systems constituting W/Fe and W/Cr were sputter deposited on Si substrates and subjected to vacuum annealing at 373 K to 873 K for duration of 1-8 h. The inter-diffusion and depth profiles were investigated using α-EBS at 3.05 MeV and NRRA involving $^{52}Cr(p,\gamma)^{53}Mn$ nuclear reaction. The investigations have established the out diffusion of Cr and Fe to the top surface regions of W. The GIXRD measurements have corroborated the IBA findings and further showed that no new additional intermetallic phases are formed. The AFM measurements un-ambiguously showed grain growth. The diffusion coefficients were determined to be 8.0×10^{-19} m^2/s at 873 K and 9.75×10^{-18} m^2/s at 773 K for Cr and Fe respectively.

Nuclear Instruments and Methods in Physics Research B 518 (2022)41

6.2 Investigations on the oxidation of zirconium nitride films in air

Thin films of transition metal nitrides such as TiN and ZrN find applications in tribology, microelectronics (as diffusion barriers) and decorative coatings due to their high hardness, chemical inertness, excellent wear resistance and prominent colouration in the visible wavelength region. In these applications thermal stability of the coatings is an important consideration, particularly in conditions wherein they are exposed to oxidative environments at high temperatures.

The thermal oxidation of DC magnetron sputter deposited thin ZrN films in air for the temperature range of 373 K – 750 K was studied by depth profiling N using nuclear reaction analysis (NRA) involving $^{15}N(^1H,\alpha\gamma)^{12}C$ resonance reaction and O using 3.05 MeV $^{16}O(\alpha,\alpha)^{16}O$ resonant scattering. The structural and morphological changes accompanying the process were also investigated. NRA and backscattering spectrometry measurements shows the formation of $ZrO_{1.8 \pm 0.1}$ at the surface due to oxidation. An interface consisting of Zr, O and N is also formed underneath the surface oxide. For an isothermal annealing, oxide layer as well as interface exhibits parabolic growth with the duration of annealing. The diffusion of oxygen through the already grown oxide layer ($D = 5.6 \times 10^{-14}$ cm^2 sec^{-1} at 475°C) forms the rate-controlling step of oxidation.

Applied Surface Science 253 (2007) 7230

6.3 Development of hard and wear resistant coatings

Ceramic coatings of metal nitrides, carbides and oxides have been successfully used in diverse fields of applications. The cutting tool industry has employed these coatings to enhance the lifespan of the tools. Decorative hard coatings are used for scratch resistance and colouring in the jewellery industry. Thin films have also been utilised as diffusion barriers in semiconductor industry. In all these applications, the deposition of inert coatings has resulted in a superior performance and higher reliability.

Various binary, ternary nitride coatings such as VN, TiN, CrN, ZrN, Ti-Zr-N, Ti-Al-N, binary carbide coatings like ZrC, TaC and NbC, multi-component alloy films like Ta-Nb-W were developed by an indigenously developed DC magnetron sputter deposition system for wear resistant applications. The performance of TaN films in Cu-metallisation was investigated for diffusion barrier applications.

Journal of Radioanalytical and Nuclear Chemistry 174 (1993) 265
Journal of Radioanalytical and Nuclear Chemistry 217 (1997) 293
Materials Letters 43 (2000) 73
Materials Letters 58 (2004) 2553

6.4 Synthesis of high quality binary, ternary and multinary sulphides powders for photovoltaic applications

Metal chalcogenides are an important class of materials with unique chemical, electrical and optical properties. Hence, they find applications in a wide range of fields that include catalysis, energy storage and conversion, and optoelectronic devices. Among chalcogens (S, Se, Te), sulphur is non-toxic, has the highest natural abundance and is the cheapest. As a result, sulphides have attracted considerable interest in recent years. Sulphur, like other chalcogens, forms binary, ternary or quaternary compounds with different metals.

CuS, In_2S_3, $CuInS_2$ and $CuGaS_2$ semiconductors were synthesised in powder form by precipitation reaction using $Na_2S{\cdot}3H_2O$ as a precipitating agent. Precipitated at about 313 K in aqueous medium, the powders of CuS crystallise in covellite (hexagonal) phase and those of In_2S_3, $CuInS_2$ and $CuGaS_2$ in tetragonal phase on heat treatment in argon atmosphere. The formation of CuS or In_2S_3 takes place due to the reaction between the metal and bisulphide ions in aqueous phase while that of $CuInS_2$ or $CuGaS_2$ involves solid state reaction between CuS and In_2S_3 or Ga_xS_y during heat treatment and is accompanied with the evolution of SO_2 gas. The powders are nearly monophasic, exhibit nanometric morphology and bear their respective stoichiometric compositions. The direct band gaps of CuS, In_2S_3, $CuInS_2$ and $CuGaS_2$ measured to be 2.06, 2.3, 1.34 and 2.38 eV respectively. The method is simple and was further extended to synthesize $CuIn_{0.8}Ga_{0.2}S_2$.

Materials Research Bulletin 79 (2016) 105

6.5 Development of a two-step thermal evaporation method for the preparation of thin copper indium sulphides films for thin film photovoltaics

Copper indium disulphide ($CuInS_2$) is an I–III–VI_2 compound semiconductor. It is a promising absorber material for thin film photovoltaics. It meets two important requisites of high solar energy conversion efficiency–it has a direct band gap of about 1.5 eV which perfectly matches the solar spectrum and is known to show high absorption coefficient.

We developed a physical vapour deposition method for producing $CuInS_2$ films with ~95% phase purity and, good optical and electrical properties. The method involves physical evaporation of a 1:1 mixture of copper sulphide (CuS) and indium sulphide (In_2S_3) powders by resistive heating followed by the vacuum annealing of the resulting films at 723 K produces $CuInS_2$ films with about 95% phase purity. Composed of sub-micron sized grains, the films bear stoichiometric or Cu-rich composition and are endowed with p-type conductivity, a band gap of about 1.5 eV and an absorption coefficient of about 4×10^4 cm^{-1} in visible region. Mechanistically, the formation of $CuInS_2$ films takes place as a result of solid state reaction among Cu_7S_4, InS and In_2S_3 in the condensed phase. These intermediate species are produced from the decomposition of $CuInS_2$ formed in the evaporating mixture due to the reaction between CuS and In_2S_3, and excess CuS. Process simplicity and the absence of a sulphurization step make this approach attractive for synthesising $CuInS_2$ absorber layers for photovoltaic applications.

Materials Research Bulletin 48 (2013) 2915

6.6 Development of Mg based thin films and bulk powders for hydrogen storage applications

IBA techniques were utilized to develop newer materials for storing hydrogen. Storage of hydrogen is the major impediment in realizing hydrogen economy. Hydrogen upon reaction with oxygen liberates tremendous amount of energy (120kJ/mol H_2) and water as a by-product. This released energy can be utilized either for transport applications or for power generation or for both (i.e. hydrogen economy). The conventional methods like compressed gas and liquid hydrogen storage methods are economically not viable as their gravimetric and volumetric efficiencies for hydrogen storage is very low. Moreover, safety and boil off are the other major issues with the compressed and liquid storage methods. In an attempt to address the hydrogen storage problem, solid state storage method is being extensively explored across the world and a tangible progress has been made in this direction. Amidst (Amongst?) ~~of~~ different metals/alloys as hydrogen storage materials, magnesium based materials exhibit superior hydrogen storage properties. Mg has 7.6 wt% hydrogen storage capacity on formation of stoichiometric MgH_2. However, MgH_2 has high thermodynamic stability, $\Delta H = -78$ kJ mol^{-1} H_2, which impedes desorption of H_2 with fast kinetics at low temperatures. On the other hand, numerous works were published on nanometric Mg/MgH_2 that exhibit fast hydrogenation/dehydrogenation kinetics at reduced/moderate temperatures. A work programme was initiated to develop Mg based materials with improved hydrogen storage properties and investigate their characteristics by IBA.

Pd-capped Mg thin films were prepared by thermal evaporation. The deposited Mg films consist of randomly oriented hexagonal platelets (Figure 8). These hexagonal platelets, defects such as grain boundaries and interfaces present in abundance, favour (de)hydrogenation. 7.6 wt% hydrogen storage

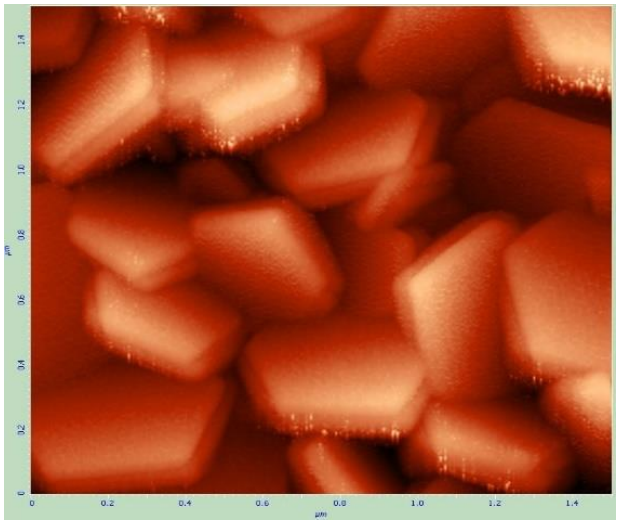

Figure 8: *Magnesium hexagonal platelets from AFM measurements*

capacity was achieved in Mg film. It is observed that the hydrogenation of Mg films involves grain boundary diffusion of hydrogen atoms. These films completely release hydrogen on dehydrogenation under dynamic rotary vacuum at 373K for 3 hours. XRD results show the formation MgH_2 phase on hydrogenation and conversion of hydride phase back to Mg phase upon dehydrogenation. The Pd/Mg films on glass substrate have shown switchable mirror properties i.e. the films which were highly

reflective/opaque before hydrogenation has become transparent after hydrogenation. Hydrogenation – dehydrogenation cyclic studies performed on these Pd/Mg films have shown that their performance is satisfactory.

Journal of Alloys and Compounds 476 (2009) 500
Journal of Alloys and Compounds 481 (2009) 714
Applied Surface Science 256 (2009)1553

6.7 Development of facile, green chemistry based synthetic protocols for nanoparticles (NP)

The nanoparticles synthesized by chemical methods are very popular and most of these protocols depend on organic solvents and toxic reducing agent usage. The chemicals employed for production are highly reactive, generate unwanted by-products and cause potential environmental and biological risks. However, the physical methods necessitate sophisticated equipment and stringent conditions and limited by low production rates, high energy consumption and high costs. When compared to physical and chemical synthetic protocols, the biosynthetic methods have received immense attention, contributing significantly towards the United Nations Sustainable Development Goals. The important features and advantages of biosynthesis are the renewability, biodegradability, biocompatibility, non-toxicity, lower cost and dual functionality (reductant and stabilizer) of biogenic resources, size and shape tailor-ability and protein capping mediated superior stability of NP at variable environmental conditions of temperature, pH and salt.

In this context, biosynthesis of metal (Ag, Au, Cu, Pd, Pt, Se), metal oxide (CuO, ZnO) and metal sulphide (CuS) NP was carried out using wide biological sources such as bacteria (*Escherichia coli, Pseudomonas aeruginosa, Bacillus cereus, Staphylococcus aureus*), leaf extracts (*Oryza sativa, Dendrophthoe falcata)*, seed extract (*Strychnos potatorum*), bulb extract (*Allium sativum)*, bacterial (*Xanthomonas campestris*) xanthan gum and plant and tree exudate gums, kondagogu(*Cochlospermum gossypium*), ghatti (*Anogeissus latifolia*), tragacanth (*Astragalus gummifer*), olibanum (*Boswellia serrata)*, biomolecules (bovine serum albumin, ascorbic acid, 4- amino hippuric acid) etc., by ambient stirring, sunlight irradiation, microwave heating and pressure cooker autoclaving. The biogenic nanoparticles are usually characterized by wide varieties of analytical techniques such as UV-visible absorption spectroscopy (UV-Vis) for surface plasmon resonance, transmission electron microscopy (TEM) for size and shape, X-ray diffraction (XRD) for crystal structure, Fourier transform infrared spectroscopy (FTIR) for functional groups of the biomolecules, thermogravimetric analysis (TGA) for thermal stability, zeta potential for surface charge, Raman spectroscopy for surface capping etc. The biosynthesized NP were utilized for multifaceted applications such as bactericide, fungicide, drug delivery agent, antioxidant, de-colourizing agent, metal sensor etc.

MethodsX, (11) (2023) 102438
Green Processing and Synthesis, 12 (2023), 20228138
Biointerface Research in Applied Chemistry 3 (2023) 1
Journal of Inorganic and Organometallic Polymers and Materials 29 (2019) 2054
IET Nanobiotechnology 3 (2019) 602
Arabian Journal of Chemistry 11 (2018) 313
Micro and Nano Letters 3 (2018) 1155
Bioresources and Bioprocessing 5 (2018) 1
IET Nanobiotechnology 11 (2017) 179
Journal of Environmental Management 181 (2016) 231
National Journal of Life Sciences 12 (2015) 127
The Journal of antibiotics 68 (2015) 88

IET Nanobiotechnology, 7 (2013) 83
Journal of Nanomaterials 2012 (2012) Article ID 869765
Process Biochemistry 47 (2012) 1516
Organic and Medicinal Chemistry Letters 2 (2012) 17
Journal of Biobased Materials and Bioenergy 6 (2012) 158
Carbohydrate Polymers 82 (2010) 670
Advanced Materials Letters 4 (2013) 548

6.8 Applications of green synthesized NP

a) Biogenic Ag NP as a bactericide and fungicide against plant pathogens

Bacterial leaf blight (BLB) and sheath blight (SB) of rice are the major destructive diseases of rice causing yield losses ranging from 20%-30% and 5%-50% in India, caused by bacterial plant pathogen *Xanthomonas oryzae* pv *oryzae (xoo)* and fungal plant pathogen *Rhizoctonia solani (R. solani)*, respectively.The biogenic Ag NP with an average size of 17 nm were synthesized with rice leaf extract were evaluated as fungicide and bactericide against these plant pathogens. The pots treated with Ag NP (15 µg/mL) *in vivo* under greenhouse showed BLB disease severity of 26.6% and % disease decrease over control of 49.2%, at a much lower NP concentration (15 µg/mL) than the previous studies. The Ag NP exhibited superior fungicidal activity (81.7%-96.7%) at a much lower concentration (10 µg/mL) than the other reported Ag NP, against *R. solani*. Thus, the present report demonstrates the effective utilization of Ag NP as microbicide towards phytopathogens under *in vitro* and *in vivo* conditions, implicating its field application towards the control and management of various plant diseases caused by pathogenic bacteria and fungi.

Bioprocess and Biosystems Engineering 44 (2021) 1975
Fungal Biology 124 (2020) 671

b) Biogenic Ag NP and Cu NP as bactericide against food and waterborne pathogens

The Ag NP (7.3 nm) synthesized by aqueous garlic extract under sunlight irradiation exhibited good antibacterial potential against both Gram-positive (*S. aureus*) and Gram-negative (*P. aeruginosa*) bacterial strains, as measured using well diffusion assay. Ag NP were stable for more than a year and retained their bactericidal potential.

Hexagonal Cu-BSA nanocomposite (Cu-BSA NC) (5 µm) consisting of embedded Cu NP (28 nm) were synthesized at pH 10 and stabilized by bovine serum albumin. Cu-BSA nanocomposite exhibited minimum inhibitory concentration of 50 µg/mL against *E. coli*. Nanocomposite caused irreversible membrane damage leading to leakage of intracellular metabolites and eventually death evident from TEM and cytoplasmic leakage analysis.

c) Metal NP as effective drug delivery vehicles for antibiotics

Highly stable, protein capped Au NP of 7.8 nm size were functionalized with aminoglycosidic antibiotics including, streptomycin, neomycin, gentamicin and kanamycin were utilized as drug delivery vehicles and evaluated against Gram-negative and Gram-positive bacteria. The antibiotic conjugated Au NP exhibited enhanced antibacterial activity, compared to pure antibiotic at the same concentration. The Au NP can act as effective carriers for drugs and might have considerable applications in the field of infection prevention and therapeutics. Also, the combined antibacterial activity of PVP capped Ag NP (16 nm) with selected antibiotics (streptomycin, ampicillin, tetracycline) was enhanced against both the Gram

classes of bacteria. The enhancement can be probably attributed to the steric stabilization of NP and improved bioavailability of the drug by PVP. The results of this study demonstrate potential therapeutic applications of silver nanoparticles in combination with antibiotics.

Gum kondagogu reduced/stabilized Ag NP (5.8 nm) were evaluated for their increased antibacterial and antibiofilm activities in combination with various antibiotics against *Staphylococcus aureus* and *E. coli* 25922, *P. aeruginosa*.The micro broth dilution assay suggested an enhanced antibacterial activity of Ag NP in combination with ciprofloxacin and aminoglycoside (streptomycin and gentamicin) antibiotics against tested strains. It was also found that Ag NP (1 μg/mL) in combination with various antibiotics at sub-MIC concentrations could inhibit 70% of the biofilm formation in bacteria as compared to the respective controls, due to the increased production of intracellular reactive oxygen species (ROS) in bacterial cells. The increased oxidative stress led to increased membrane damage and higher levels of potassium ion release from the cells. The results suggested that the combination of antibiotics with AgNP have improved the antibacterial effects and AgNP could potentially be used as *in vivo* antibacterial agents in combination with antibiotics to overcome the problem of antibiotic resistance.

Applied Nanoscience 5 (2015) 535
Bioinorganic Chemistry and Applications, 2013 (2013), Article ID 871097
Materials Science and Engineering C 32 (2012) 1571

d) Gum capped Se NP as an antioxidant

Selenium (Se) is an important metalloid micronutrient and a constituent of selenoenzymes, which protect the cells against the ROS mediated oxidative stress and damage. It is significant to note that the chemical form and dosage are the two key factors in determining the biological activity of Se. When compared to the ionic forms of Se [sodium selenite and selenium dioxide (SeO_2)], the nanoparticulate elemental Se is known to be a potent antioxidant. This is mainly attributed to the enhanced bioavailability and biological activity and reduced toxicity of Se NP.

In this scenario, gum kondagogu capped Se NP (106 nm) were studied for antioxidant potential utilizing *in vitro* radical scavenging assays. In comparison to ionic Se (SeO_2), the gum capped Se NPs exhibited superior 1,1-diphenyl-2-picrylhydrazyleand 2,2-azinobis-(3-ethylbenzthinzoline-6- sulphonic acid) radial scavenging activities of 73.2 and 92.2%, respectively, at 25 μg/ml. Se NP exhibited growth inhibition activity against *Bacillus subtilis* and *Micrococcus luteus* with respective inhibition zones of 6.3 and 8.6 mm at 12 μg. Thus, the present study demonstrates the applicability of tree gum stabilized Se NP as a potent antioxidant nutrition supplement at a much lower dose, in comparison with ionic Se.

IET Nanobiotechnology 12 (2018) 658

e) Biogenic metal NP as dye decolourizing agent

Various manufacturing industries such as pulp, paper, paint, printing, rubber, textile, plastic, leather, concrete, cosmetic, food, pharma, medical etc., employ vast quantities of synthetic dyes for multiple applications. These industries mandate large volumes of water use at different steps and generate enormous quantities of effluents contaminated with dyes. Presence of dyes in waters increases biological and chemical oxygen demand; drastically reduces sunlight penetration and decreases the photosynthesis of aquatic flora leads to reduced dissolved oxygen, reduced biodiversity and ecological imbalance in the native aquatic ecosystems. As the dyes are persistent, it may lead to bioaccumulation and biomagnification. Being a peril to aquatic organisms, the aesthetics of the water bodies are also affected making them unsuitable for human usage. This in turn demands the development of protocols for decolourization and removal of synthetic, toxic, persistent dyes from industrial effluents and their safer

discharge into aquatic bodies. Traditional wastewater effluent decolourization methods, such as sedimentation, flocculation, precipitation, membrane filtration, ion exchange etc., are not efficient due to complex molecular structure, degradation resistance of dyes; sludge formation and high process cost.

In this context, biogenic Ag NP (5 nm) and Pd NP (7 nm) were utilized as nano catalysts for dye decolourization of rhodamine B (RB) and methylene blue (MB). The effect of varying concentration levels of Ag NP (0.5-5 µg/mL), Pd NP (0.025-0.3 µg/mL) and RB (2.5-7.5 µg/mL) and MB (5-15 µg/mL);and reaction time (1-8/0.25-2 min) was investigated at ambient conditions. Ag NP and Pd NP showed corresponding rate constant (k) values of 0.189 min^{-1} and 0.367 min^{-1}; and 0.111 min^{-1} and 304 min^{-1} towards RB and MB, receptively. Thus, the decolourization capability of NP can have wide functions in the ecofriendly ecological remediation of diverse wastewaters contaminated with noxious, mutagenic, carcinogenic, dangerous dyes and pigments.

Arabian Journal of Chemistry 11 (2018) 1097
Industrial Crops and Products 81 (2016) 1
IET Nanobiotechnology 9 (2015) 362

f) Biogenic NP as a sensor for mercuric and aluminium ions

i. **Hg:** Mercury, a toxic heavy metal occurs in as metallic (Hg^0), inorganic (mercurous (Hg_2^{2+}), mercuric (Hg^{2+}) and organic mercury (methyl, ethyl, phenyl mercury) forms. Hg contamination in environment is due to anthropogenic cactivities and among the forms; Hg^{2+} is the most stable and exists in surface waters due to higher water solubility. Regulatory bodies, EPA and WHO stipulated the maximum permitted limits for Hg in drinking water as 10 nM and 30 nM. Excellent standard , selective and sensitive techniques used for Hg detection such as CVAAS, AAS/AES, ICP-MS, AFS, HPLC, ISE etc., are limited for routine detection due to the expensive and complex instrumentation, time-consuming sample preparation and preconcentration.

Pt NP: In this context, biogenic green Pt NP (4.4 nm) were utilized as Hg^{2+}colourimetric sensor based on peroxidase activity which catalyzes the oxidation of 3,3,5,5-tetramethylbenzidine (TMB) to a blue colour product, in the presence of H_2O_2. Peroxidase activity of NP was selectively inhibited by Hg^{2+}due to the formation of amalgam and the inhibition was not affected by other metal ions at 5 µM concentration. The decrease in oxidized TMB intensity at652 nm (blue colour), upon addition of $Hg^2$was linear in the range of 50-500 nM for MilliQ, tap and ground waters and the respective limit of quantification values were 16.9, 26 and 47.3 nM. The method was applied for the determination of Hg^{2+}in various ground waters and verified with CVAAS and is advantageous in terms of green nanozyme synthesis, smaller particle size, superior stability, lower nanozyme conc. and ease of detection. We envisage that the biogenic Pt NP based colourimetric probe can have promising applications in the screening and field detection of Hg^{2+}in various water bodies and public drinking water distribution systems and environment.

Sensors and Actuators B: Chemical 254 (2018) 690

Ag NP: A highly sensitive and selective method for the colourimetric detection of Hg^{2+} in aqueous system by using label free GK-Ag NP was developed. The bright yellow colour of Ag NP was found to fade in a concentration dependent manner with the added Hg^{2+} ions. This response was found to be highly selective for Hg^{2+} and unaffected by Na^+, K^+, Mg^{2+}, Ca^{2+}, Cu^{2+}, Ni^{2+}, Co^{2+}, As^{2+}, Fe^{2+}, Cd^{2+}, etc. The metal sensing mechanism is explained based on the turbidometric and XRD. The proposed method was successfully applied for the determination of Hg^{2+} in various ground water samples and also total Hg^{2+} in samples, wherein the organic mercury is first oxidized to inorganic form by UV irradiation. The limit of

quantification for Hg^{2+} was 50 nM. The proposed method has potential application for on-field qualitative detection of Hg^{2+} in aqueous environmental samples.

Talanta 118 (2014) 111

Cu NP: Cu-BSA NC based vapor generation approach as a simple, rapid, reliable and sensitive determination of mercury in waters was developed. Cu NP in the form of Cu-BSA NC acted as reductant for conversion of Hg^{2+} to Hg^0 at pH at ≥ 4.0 and 90°C, which was subsequently quantified using CVAAS and on-line flow injection ICPMS (FI-ICPMS). The absolute limits of detection of VG method in conjunction with FI-ICPMS were 2.8 pg and 4.1 pg for iHg and MeHg, respectively. The proposed VG method was applied to the analysis of total mercury in various natural water samples.

Journal of Analytical Atomic Spectrometry 29 (2014) 721

Au NP: Peroxidase mimicking activity of 4-aminohippuric acid (4-AHA) reduced/stabilized Au NP (5.9 nm) was selectivity enhanced in the presence of Fe^{3+} and Hg^{2+}, attributed to generation of hydroxyl radical and accelerated electron transfer. The assay was made selective for iron with cysteine addition in acetate buffer and selective for mercury was achieved with citrate buffer. The linear ranges for the determination of Fe^{3+} and Hg^{2+} in deionized water were 5-50 ppb and 5-200 ppb, respectively. The limits of quantification for Fe^{3+} and Hg^{2+} were 4 and 2.5 ppb, respectively. The assay was applied for the determination of Fe^{3+} andHg^{2+} in drinking and ground water samples. The method holds potential for the on-field screening of these metal ions in real environmental samples.

Spectrochimica Acta Part A: Molecular and Biomolecular Spectroscopy 228 (2020) 117805

ii. **Al:** A method for the selective and sensitive detection of Al^{3+} in aqueous systems was developed by the selective aggregation of ascorbic acid capped Au NP (AA-AuNP),evident from change in colour from bright red to purple decrease in characteristic absorption peak (520 nm) and emergence of second peak (652 nm) after the addition of Al^{3+}. The ratio of A652/A520 was used to quantify the Al^{3+}concentration and the method was linear from 20 ppb-100 ppb in drinking water with a detection limit of 6.5 ppb. The proposed method did not suffer any interference from concomitant transition metal ions (Mn^{2+}, Ni^{2+}, Zn^{2+}, Sn^{2+}, Li^{2+}, Co^{2+}, Hg^{2+}, Fe^{2+}, and Pb^{2+} at5 ppm) and anions (Cl^-, F^-, SO_4^{2-}, NO^{3-}, PO_4^{3-} at 250 ppm). However, Ca^{2+} (≥15 ppm) was found to interfere and the interference was eliminated by passing the water through an anion exchange oxalate resin. After the pre-treatment the linearity range in ground water was 100-350 ppb and LOD of 12.5 ppb. The simplicity and rapidity of the developed method shows great potential for screening drinking water samples for aluminium toxicity.

Sensors and Actuators B 248 (2017) 124

g) Biogenic Pd NP as colourimetric sensor for glucose and cholesterol

Glucose: Intrinsic peroxidase catalytic activity of GK-Pd NP was dependent on pH, temperature and NP concentration. The steady-state kinetic of GK-Pd NP followed typical Michaelis-Menten kinetics and showed good affinity towards H_2O_2 (K_m-23 mM) and TMB (K_m-195 µM). Based peroxidase activity, a simple and selective colourimetric assay for the determination of glucose and the assay had a linear range of 10-1000 µM and a detection limit of 6.0 µM. Use of GK-Pd NP in place of routine HRP makes the assay advantageous in terms of low production cost, easy room temperature storage and high stability.

The study opens up the possibilities of exploiting the peroxidase mimicking properties of GK-Pd NP in various other clinical and diagnostics as an efficient substitute for peroxidase enzyme.

Sensors and Actuators B 240 (2017) 1182

Cholesterol: Based peroxidase activity, the absorbance was proportional to the concentration of cholesterol over the range of 5-100 µM and the limit of quantification was 8.5 µM. The practicability of the assay in the detection of cholesterol in human serum was validated with clinical samples and has potential application in clinical diagnosis due to its selectivity and sensitivity.

Current Research in Biotechnology 3 (2021) 42

7. Quality Control Activities of NCCCM (ISO 17025 & ISO 17034)

Chemical metrology is an essential component of progress in industrial development of any nation. The National Centre for Compositional Characterisation of Materials (NCCCM), a division under Chemistry Group, is accredited for ISO 17025:2017 as a Testing Laboratory since 2009. And in the year 2018 NCCCM got the accreditation for ISO 17034:2016 as a Reference Material Producer by NABL, New Delhi. NCCCM management is committed to provide analytical data of highest quality using validated and appropriate methods for analysis and state-of–the-art instruments. It ensures consistent operation to meet customer needs. NCCCM provides specialized analytical services for the determination of constituents down to parts per billion levels in samples of different matrices, meeting the requirements of ISO 17025:2017 standard, which deals with the general requirements for the competence of testing and calibration laboratories. This objective is being catered to different government and private organizations. The laboratory regularly participates in proficiency testing programs, demonstrating the competence in the scope of testing. The laboratory conducts internal auditing, management reviews and intermediate checks periodically as per the ISO 17025 standard, to ensure the quality control of the testing activities (Table 2).

Table 2: *The testing activities under the scope of accreditation of ISO 17025:2017*

S. No.	Category	Matrix	Analyte parameter
1	Water	Water	pH, alkalinity, conductivity, Ca, Mg, Total hardness
2	Residues in water	Water	Cd, Cu, Pb, Mn, Hg, B, Fe, Zn
3	Ores & Minerals	Quartz	Al, Ca, Fe, Mg, K, Na, Ti
		Dolomite	CaO, MgO, Al_2O_3, Fe_2O_3, BaO, SrO
		Bauxite	Al_2O_3, Fe_2O_3, Cr_2O_3, SiO_2, TiO_2, MnO, MgO, V_2O_5, LOI
4	Metals & Alloys	Cast Iron	P, Si, Mn, Ti
5	Residues in Food products	Noodle Powder	Pb
		Tea powder	K, Mg, Ca, Sr, Ba, Al, P, Mn, Fe, Cu, Zn, As, Cd, Hg, Pb
		Wheat flour	Fe, Zn

The NCCCM management has committed to ensure and maintain quality aspects of Certified Reference Material production, storage and distribution and has documented policies and objectives. Its objective is to produce Certified Reference Materials (CRMs) for its intended use and conforming to ISO Guide 35 (statistics) and 31 (contents of certificates, labels) which will satisfy the customers and meet their needs. Materials produced will be of international quality and its process of production will meet the requirements of ISO 17034:2016 standard (Table 3).

Table 3: *The list of CRMs under the scope of accreditation of ISO 17034:2016*

S. No.	CRM	Analyte Parameter
1	Quartz	Al, Ca, Fe, K, Mg, Na, Ti
2	Noodle powder	Pb
3	Dolomite	Al_2O_3, BaO, CaO, Fe_2O_3 ,MgO, SrO
4	Bauxite	Al_2O_3, CrO, Fe_2O_3, MgO, MnO, SiO_2, TiO_2, V_2O_5, LOI
5	Tea Powder	Al, Ba, Ca, Cd, Cu, Fe, Hg, K, Mg, Mn, P, Pb, Sr, Zn

8. Environmental Analytical Chemistry

8.1 On-line speciation of inorganic arsenic in natural waters using polyaniline (PANI) with determination by flow injection-hydride generation-inductively coupled plasma mass spectrometry at ultra-trace levels

The toxicity of arsenic depends on its chemical form. The determination of inorganic arsenic species—arsenite [As(III)] and arsenate [As(V)]—in water/groundwater is very important in view of (i) their established toxicity through consumption of arsenic tainted water and, (ii) the various arsenic remediation technologies critically dependent on the predominant chemical form of arsenic in a particular water source.

As the concentration of arsenic species in natural water is at ppb levels and its ionization potential is high, special sample introduction methods are required to improve sensitivity for its determination by ICPMS. Hence a Flow injection Hydride Generation-ICPMS method was developed, which has the advantage of low volume sample introduction and offers the flexibility to include online separation techniques based on ion-exchange. Polyaniline (PANI) is well known for both its ion-exchange properties. A home-made PTFE micro-column loaded with polyaniline (50mg), prepared freshly by a chemical method was used for the on-line separation of As(III) and As(V). The species were determined using time resolved mode of data acquisition, by monitoring ^{75}As. The volume of sample injected was 100µl. As(III) elutes in void volume and As(V) is subsequently eluted using HNO_3. Both the species eluted within 3min. The detection limits were calculated to be 0.05 and 0.09 µg L^{-1} for As(III) and As(V) respectively and the precision (%RSD) at 1 µg L^{-1} level was found to be 2.0% for As(III) and 2.5% As(V). The method validation was carried out by analyzing two BCR groundwater certified reference materials, BCR609 and BCR610, certified for total arsenic. The developed speciation method has been applied to groundwater samples collected from West Bengal, India. The concentration of As(III) and As(V) in these samples ranged between 50-120 µg L^{-1} and 100-450 µg L^{-1} respectively.

Journal of Analytical Atomic Spectrometry 25 (2010) 1348

8.2 Development of on-line UV-induced volatile species generation for selenium speciation [Se(IV) and $SeCN^-$] by ion chromatography-inductively coupled plasma mass spectrometry in petroleum refinery wastewater

Selenite [Se(IV)] and selenate [Se(VI)] are the primary Se species reported in aqueous ecosystems, while selenocyanate [$SeCN^-$] is found at significant concentrations in petroleum refinery wastewaters. $SeCN^-$ is formed by the reaction of elemental selenium with cyanide in refinery wastewaters. The removal of selenium from oil refinery wastewaters is usually achieved by co-precipitation/coagulation, whose efficiencies depend on the species distribution. The US EPA has set a selenium regulatory discharge limit of 5 µg L^{-1} for wastewaters. As the toxicities of various species are different it is essential to determine their concentrations in industrial discharges and environmental water samples. An on-line UV-induced vapor generation method was developed that allows simultaneous conversion of [$SeCN^-$] and [Se(IV)] to volatile species for their subsequent determination by IC-ICPMS with improved detection limits. The species present in the sample were separated on an anion-exchange column using a step gradient with NaOH as the eluent, and were subsequently converted to their volatile forms by UV irradiation in the presence of a mixture of HCOOH–HNO_3 followed by determination using

ICP-MS. Employing a 200 µL sample injection loop, the species separation was achieved within 7 min and with the best detection limits achieved at 0.01 µg L^{-1} and 0.06 µg L^{-1} for $SeCN^-$ and Se(IV) respectively while the reproducibilities achieved for retention times and peak areas in the chromatograms were better than 1.3% and 5.0% respectively. The method was employed to study the quantitative speciation of selenium in three petroleum refinery wastewaters and the accuracy of the results was validated by two independent methods. In addition, the method was validated by analyzing a certified reference material BCR-713, wastewater effluent. Quantitative recoveries (>95%) were observed for both Se(IV) and $SeCN^-$ in refinery wastewater.

Journal of Analytical Atomic Spectrometry 32 (2017) 796

8.3 Determination of Selenium (IV) at Ultra trace Levels in Natural Water Samples by UV-assisted Vapor Generation - 'Collect and Punch' - Inductively Coupled Plasma Mass Spectrometry

A UV-assisted vapor generation combined with a sensitive 'collect and punch'- ICPMS method is described for the determination of Se(IV) at ultra-trace levels in natural water samples. Volatile Se species were formed by UV irradiation in the presence of formic acid. The vapors were collected in a glass chamber before injection into the plasma in the form of a plug. This arrangement provided a 6–7 fold enhancement in sensitivity compared with continuous vapor injection. A detection limit of close to 50 parts per trillion (0.05 µg L^{-1}) was achieved. A precision of 1.2% (RSD, n=6) was obtained for a 0.5 µg $L^{-1}$of Se(IV) solution. The method is specific for Se(IV) and was used for the determination of Se(IV) in tube well water samples of Punjab, India. The concentration of Se(IV) ranged from 0.5–5.0 µg L^{-1} in the water samples analyzed. The values obtained for Se(IV) by the UV assisted vapor generation method agreed well with the conventional HG-ICPMS method. However, the total selenium contents determined by HG-ICP-MS after reduction of Se(VI) to Se(IV) in many of these samples were greater than 50 µg L^{-1}, demonstrating that the major species in these water samples are Se(VI).

Atomic Spectroscopy 29 (2008) 129

8.4 A simple and rapid copper-assisted micro-precipitation method for the on-site separation of inorganic arsenic species in water samples

A micro-precipitation procedure was developed using copper (Cu^{2+}) as precipitating agent for the separation–preconcentration of inorganic arsenic species (As(III) and As(V)) in waters prior to their determination by hydride generation atomic fluorescence spectrometry (HG-AFS). This procedure is based on selective precipitation of anionic species of As(V) with Cu^{2+}, leaving neutral As(III) in the filtrate. The complexation of As(V) with Cu(II) entails the precipitation as copper arsenate, $Cu_3(AsO_4)_2$ due to its low solubility product. Optimum conditions for efficient micro-precipitation process are; pH: 5 to 6, Cu/As mass ratio: 100, equilibration time: 2-3 min. and eluent volume: 2 mL of 0.03 mol L^{-1} HCl. A process time of 2 min. is enough for the on-site separation of As(III) and As(V) with the detection limits (LOD) 0.012 and 0.034 µg L^{-1} respectively. The recoveries were found to be in the range of 98-102%. This method was successfully utilized for the on-site separation of As(III) and As(V) in wide variety of water samples collected in and around Kiradalli Tanda village, Karnataka state, India, where severe arsenic-contamination exists in various water bodies.

Spectrochimica Acta Part B, 211 (2024) 106833

8.5 Dispersive liquid–liquid microextraction for simultaneous preconcentration of platinum group elements (Pd, Os, Ir, and Pt) and selected transition elements (Ag, Cd, Ta, and Re) at parts per trillion levels in water and their determination by inductively coupled plasma-mass spectrometry

The main emission source of platinum group elements (Pd, Os, Ir, Pt) (PGEs) and selected transition elements (Ag, Cd, Ta, Re) into the environment is due to increased anthropogenic activities due to rapid industrialization. Another significant source of environmental pollution with PGEs is hospital effluents, particularly those with chemotherapy departments, which find their way into municipal wastewater systems. The concentrations of PGEs in natural waters are generally in parts per trillion levels. An environmentally friendly procedure for the simultaneous determination of PGEs and selected transition elements of industrial importance in water was developed. The elements were extracted as their chloro and/or fluoro complexes by dispersive liquid–liquid microextraction (DLLME) and determined by ICPQMS. The anionic complexes formed in the presence of 1 mol L^{-1} HCl and 0.5 mol L^{-1} F^- were extracted into chloroform in the presence of Aliquat® 336 at room temperature. Analytes were back extracted from the chloroform layer with a mixture of perchloric acid and nitric acid for their determination by ICPMS. The preconcentration factors of the above elements ranged from 27–75 for 35 mL of water samples for determination by ICP-QMS. The limits of detection ranged between 0.04–0.3 ng L^{-1}. The proposed DLLME procedure was applied to the analysis of lake water contaminated with industrial effluents and hospital wastes, collected from different locations in Hyderabad, India. The concentration of Pt group elements ranged between 2 – 20 ng L^{-1}, while concentration of Cd was significantly higher in all samples (100-600 ng L^{-1}). The method was validated by comparing the results obtained by HR-ICPMS.

Journal of Analytical Atomic Spectrometry 31 (2016) 1131

8.6 Dispersive liquid–liquid micro extraction of boron as tetrafluoroborate ion (BF_4^-) from natural waters, wastewater and seawater samples and determination using a micro-flow nebulizer in inductively coupled plasma-quadrupole mass spectrometry

The potential sources of boron contamination in water are either anthropogenic (sewage effluents, boron enriched fertilizers, landfill leachates and discharge from soap and detergent manufacturing) or natural (e.g., water–rock interactions, sea water encroachment, mixing with fossil brines or hydrothermal fluids). Due to its interaction with the environment, the boron concentration in both drinking water and wastewaters should be limited. The WHO - maximum permissible limit of boron in drinking water is 0.5 mg L^{-1} and at 1 mg L^{-1} in the case of wastewaters. Thus the determination of boron content in different water resources is important. Boron, present in groundwater and seawater, is extracted as tetrafluoroborate anion by dispersive liquid–liquid microextraction (DLLME) and determined by ICP-QMS. In this method, the tetrafluoroborate anion formed in the presence of 0.9 mol L^{-1} H_2SO_4 and 0.1 mol L^{-1} F^- was extracted into chloroform in the presence of Aliquot 336 at room temperature. The bulky cationic surfactant, Aliquot 336, acts as a phase transfer agent, which not only forms an ion-pair complex with tetrafluoroborate anion but also helps in the rapid conversion of boric acid to BF_4^- ion. The tetrafluoroborate anion is back extracted from the chloroform layer with nitric acid for determination by ICP-QMS. Under optimum conditions, an average preconcentration factor of 18 was obtained for 8 mL of water sample, with a limit of detection of 0.3 µg L^{-1}. The precision was close to 3% RSD. The method was applied to determine boron in bottled mineral water, groundwater, wastewater and seawater samples.

The recoveries obtained for the boron spiked to 30 µg L^{-1} levels in these water samples were 97–102%. The method was validated using azomethine-H as the reference method.

Journal of Analytical Atomic Spectrometry 28 (2013) 142

8.7 Environmental screening, monitoring and detection of waterborne bacterial pathogens in Hussain Sagar lake

Hussain Sagar is a man-made lake originally designed for drinking water purpose that receives domestic sewage and industrial effluents through drainage canals due to rapid residential and industrial growth. Also, every year thousands of idols are immersed into the lake during festivals. In this context, a comprehensive study was initiated for monitoring the lake water quality and physico-chemical parameters such as temperature, pH, EC, TDS, COD and chlorophyll a were analyzed using APHA standard methods Water was also monitored for heterotrophic bacteria, total coliforms, *Escherichia coli* and antibiotic resistant bacteria. The average values for heterotrophs were found to be 8.6×10^4 and 2.8×10^4 CFU/mL before and after idol immersion, respectively. While the average values for total coliforms and *E. coli* were 5×10^4 and 5×10^2; 1.2×10^4 and 7.2×10^1 CFU/mL, for the respective sampling periods. The mean values for ampicillin and gentamicin resistant bacteria were 5.9×10^3 and 6.9×10^2; and 2.2×10^3 and 5.4×10^2 CFU/mL, respectively. It was found that TDS, COD and chlorophyll a values were decreased after idol immersion due to extensive cleaning. The statistical results showed no correlation between faecal bacteria and physico-chemical parameters and one way-ANOVA indicated statistically significant differences between the mean values of different sampling locations, with respect to COD and *E. coli* at 95% confidence. However, enormous load of coliforms and *E. coli* indicated severe contamination of the lake with domestic sewage and human excreta. Thus, the water is not suitable for human consumption/drinking purpose. Notably, incidence of antibiotic resistant bacteria in lake water is a potential threat to both public health and the environment. Thus, regular monitoring and applying appropriate corrective actions are needed to improve the water quality.

Water Science 31 (2017) 24

9. Analytical and Atomic Spectroscopy Studies using Lasers

9.1 Determination of isotope ratios in lithium by resonance ionization mass spectrometry

The selectivity of the isotope selective photoionization scheme due to narrow bandwidth of the excitation laser and isotope shift limits the measurements of isotope ratios using resonance ionization mass spectrometry. Spectral simulation method was utilized for the estimation of isotope selectivities and isotope ratio enhancement factors by taking into account the isotope shifts, bandwidth of the excitation laser, residual Doppler widths and abundance of the constituent isotopes for the $2s\ ^2S_{1/2} \rightarrow 4s\ ^2S_{1/2}$ two-photon transition in lithium.

A XeC1 excimer laser with a pulse repetition frequency of 200 Hz and pulse energy of 300 mJ was used to pump a grazing incidence dye laser. The dye laser beam was tuned to the two-photon resonance of lithium (571.0733 nm). An indigenously built Wiley-McLaren type linear time-of-flight mass spectrometer (TOF-MS) was utilized to mass separate the laser produced photo ions. Significant isotope selectivities for the ^{6}Li and ^{7}Li are achieved due to the larger value of two-photon isotope shift (14.65 GHz). By estimating the selectivity and isotope ratio enrichment factors, the ^{6}Li/^{7}Li isotope ratio was determined to be 0.0413 $\pm$ 0.009. The result was in agreement with the lithium isotope ratio value of 0.0407 $\pm$ 0.002 which was determined by inductively coupled plasma-mass spectrometry (ICP-MS).

International Journal of Mass Spectrometry and Ion Processes 173 (1998) 177

9.2 Development of resonance ionization mass spectrometer (RIMS) using high repetition rate DPSS pumped Ti:Sa lasers for low level detection of uranium

The determination of the isotopic composition of uranium is of immense importance in a number of fields like nuclear technology, environmental analysis after nuclear accidents and weapons tests and effluent/reprocessing control.

Analytical instrument for trace analysis of uranium based on resonance ionization mass spectrometry was developed. The RIMS instrument is developed by integration of three tunable high repetition rate pulsed Ti: Sapphire lasers, graphite crucible based atomizer and a time-of-flight mass spectrometer (TOFMS). In order to quantitatively determine various isotopes of uranium, mass resolution of ~600 is essential to completely resolve the neighbouring isotopes. By utilizing a delayed pulsed extraction method and optimizing the reflectron grid potentials a resolution >800 at the mass of 238 was achieved. Five two-colour resonant three-photon ionization schemes were investigated for their efficiency and spectral resolution. The optical selectivity of the isotopes of uranium as function of the excitation laser frequencies for different schemes was evaluated (Figure 9). Further, the saturation behavior with respect to the power of first excitation transition is investigated. Typically ~3 to 5 mW was sufficient to saturate the transition. The overall detection efficiency (ε_{RIMS}) of the developed resonance ionization spectrometer was determined to be ~1×10^{-10}. The ε_{RIMS} of the RIMS instrument is rather limited due to loss of atoms as oxide instead of free neutral atoms and non-resonant photoionization step. Assuming a total integrated counts of ~30 for unambiguous identification of the TOF signal due to RIMS, the detection limit was estimated to be ~ 10^{10} atoms or 3 *pg*, for the two-step resonant three-photon ionization scheme.

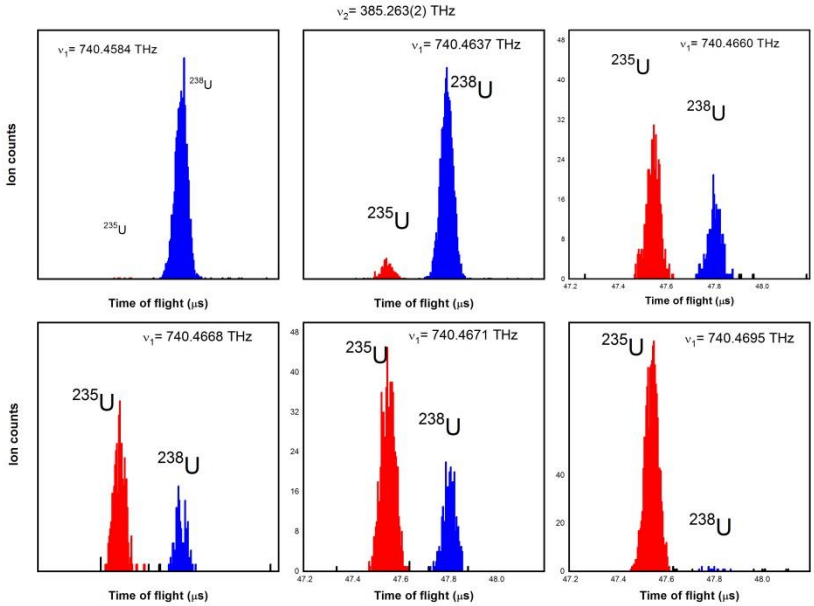

Figure 9: *The isotopic selectivity of ^{235}U isotope as a function of first excitation transition frequency*

9.3 Development of Laser Enhanced Ionization for trace level detection in flames

Laser enhanced ionization (LEI) in flames is capable of achieving very low detection limits for several elements. The basic principle of this technique relies on the increased collisional ionization of the atoms that are excited to higher levels by resonant laser radiation. Consequently, the impedance change within the flame is monitored by applying an electric field along the region of laser interaction. Excimer pumped pulsed dye lasers were tuned to the resonance transition of the analyte of interest to excite the atoms in the conventional air-acetylene flame. The laser beam interacts with the analyte atoms typically ~1 cm above the burner. By applying a voltage of -2000 V to the 0.6 mm thick SS plates (2.5 cm height and 10 cm length) as split cathode across the flame with burner head as anode, the change in impedance due to laser excitation is measured. A RC filter separates the LEI signal pulses from the DC background arising from ionization in the flame. Two-step LEI investigations were carried on sodium standard solutions. Good calibration was obtained for 1 ppb to 100 ppb range for aqueous standard solutions of Na. This technique was applied for the measurement of sodium in raw and purified quartz and the results of LEI were in agreement with that of flame atomic absorption spectrometry technique.

9.4 Development of high-resolution spectroscopic techniques for the measurements of isotope shift, hyperfine structure constants and absolute frequencies

In general, the Lorentzian line profile with the natural linewidth ($\delta\nu_n$) cannot be observed without special techniques, because it is more often than not completely concealed by other broadening effects. One of the major contributions to the spectral linewidth in gases at low pressures is the Doppler broadening, which is due to the thermal motion of the absorbing or emitting atoms. It is directly proportional to the square root of temperature and inversely proportional to the square root of mass. The first approximate of calculations show that Doppler broadening limits optical spectroscopy to a resolution ($\nu/\Delta\nu$) of $\sim 10^6$ even for heavy elements. The Doppler widths of atomic transitions are usually 100 or

1000 times larger than the natural width and in general, the fine spectral features of atomic transitions are obscured. Therefore, to overcome the limitation of Doppler broadening and achieve higher resolving power, techniques like (i) *Doppler-free two-photon Spectroscopy*, (ii) *Crossed atomic beam technique*, (iii) *Saturation absorption spectroscopy and* (iv) *Optogalvanic Spectroscopy* must be developed. Laser laboratory had developed these techniques and applied them to various atomic systems. In principle, measurements of isotope shifts and hyperfine structure of odd isotopes is carried out using a stabilized Fabry-Perot interferometer (FPI) as a marker cavity for calibrating the laser frequency scan. A simpler method of using an electro-optic modulator for frequency measurements was adopted. The calibration technique provides stability and precision without the exacting mechanical and thermal requirements associated with interferometric methods.

9.4.1 Development of Doppler-free two-photon spectroscopy

Doppler-free two-photon spectroscopy uses two counter-propagating laser beams for excitation. The atom perceives an equal and opposite Doppler shift for each beam and these shifts cancel out in the sum of the frequencies of the two counter-propagating photons absorbed by the atom. This absorption condition is independent of the atomic velocity and the absorption line is not broadened by the Doppler effect. All the atoms absorb two photons at the same angular frequency and this produces a narrow resonance limited only by the natural width.

Very precise hyperfine constants of the alkalis are required for a large variety of atomic physics experiments. More accurate hyperfine structure measurements have revitalized their use in studies and tests of nuclear physics and fundamental symmetries in nature. Doppler-free two-photon spectroscopy technique was developed to precisely measure the absolute frequency, isotope shift, hyperfine structure constants of excited states in Na, K, Rb and Cs.

i. Isotope shift and hyperfine structure measurements of $4s\ ^2S_{1/2} \rightarrow 6s\ ^2S_{1/2}$ ***transition in Potassium***

The hyperfine splittings for the ^{39}K and ^{41}K isotopes and the isotope shift for the two-photon transition was measured using Doppler free two-photon spectroscopy in a reference gas cell. An electro-optic modulator based frequency calibration method was utilized. The resulting hyperfine splitting values of 418.2 (5) MHz and 230.4 (1.3) MHz for ^{39}K and ^{41}K isotopes respectively were found to be in agreement with previous measurements. From the hyperfine splitting measured (ΔHFS) and the known value of A ($4s\ ^2S_{1/2}$), the magnetic dipole constant of the 6s state A ($6s\ ^2S_{1/2}$) for the ^{39}K isotope and ^{41}K is determined to be 21.8(5) MHz and 11.8 (1.3) MHz which is consistent with the reported values of 21.81 (18) MHz and 12.03 (40) MHz respectively. The transition isotope shift for the two-photon transition was measured to be 500.8 (6) MHz. Our measured isotope shift is about 19 MHz lower than the previously reported value. Furthermore, the precision of the absolute frequency values for the two-photon transition was improved by about two orders.

Journal of Physics B: Atomic, Molecular and Optical Physics 44 (2011) 055003

ii. Measurement of the hyperfine splitting of the 9 $S_{1/2}$ level in Cesium by Doppler-free two-photon spectroscopy

The studies on the hyperfine structures for alkali atoms is always attractive in atomic physics, in particular the structures of cesium. A spectroscopy technique based on frequency calibration markers from 150 MHz free spectral range (FSR) confocal Fabry-Perot Interferometer (FPI) was adopted. The frequency separation between the hyperfine components was determined to be ~8754 (4) MHz. Additionally, by locking the laser to the hyperfine peak by phase modulating (PM) the RF side bands generated by passing the laser beam through a broadband electro-optic phase modulator (EOM) better precision is achieved. The experimental determination of frequency separation was utilized to calculate the magnetic dipole coupling constant (A) for the excited 9 $^2S_{1/2}$ state for the ^{133}Cs isotope to be 109.7 (5) MHz. The measured value for magnetic dipole coupling constant of 9s state was in good agreement with the only previously reported by femto second frequency measurement value of 109.93 (9) MHz carried out using stepwise excitation.

Optics Communications 285 (2012) 1838

iii. Precise measurement of the hyperfine structure of the 7d $^2D_{3/2}$ level in Cesium by Doppler-free two-photon spectroscopy

We utilized two identical Doppler-free two-photon spectroscopy setups by splitting the laser power equally into each of the Cs cells. The hyperfine separations were measured by locking the laser to one of the hyperfine transitions using a Doppler-free two-photon technique in the first cell and the precise frequency of the acousto-optic modulator (AOM) was measured. Another AOM in the path of the laser beam into the second Cs cell was utilized to scan the stabilized laser about the resonance of the neighboring hyperfine transition (i.e., another hyperfine transition). The AOM is locked to this neighboring component and thus difference in the two AOMs was utilized to measure the hyperfine separation between the two locked peaks. This technique enabled the direct measurement of the frequency separation between the two hyperfine transitions. The advantage of this technique is that, the systematic errors are minimized by varying the locking frequency across various components of the hyperfine spectrum. Both the hyperfine coupling constants (A and B) for the excited 7d $^2D_{3/2}$ state were determined. The results (Table 4) were in consistent with earlier measurements carried out by step-wise excitation through an intermediate state using radio-frequency phase modulation technique, femto second frequency comb technique and also Doppler-free two-photon spectroscopy.

Table 4: *Comparison of the measured A and B values with previous reports*

Hyperfine coupling constants		**Reference**
A (MHz)	**B (MHz)**	
7.38 (0.01)	-0.18 (0.1)	This work
7.36 (0.07)	-0.88 (0.87)	Appl. Phys. B (2011) 105:391–397

7.386 (0.015)	-0.18 (0.16)	Phys. Rev. A 81, (2010) 043840
7.36 (0.03)	-0.1 (0.2)	Phys. Rev. A 77, (2008) 062505

Phyical Review A 87 (2013) 012503

iv. Precision measurement of the hyperfine structure hyperfine structure of 8d $^2D_{3/2}$ state by radio-frequency phase modulation technique

The hyperfine structure in the *8d* $^2D_{3/2}$ state of ^{133}Cs isotope was measured using Doppler free two-photon fluorescence spectroscopy in a gas cell. The frequency separations between various hyperfine transitions were calibrated by the precisely imprinting radio-frequency sidebands to the fluorescence spectrum using an electro-optic modulator. The spectra recorded for the $6s\ ^2S_{1/2} \rightarrow 8d\ ^2D_{3/2}$ two-photon transition along with lower order and higher order sidebands generated by phase modulation at 70 MHz were utilized to measure the frequency separations between various hyperfine components. From the measured hyperfine separations between the adjacent components of the *8d* $^2D_{3/2}$ state of ^{133}Cs isotope, a set of coupled linear equations using the Casimir formula were obtained. Using the method of least squares minimization of the coupled linear equations the magnetic dipole coupling constant *A* and the electric quadrupole coupling constant *B* were determined. From the least squares minimization routine, the values 3.98 (0.01) MHz and -0.03 (0.09) MHz for *A* and *B* respectively were obtained. The deduced magnetic dipole coupling constant (A) value was thus by far the most precise and was in good agreement with the 3σ level with the earlier reported values. The electric quadrupole coupling constant (B) value for the 8d $^2D_{3/2}$ state was reported for the first time.

Optics Communications 320 (2014) 77

v. Measurement of Hyperfine structure of 4s $^2S_{1/2}$ state of sodium by Electro-Optic phase modulator technique

The hyperfine splitting of the 4S state of Na was precisely measured by Doppler-free two-photon spectroscopy technique. The Na vapour cell was heated to ~400^{o}C to increase the atom density in the cell. Free Spectral Range (FSR ~150 MHz) of marker cavity of confocal Fabry-Perot Interferometer(FPI) was measured by passing the laser beam through a broadband electro-optic phase modulator (EOM) and was found to be ~149.5(2) MHz. The electro-optic modulator phase modulates the Ti:Sa laser beam at a frequency of~ 66 to 75 MHz to produce sidebands and the number of sidebands depends on the rf-power coupled to the EOM. The peak center positions of the fluorescence spectrum and the cavity peaks of 150 MHz interferometer and its side bands were determined by fitting a multi-peak Lorentzian function. A non-linear least-squares curve fitting procedure based on the Levenberg-Marquardt residual minimization algorithm was used to identify the centers of the hyperfine transitions. From the repeated experiments carried out, the hyperfine splitting for the two-photon transition is determined to be ~ 682.4 MHz and the precision was ~300 kHz.

9.4.2 Development of crossed atomic beam fluorescence technique

A crossed atomic beam fluorescence technique is a simple and elegant technique to reduce the Doppler Effect on a transition. A thin vertical slit or a circular aperture collimates the atomic beam to give a small angular spread. The laser beam intersects the atomic beam at right angles and the emitted

fluorescence is detected perpendicular to both the atomic beam and laser beam. This technique was developed to carry out high resolution atomic experiments on Na, Rb, K, Yb, Eu, Sm and Ce.

i. Isotopic shift studies on first excited states of samarium (Sm) for laser based enrichment applications

Specific isotopes of samarium (Sm) (viz., ^{144}Sm, ^{149}Sm and ^{152}Sm) have important applications in medical and nuclear industry. Department of Atomic Energy (DAE) is actively pursuing multi-step laser based isotope selective ionization process of Yb, Sm and Lu isotopes. The fluorescence emitted from the excited atoms is detected as the laser frequency is scanned across the transition. A mode-hop free (MHF) scan of ~ 6 GHz was e carried out by varying the length of thermally stabilized reference cavity of the cw-ring dye laser. For the precise calibration of the laser scan, the cavity length of 750 MHz confocal Fabry Perot (FP) etalon was stabilized (locked) to a reference He-Ne laser frequency.

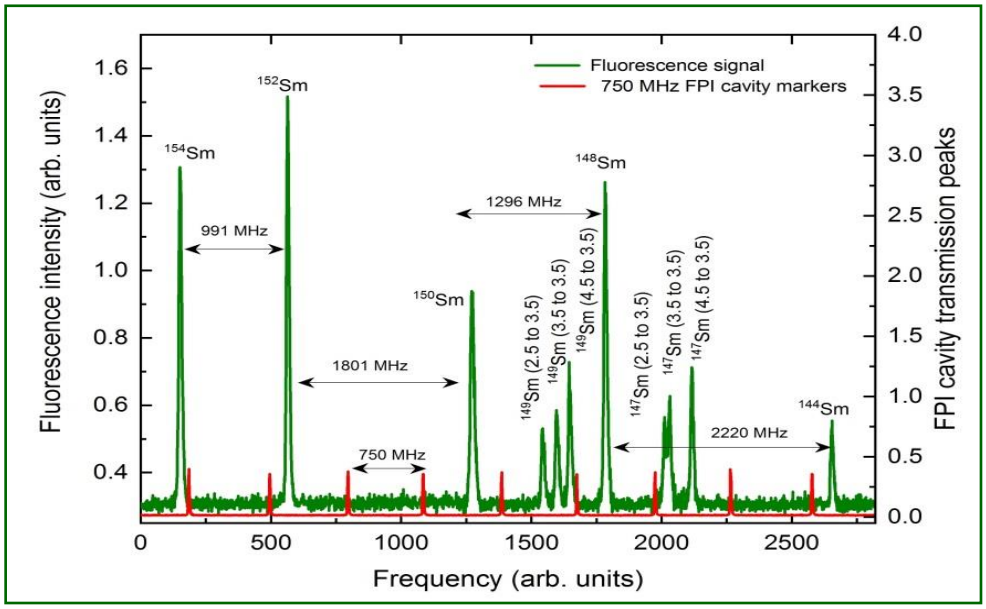

Figure 10: *IS and HF splitting in the Sm I 570.67nm line. The mass numbers of the isotopes are indicated. There are three HF components for each odd isotope (nuclear spin I = 7/2).*

The spectral width was estimated to be ~26 MHz and is dominated by the residual Doppler broadening determined by the collimator geometry (Figure 10). The excitation laser power was ensured to be very less so that the power broadening and optical pumping effects are negligible. By the precise calibration of the laser scan, the transition isotope shifts between various isotopes for about 15 transitions were determined with uncertainties ranging from 1 MHz to 3 MHz largely depending on the relative strengths of the peaks (A_{21} values) and also the Boltzmann distribution of the population in the lower level.

ii. Precision hyperfine structure and isotope shift measurements of the 601.8154 nm transition in Eu I

The atomic beam of Eu effusing out of the self-collimating graphite crucible maintained at 1200K is further collimated by a 75 mm long solid block collimator with an aperture of 7 mm placed at about 5 mm downstream. The atomic beam interacts with the laser beam in orthogonal direction. The fluorescence is imaged onto a photomultiplier tube from a directional orthogonal to both the atomic beam and laser beam propagation. The isotope shift of the 601.8154 nm transition and the hyperfine structure constants of the states involved in the transition for stable Eu isotopes were measured by a combination of AOM frequency locking technique and continuously calibrated wavemeter. The isotope shift between the ^{151}Eu and the ^{153}Eu isotopes is 3549.3 (5) MHz was determined with a higher precision. The values of the magnetic dipole constant (A) for the ^{151}Eu and ^{153}Eu isotopes for the $4f^7 6s6p$ ($^8P_{9/2}$) level were determined to be 664.73 (9) MHz and 295.15(7) MHz respectively. While, the values of the electric quadrupole constant (B) for the ^{151}Eu and ^{153}Eu isotopes were determined to be 290(3) MHz and 727(2) MHz respectively. The determined values of hyperfine structure constants for the ground state are consistent with the reported values by atomic beam magnetic resonance technique.

Journal of Quantitative Spectroscopy & Radiative Transfer 133 (2014) 251

9.4.3 Development of Saturation Absorption Spectroscopy

Saturated absorption spectroscopy is a simple and frequently used technique for measuring narrow-line atomic spectral features, from an atomic vapor with large Doppler broadening of $\Delta\nu_{Dopp}\sim$ 1 GHz. Two counter propagating laser beams (a weak probe beam and a strong pump beam) from the same laser are sent through an atomic vapor cell from opposite directions. As the laser frequency is scanned, the probe beam intensity is measured by a photo detector. The saturation absorption spectroscopy technique was developed and the high resolution spectra for Rb D1 and D2 isotopes were recorded. The spectral width (Figure 11) achieved was ~ 15 MHz. The spectral resolution ($\nu/\Delta\nu$) was improved to ~ 2.5 x 10^7.

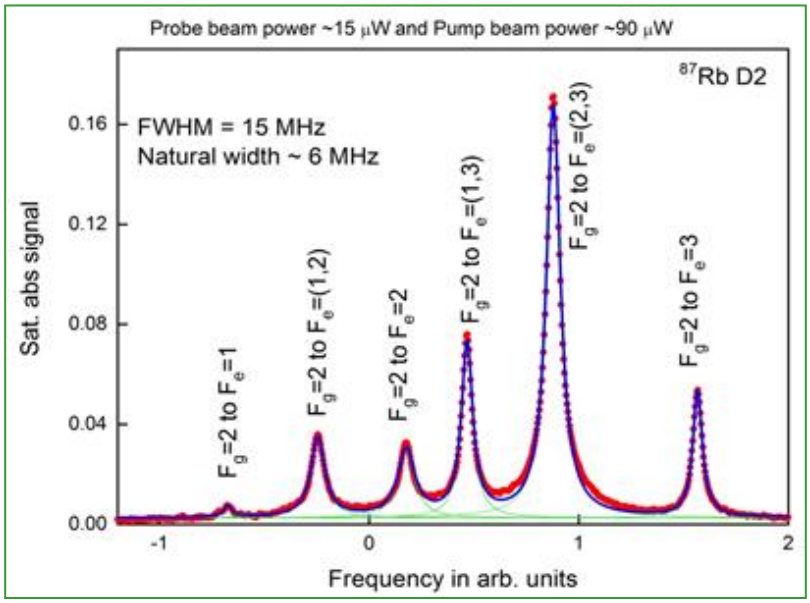

Figure 11: *Saturation absorption spectrum for D2 transition of ^{87}Rb isotope*

9.4.4 Development of Optogalvanic spectroscopy

Optogalvanic spectroscopy (OGS) is a simple and sensitive spectroscopic technique for investigating the electronic transitions in atoms and molecules. The impedance change in the discharge due to excitation of the sputtered atoms from the cathode or buffer gas atoms is measured by phase sensitive detection (PSD) using lock-in-amplifier (LIA). The necessary amplitude modulation is accomplished by modulating the excitation laser beam using a mechanical chopper or acousto-optic modulator (AOM) or alternatively by modulating the HCL source.

The absolute frequencies of the major hyperfine components of 579.13 nm transition in ^{139}La I were measured with an accuracy of ~50 MHz by frequency modulation of cw-ring Dye laser. The cavity length of a Fabry-Perot Interferometer (FPI) was locked to a stabilized He-Ne laser by phase modulating the He-Ne laser beam using an electro optic phase modulator. This stabilized FPI cavity was used to precisely calibrate the frequency scale of the optogalvanic spectrum for 579.13 nm transition in La I. Measurements to determine the hyperfine coupling constants (HCCs) for the lower and upper levels of the 579.13 *nm* transition were carried out and the determined HCCs from least squares fitting method were found to be consistent with earlier reported values. The necessary frequency discriminant signal for locking of the laser frequency was obtained by phase sensitively detecting variations in the impedance of the discharge due to laser excitation with a lock-in amplifier. Our experimental results in a closed-feedback loop to *cw*-dye laser indicate frequency instability of ~5-9 MHz. The OG technique gives the flexibility of accessing transitions originating from high lying metastable levels, thereby greatly enhancing the range of frequencies to which the laser can be locked. Therefore, the technique is suited for applications requiring laser stabilization in the visible region.

Applied Optics 20 (2021) 3430

9.5 Theoretical studies

High selectivity and efficient ionization through a multi-step (photon) excitation process involving a ladder of atomic transitions is feasible due to the availability of tunable lasers with narrow bandwidth and high spectral brightness. The potential application of multi-step photoionization of atoms by laser photons is Atomic Vapor Laser Isotope Separation (AVLIS) and detection of rare isotopes. Conversely, there is a growing demand for large number of enriched natural isotopes like (^{41}Ca, ^{90}Sr, ^{168}Yb, ^{176}Yb, ^{144}Sm, ^{149}Sm, ^{152}Sm, ^{176}Lu, ^{152}Gd, ^{155}Gd, ^{157}Gd and ^{102}Pd) as they have specific applications in the field of nuclear medicine and industry.

The selectivity in a multi-step excitation process has a complex interdependence on atomic and laser parameters, hence, a complete and realistic theoretical model is very essential to evaluate the suitability of particular excitation pathway for its best selectivity and ionization efficiency. Density Matrix Approach (DMA) is an elegant theoretical model that can realistically measure the observable quantities of a coherently or incoherently excited system of atoms and molecules. The numerical model based on DMA incorporates realistic experimental conditions by properly taking into account of the Doppler width, the angular distribution of atoms effusing from a collimated atom source, magnetic sub-level degeneracies, laser's temporal pulse and finite spectral bandwidth. These theoretical calculations provide foresight of the ionization lineshape dependency on the bandwidth of the excitation lasers and can assist one to optimize the intensities for best selectivity without sacrificing the ionization efficiency.

This numerical model is applied both to multi-step excitation involving single photon resonance and two-photon excitation schemes. We have derived optimum conditions for laser bandwidth, residual

Doppler width and intensities of the excitation and ionization lasers for isotope selective excitation of ^{91}Zr, ^{176}Yb and ^{168}Yb isotopes.

i. Isotope selective photoionization of ^{91}Zr

Zirconium has five naturally occurring isotopes. The only odd isotope, ^{91}Zr, has the largest neutron absorption cross section (1.2b) and accounts for ~73% of the thermal neutron absorption in natural zirconium. Zirconium depleted in the ^{91}Zr isotope is known to improve the neutron economy of reactors. Atomic vapor laser isotope separation (AVLIS) is the most attractive method for the selective removal of ^{91}Zr from the rest of the isotopes, since this requires the removal of the middle ^{91}Zr isotope. Therefore, optical selectivity calculations were carried out for the ^{91}Zr isotope for two-colour resonant three-photon photoionization schemes. The density-matrix equations of motion were solved numerically for collinear, counter propagating linearly polarized laser beams having Gaussian temporal profile. The selectivities and ion yields were determined for various Rabi frequencies and ionization rates. Thereby, the optimal Rabi frequencies for the first and second excitation steps and ionization rate for the ionization step were determined. The ionization efficiency as a function of detuning of the excitation lasers was also investigated. Two of the photoionization schemes investigated yielded a selectivity of ~10, with an ion yield of ~23%.

Journal of the Optical Society of America B: Optical Physics 20 (2003) 1807

ii. Isotope selective photoionization of ^{176}Yb

Ytterbium enriched in ^{176}Yb is used for the production of the ^{177}Lu radioisotope, which has applications in cancer treatment. A detailed theoretical study to evaluate the effect of the laser line shape on the excitation profile was carried out. Calculations were carried out to identify the optimized Rabi frequencies for evaluating the separation factor. The separation factor for various Doppler widths was evaluated, and it is found that even for Doppler widths as large as 500 MHz, a large separation factor for the ^{176}Yb isotope is feasible. Further, the separation factor for broader laser linewidths was also estimated, and even in such cases, appreciable loss in selectivity is not observed for laser linewidths as large as 500 MHz. From the theoretical studies, a large separation factor of ~5000 for the ^{176}Yb isotope was achieved.

Journal of the Optical Society of America B: Optical Physics 25 (2008) 1820

iii. Isotope selective photoionization of ^{168}Yb for an optical double-resonance (ODR) ionization scheme

^{168}Yb isotope is of great importance due to their applications in the field of nuclear medicine and industry. Naturally occurring Yb contains only 0.13% of ^{168}Yb, thus, the precursor to the reactor produced ^{169}Yb needs to be enriched by two orders of magnitude. With the optimization studies, the laser intensities of both the excitation steps for efficient and selective ionization of ^{168}Yb isotope are evaluated. The evaluated saturation intensities are in agreement with earlier reported experimental results. Quantitative estimation of interference of the neighboring isotopes on the selective ionization was carried out by taking into account the finite laser bandwidths. The dependence of Autler-Townes doublet peaks of neighbouring isotopes on the spectral bandwidth of the excitation lasers and their consequent influence on the ionization lineshape was investigated. The theoretical results indicated that the 91% degree of enrichment is feasible for the low abundant ^{168}Yb isotope with an ionization efficiency of $\leq$32%.

Journal of Quantitative Spectroscopy & Radiative Transfer 277 (2022) 107995

iv. Simultaneous non-selective excitation of plutonium isotopes

Additionally, this theory was also applied for simultaneous non-selective ionization of the Pu isotopes. Theoretical calculations were carried out for the non-selective excitation of the isotopes of plutonium for triple resonance excitation scheme with $\lambda 1 = 420.77$ nm, $\lambda 2 = 847.28$ nm and $\lambda 3 = 767.53$ nm. The isotopic bias between the resonant and off-resonant isotopes under the optimized conditions was not more than 3%. The threshold powers and bandwidth of the excitation lasers required for indiscriminate excitation of all the isotopes of plutonium in a three-step resonance excitation scheme were identified by using density matrix formalism. Maximum excitation efficiency was ~23% for the resonant isotope. Under the optimized conditions, the isotopic bias between the resonant and the farthest lying off-resonant isotope was ~3%. The optimized powers for the indiscriminate excitation of all the plutonium isotopes were 540mW, 250mWand 1138mW for the first, second and third excitation steps, respectively, while the bandwidth requirement of the excitation lasers is~10 GHz.

International Journal of Mass Spectrometry 254 (2006) 94

v. Optical selectivity calculations of ^{41}Ca and ^{90}Sr

Detection of rare calcium (^{41}Ca) and strontium (^{90}Sr) isotopes (abundance $<10^{-10}$) in the presence of an excess of major isotopes is of interest because of their applications in biomedical research, the nuclear industry, and environmental assessment. Numerical integration of the density matrix equations for double-resonance ionization were carried out by incorporation of the effects of Doppler broadening, velocity-dependent interaction times, time-varying Rabi frequencies, and laser bandwidths. The optimum conditions for selective excitation of rare isotopes were derived. The dependence of Doppler induced structures on the atomic-beam angular divergence and their influence on optical selectivity and ionization efficiency were investigated in detail. The studies resulted in five new photoionization pathways (two for calcium and three for strontium) whose optical selectivities were about 2 to 4 orders higher than the previously studied photoionization schemes.

Journal of the Optical Society of America B: Optical Physics 21 (2004) 1369

vi. Isotope selective near-resonant two-photon ionization of calcium isotopes

A near resonant two-photoionization scheme $4s\ ^1S_0 \xrightarrow{422.8nm,420.4nm} 4s10s\ ^1S_0 \xrightarrow{514.5nm} Ca^+$ was investigated for the isotope selective excitation of ^{41}Ca isotope for its applications as a tracer in bio-medical studies. The ionization efficiency and optical selectivity were calculated for various powers of the excitation and ionization laser. Under the optimized excitation/ionization laser powers the ionization efficiency and the selectivity for the studied scheme are found to be 1.3×10^{-4} and $\sim 1.0 \times 10^4$, respectively. The ionization efficiency is two orders of magnitude higher than the step-wise excitation process. In combination with a mass spectrometer, an overall selectivity of $\sim 10^{10}$ was obtained and is adequate for bio-medical applications

Journal of Physics D: Appl. Phys. 40 (2007) 288

10. Major Analytical Services

i. Sample analysis carried out for DAE Units

S.No.	Sample Name	Technique	Analytes	Application	DAE unit
1	^{10}B enriched B_4C powder	Titration, ICP-AES	Total boron, Al, Ca, Mg, Ni, Fe, Si and W.	Control rod for PFBR	MPD/BARC
2	BeO	ICP-AES	Al, B, Ca, Co, Cr, Cu, Fe, Li, Mg, Mn, Na, Ni, Si and Zn	Neutron moderator and reflector	PMD/BARC
3	B_4C+ZrO_2, BSiMoCrTi alloy	ICP-AES	B	Submarine project	MPD/BARC
4	B:Al:Zr	ICP-AES	B	Ceramic boride (shielding material)	MPD/BARC
5	U_3O_8 and $U_3O_8+ThO_2$	ICP-AES	Al, Ca, Cd, Cr, Fe, Mg, Mo	Reference Material	NFC and BARC
6	Cu, Zn, Co ores	ICP-AES and Spectrophotometry	Ge, Te, In & Ga	Exploration in ores	ACD/BARC
7	Uranium	ICP-AES	Fe, Ni, Cu, Mn, Si,Ta&W	Fuel	L& PTD/BARC
8	Pt-Ir alloy	ICP-AES	Pt-Ir-Rh	Super alloy	Isotope Division/ BARC
9	SiC	ICP-AES	Si	High temperature - nuclear material	MPD/BARC
10	Graphite	ICP-AES	B	Reference Material	ACD/BARC
11	Niobium	ICP-AES	Ta, Mo, W, Ti&Zr	Fuel cladding material	MPD/BARC
12	NdB_6	ICP-AES	Nd, B, W&Co	Strategic application	BARC
13	Filter paper	Ion Chromatography	F	Environmental monitoring	PMD/BARC
14	Silicon	ICP-AES	Al, Fe, Cu, Cr, Ag, Co, In	Semiconductor	HWD/BARC
15	BF_3-CaF_2	EDS	Si, Mg, O	Neutron Sensor	BARC

	Powder				
16	B_4C	PIGE	^{10}B, ^{11}B Isotopic Abundance	Control Rod	BARC
17	B_4C	PIGE	^{10}B, ^{11}B Isotopic Abundance	Control Rod	BARC
18	Graphite	NRRA	B	Nuclear Application	ACD/BARC
19	B_4C/Si	RBS	Thickness & Composition	R&D	BARC
20	ZrO_2+ B_4C pellets	PIGE	^{10}B, ^{11}B, B/C Ratio, Zr, Fe,F	R&D	BARC
21	Gadolinium Zirconate	PIGE, RBS	NbO_5	R&D	AFD/BARC
22	Air Particulate Matter samples	PIGE, PIXE	S, Cl, K, Cs, Ti, Cr, Mn, Fe, Co, Zn, Br, Pb	Environmental Studies	BARC
23	Zirconium Borides	NRRA, PIGE , RBS	Zr, B	R&D	Energy Conversion Materials Section, BARC
24	Transition element compounds	PIXE	Heavy Ions	R&D	NPD/BARC
25	NdF_3 films	XRD	Phase identification	R&D	BARC
26	Ag-VO_2 & AgO_2 Thin Films	RBS	Film Thickness	Optical coatings	BARC
27	Thin film HfO_2 on Si substrate	XRD	HfO_2 Phase	Optical applications	BARC
28	High purity Germanium (x4)	Matrix volatilazation, GFAAS, ICP-MS		Detectors	Chemistry Division/BARC
29	Single crystal Silicon	Matrix volatilazation, GFAAS, ICP-MS	B, Fe, Al, Mo, Au, Ni, K, W, Cr, Co, In, As, P, Ag	Integrated Circuits	HWD/BARC
30	Poly crystal Silicon	Matrix volatilazation, GFAAS, ICP-MS	B, Fe, Al, Mo, Au, Ni, K, W, Cr, Co, In, As, P, Ag	Integrated Circuits	HWD/BARC
31	Stainless steel rod	GD-QMS	All major and minor constituents	Hydrogen mitigation	BARC

32	Seawater (x7)	GFAAS	Be	Be processing plant	PMD/BARC
33	Filter paper (x3)	GFAAS	Be	Be processing plant	PMD/BARC
34	Sea sludge	GFAAS	Be	Be processing plant	PMD/ BARC
35	Water	GFAAS, Spectrophotometry	Cr(VI), phenol, pH, turbidity	NABL	BARC Canteen
36	UO_2/Cu/Ni coatings on inconel	RBS, XRD	Thickness and composition	Neutron sensing material, High temperature fission chambers (PFBR)	BARC/ECIL
37	Cu-Ag alloy Copper SS sheet Solder Al-alloy	ICP-AES	Cu and Ag P, Fe, Ni, Cu, Pb, Zn, As Si, Ni, Ti, Mn & Cr Pb, Sb	Neutron detector Quality control Quality control Quality control	ECIL
38	B_4C	ICP-QMS	$^{10}B/^{11}B$ Isotopic ratio; % ^{10}B Isotopic Abundance	Control Rod	ECIL
39	Tantalum	ICP-AES	Nb, Fe, Al, Cr and Mg	Fuel cladding material	NFC
40	Zr-Nb	ICP-AES	B	Coolant and Fuel cladding tubes	NFC
41	Clad Tubes	RBS	C-Thickness	PHWR Clad Tubes	NFC
42	Tantalum disc	GD-QMS	All major and minor constituents	Capacitors	NFC
43	Nb metal	GD-QMS	Trace and ultratrace elements	Zr alloy	NFC
44	Hard Faced SS Coupons	NRRA	B	Nuclear Industry	IGCAR & FCD/BARC
45	Sn-Bi alloy	Gravimetry and Titration	Sn and Bi	Liquid sealant for PFBR	IGCAR
46	Sb and Pb-Sb alloy	ICP-AES	Sb, As, Pb, Cu, Ni, Fe and Sn	Pb-Sb bricks for PFBR	IGCAR
47	Heating parts (Nichrome),	ICP-AES	Co and B	Inclined Fuel Transfer	IGCAR

	Insulator (MgO) and sheath (SS)			Machine (IFTM) of PFBR	
48	Ni- Samples	RBS	F depth profiling	Corrosion Test	IGCAR
49	Ni Samples	NRRA	F-depth profiling	Corrosion Test	IGCAR
50	(Ca/Sr)SiO3: Eu2+, LaF3, SrBPO5	XRD	(Sr/Ca)SiO3 Phase	Luminescence materials	IGCAR
51	Monazite	ICP-AES	Ce, La, Pr, Sm, Eu, Y, Gd, Dy, Tb, Ho, Yb&Lu	For recovery of REE	AMDER
52	Niobite and Tantalite	ICP-AES	Nb, Ta, Fe, Mn, Ti, W and Zr	Fuel cladding material	AMDER
53	Sillimanite	ICP-AES	Fe, Mn, Ti, Ba and Al	Refractory alumina bricks.	AMDER
54	Spodumene	ICP-AES	Li and Al	Li extraction	AMDER
55	^{10}B enriched B_4C pellet	Titration, ICP-AES	Total boron, Al, Ca, Mg, Ni, Fe, Si and W.	Control rod for PFBR	BHAVINI
56	Boric acid	ICP-QMS	$^{10}B/^{11}B$ Isotopic ratio	^{10}B enrichment	HWP & BHAVINI
57	^{10}B enriched Boron powder	Titration, GFAAS, ICP-AES, Spectrophotometry	H_3BO_3, boron, $^{10}B/^{11}B$, Al, Ca, Mg, Ni, Fe, Si, W, Cl and F	For production of B_4C powder	HWP
58	Neutral filter	ICP-AES	Pb, Fe, Cr, Al, Mo&Ce	solid-liquid separator.	HWP
59	SS	PIGE	B, N	Synchrotron beamline	RRCAT
60	Hydrogenated diamond like carbon (HDLC) films	NRRA	H Depth profiling	R&D	ACD/VECC
61	Zircon	ICP-AES and Spectrophotometry	Zr, Si, P, V, Nb, Ti, Al, Ca, Cr, Mg, Mn, Fe, Pb, Zn, Hf & Th	Zr recovery	IRE
62	Ni-Fe crystal	ICP-AES	Fe, Cu, Ni, Mn&Cr		IPR
63	Pb-Li alloy	ICP-AES	Li, Fe, Cu, Ni, Mn & Cr	Heat extraction in nuclear industry	IPR
64	Brass samples	PIGE, PIXE	Elemental profile	R&D	TIFR

ii. Sample analysis carried out for IAEA

S.No.	Sample Name	Technique	Analytes	Organization
1	Lichen	Flame AAS and ICP-AES	Na, K, Ca, Mg, Cu, Zn, Mn, Fe, Sr, Al and Hg	IAEA
2	Mosses	Flame AAS and ICP-AES	Na, K, Ca, Mn, Mg, Cd, Cu, Cr, Fe, Ni, Zn, Al , Co	IAEA
3	Coal fly ash	HG-Flame AAS and ICP-AES	Al, As, Ca, Cu, Cr, Fe, Mg, Mn, V, Zn	IAEA
4	Egg Powder	ICP-QMS	Ba, Cu, Mn, Sr, Zn	IAEA
5	Tuna fish	ICP-QMS	Cd, Pb, Cr, Cu, Mn	IAEA
6	Scallop Tissue	ICP-QMS	Cd, Cr, Cu, Mn, Zn	IAEA
7	IAEA-436, Fish Homogenate	ICP-QMS	Al, Cd, Cr, Cu, Fe, Hg, Li, Mn, Se, Sn, Sr, Zn	IAEA
8	IAEA-457, Sediment	ICP-QMS	Cd, Co, Sr, Ni, Mn, Zn, Pb, Cu, Cr	IAEA
9	Fish	GFAAS	Pb, Cd	IAEA

iii. Sample analysis carried out for other Government Industries / Institutions, Public Sector Units and Academia

S. No.	Sample	Technique	Analytes	Organization/Industry
1	Shape memory alloy	ICP-AES	Ni, Co, Cu, Cr, Fe and Nb	MIDHANI, Hyderabad
2	Fluorspar, ESR slag	ICP-AES	CaF_2, $CaCO_3$, CaO, SiO_2, Al_2O_3	MIDHANI, Hyderabad
3	Ti-6Al-4V	NRRA	O, H, N Depth Profiling	MIDHANI / VSSC, Hyderabad
4	Ni based superalloy	ICP-AES	Pb, Ag, In, Tl, Cu, Co, Al, Cr, Fe, Mo, W, Sn & Bi	DMRL, Hyderabad
5	SiC	GD-QMS	Trace and ultratrace elements	DMRL, Hyderabad
6	Ti alloy	GD-QMS	Ti, Zr, Ni, Cu, Mo	DMRL, Hyderabad
7	Ni-based Superalloys	GD-QMS	All major, minor, trace and ultratrace constituents/impurities	DMRL, Hyderabad
8	Bronze	ICP-AES	Zn, Pb, Sb, Bi & Fe	NFTDC, Hyderabad

9	Ni-Al Bronze	ICP-AES	Al, Fe, Ni & Mn	NFTDC, Hyderabad
10	Ti-Al-Nb	ICP-AES	Al, Fe & Nb	NFTDC, Hyderabad
11	Ti-Al-V	ICP-AES	Al, Fe & V	NFTDC, Hyderabad
12	Cu	ICP-AES	Zr, Cr	NFTDC, Hyderabad
13	$MoSi_2$	ICP-AES	Mo, Si, Fe, Al & Ca	NFTDC, Hyderabad
14	Graphite	ICP-AES	Zr, Cr&Cu	NFTDC, Hyderabad
15	ZnS	ICP-AES	Li, Cr, Al, Pb, Ni, Fe, Mn, Co &Sn	ARCI, Hyderabad
16	Yellow beads	GFAAS	Cd, Hg, Pb	CMET, Hyderabad
17	SiOCB ceramic powder	ICP-AES	Si & B	C-MET, Trissur
18	SiC	GD-QMS	Trace and ultratrace elements	SSPL, Delhi
19	Ti-Al-Sn Alloy	NRRA	H Depth Profiling	VSSC-ISRO, Trivandrum
20	Triple junction solar cells	RBS	Composition & Thickness measurement	ISRO
21	Graphite Anode and Cathode	XRD	Phase identification	ISRO
22	Copper disc	GD-QMS	All major and minor constituents	ISRO
23	H_2O_2	GFAAS	Al, As, Ba, Bi, Be, Ca, Cd, Co, Cr, Cu, Fe, Ga, K, Li, In, Mg, Mn, Mo, Na, Ni, Pb, Sn, Sb, Sr, Tl, V, Zn	SCL-ISRO
24	IPA	GFAAS	Al, As, Ba, Bi, Be, Ca, Cd, Co, Cr, Cu, Fe, Ga, K, Li, In, Mg, Mn, Mo, Na, Ni, Pb, Sn, Sb, Sr, Tl, V, Zn	SCL-ISRO
25	Acetone	GFAAS	Al, As, Ba, Bi, Be, Ca, Cd, Co, Cr, Cu, Fe, Ga, K, Li, In, Mg, Mn, Mo, Na, Ni, Pb, Sn, Sb, Sr, Tl, V, Zn	SCL-ISRO
26	Ethylene glycol	GFAAS	Al, As, Ba, Bi, Be, Ca, Cd, Co, Cr, Cu, Fe, Ga, K, Li, In, Mg, Mn, Mo, Na, Ni, Pb, Sn, Sb, Sr, Tl, V, Zn	SCL-ISRO
27	Ethyl lactate	GFAAS	Al, As, Ba, Bi, Be, Ca, Cd, Co, Cr, Cu, Fe, Ga,	SCL-ISRO

			K, Li, In, Mg, Mn, Mo, Na, Ni, Pb, Sn, Sb, Sr, Tl, V, Zn	
28	Tetramethyl ammonium hydroxide	GFAAS	Al, As, Ba, Bi, Be, Ca, Cd, Co, Cr, Cu, Fe, Ga, K, Li, In, Mg, Mn, Mo, Na, Ni, Pb, Sn, Sb, Sr, Tl, V, Zn	SCL-ISRO
29	N-methyl pyrrolidone	GFAAS	Al, As, Ba, Bi, Be, Ca, Cd, Co, Cr, Cu, Fe, Ga, K, Li, In, Mg, Mn, Mo, Na, Ni, Pb, Sn, Sb, Sr, Tl, V, Zn	SCL-ISRO
30	Photoresist	GFAAS	Ca, Cu, Fe, K, Na	SCL-ISRO
31	Tetra ethyl orthosilicate	GFAAS	Al, As, Ba, Bi, Be, Ca, Cd, Co, Cr, Cu, Fe, Ga, K, Li, In, Mg, Mn, Mo, Na, Ni, Pb, Sn, Sb, Sr, Tl, V, Zn	SCL-ISRO
32	Methanol	GFAAS	Al, As, Ba, Bi, Be, Ca, Cd, Co, Cr, Cu, Fe, Ga, K, Li, In, Mg, Mn, Mo, Na, Ni, Pb, Sn, Sb, Sr, Tl, V, Zn	SCL-ISRO
33	Ammonium Hydroxide	GFAAS	Al, As, Ba, Bi, Be, Ca, Cd, Co, Cr, Cu, Fe, Ga, K, Li, In, Mg, Mn, Mo, Na, Ni, Pb, Sn, Sb, Sr, Tl, V, Zn	SCL-ISRO
34	HCl	GFAAS	As, Fe, Na, Pb	SCL-ISRO
35	Choline Hydroxide	GFAAS	Al, Ca, Cr, Cu, Fe, K, Mg, Na, Ni	SCL-ISRO
36	ELM C30	GFAAS	Ag, Ca, Cr, Cu, Fe, K, Mg, Na, Ni, Pb, Zn	SCL-ISRO
37	MPS	GFAAS	Ag, Ca, Cr, Cu, Fe, K, Mg, Na, Ni, Pb, Zn	SCL-ISRO
38	PGMEA	GFAAS	Al, Ag, Cd, Ca, Cu, Fe, Pb, Li, Mg, Mn, Ni, K, Na, Zn	SCL-ISRO
39	HF	GFAAS	Al, As, Ca, Cr, Cu, Fe, K, Na, Mg, Ni, Pb	SCL-ISRO
40	Mixed nitric HF	GFAAS	Al, As, Ba, Bi, Be, Ca, Cd, Co, Cr, Cu, Fe, Ga,	SCL-ISRO

			K, Li, In, Mg, Mn, Mo, Na, Ni, Pb, Sn, Sb, Sr, Tl, V, Zn	
41	Hexamethyl disilazane	GFAAS	Ca, Cu, Fe, K, Na, Mn, Mg	SCL-ISRO
42	Cast iron	Spectrophotometry	P	Indian Railways
43	Pt-Rh	Spectrophotometry and Flame AAS	Pt and Rh assay and impurities (Pd, Au, Fe, Cu, Mn, Ca, Cr, Mg, Ni)	Rashtriya Fertilizer and Chemicals Ltd
44	Pd-Au	Spectrophotometry and Flame AAS	Pd and Au assay and impurities (Rh, Fe, Cu, Mn, Ca, Cr, Mg, Ni)	Rashtriya Fertilizer and Chemicals Ltd
45	Virgin Rhodium	Spectrophotometry	Rh assay	Rashtriya Fertilizer and Chemicals Ltd
46	Pd-Ni	ICP-AES	Pd, Ni and impurities	Rashtriya Fertilizer and Chemicals Ltd
47	Pt, Pd, Au and Rh	Spectrophotometry and Flame AAS	Assay and impurities	Rashtriya Fertilizer and Chemicals Ltd
48	Naphtha	ICP-AES, ICP-QMS, Spectrophotometry	P, Pb, Ni and V	National Organic Chemical Industries Ltd
49	Ti-Ni Films	RBS	Compositional Analysis	HAL, Bangalore
50	Ore	Flame AAS and Spectrophotometry	Au	NGRI, Hyderabad
51	Sludge leaching	ICP-AES	Zn, Fe, Mn&Mg	EPTRI, Hyderabad
52	Ore	Flame AAS and Spectrophotometry	Au	Commissioner of Mining, Gujarat
53	Ore	Flame AAS and Spectrophotometry	Au	Commissioner of Mining, Gujarat
54	Ni implanted Inconel & SS 316	NRRA	Ni depth profiling	IIT-Delhi
55	Ultrathin silicon nitride films	NRRA	N	IIT-Mumbai
56	TiO_2	RBS	Thickness & Composition	IISc-Bangalore
57	Depth profile of N in DLC films	NRRA	N	IISc-Bangalore
58	Ferrocene (FC) and FC grafted polymer	ICP-AES	Fe	University of Hyderabad (HCU)
59	GaN films	RBS	Thickness	Hyderabad Central

				University (HCU)
60	La magnite LaKNaLiMnAg Bi alloy	ICP-AES	La, K, Na, Li, Mn, Ag, Bi	Osmania University, Hyderabad
61	ZnO, CeO_2 and In_2O_3 films	XRD	zinc oxide & Cerium oxide Phase	Osmania University, Hyderabad
62	Alumina powder	ICP-AES	Al, Fe	BITS Pilani, Hyderabad
63	Medicinal plants	PIXE	K, Ca, Mn, Fe, Cu, Zn	Manipur University
64	Bacterial sample	ICP-AES	Fe	CDFD, Hyderabad
65	Bacterial pellets (x8)	GFAAS	K	CDFD, Hyderabad
66	Saliva	ICP-AES, Ion Chromatography	P, Mg, Ca, Na and K	Army Dental College, Hyderabad
67	Medicinal plants	PIGE	F, Na, Al, Mg, P	Manipal University
68	Polyimide and glass	RBS	Ag depth profile	University of Pune
69	Al_2O_3-TiO_2, Alunimna-SiO_2 powder samples	XRD	Phase identification	Tripura University, Agartala
70	Medicinal Powders	XRF	K, Ca, S, Se, P, Fe, Pb, Hg, Cr, Mn	Andhra University, Visakhapatnam
71	Rice Powders	XRF	K, Ca, S, P, Fe	Andhra University, Visakhapatnam
72	Fish tissue Powders	XRF	K, Ca, S, Se, P, Fe, Pb, Hg, Cr, Mn	Andhra University, Visakhapatnam
73	Ti-Ni films	RBS	Compositional analysis	PSG College, Coimbatore & DMRL
74	High Purity Chemicals	ICP-QMS	Multi-element	IICT, Hyderabad
75	Geological samples (water and process samples)	ICP-QMS	Rare Earth Elements	GSI, Hyderabad
76	Blood Samples	PIGE, PIXE	F	Osmania General Hospital, Hyderabad
77	H_2SO_4	GFAAS	Al, As, Ba, Bi, Be, Ca, Cd, Co, Cr, Cu, Fe, Ga, K, Li, In, Mg, Mn, Mo, Na, Ni, Pb, Sn, Sb, Sr, Tl, V, Zn	IICT-CSIR, Hyderabad
78	Trimethyl phosphate	GFAAS	Al, As, Ba, Bi, Be, Ca, Cd, Co, Cr, Cu, Fe, Ga,	IICT-CSIR, Hyderabad

			K, Li, In, Mg, Mn, Mo, Na, Ni, Pb, Sn, Sb, Sr, Tl, V, Zn	
79	H_3PO_4	GFAAS	Al, As, Ba, Bi, Be, Ca, Cd, Co, Cr, Cu, Fe, Ga, K, Li, In, Mg, Mn, Mo, Na, Ni, Pb, Sn, Sb, Sr, Tl, V, Zn	IICT-CSIR

iv. Sample analysis carried out for Private Industries

S. No.	Sample	Technique	Analytes	Private Industry
1	Quartz Purification			M/s. Gimpex, Chennai
2	Quartz	ICP-AES, Flame AAS	Na, K, Li, Ca, Mg, Al, Fe, Mn and Ti	M/s. Gimpex, Chennai Nanofold India, Bangalore
3	Barite	ICP-AES	Ba, Ca, Si, Al, Ti, Fe	M/s. Gimpex, Chennai
4	Litharge	ICP-AES	PbO, Pb, Pb_3O_4 , Al_2O_3, Cr_2O_3, Fe_2O_3 , ZnO, CuO, Ceramic and TiO_2	M/s. Videocon Narmada Electronics Limited, Baroda
5	Dolomite	ICP-AES	CaO, MgO, SiO_2 , Fe_2O_3, Al_2O_3	M/s. Videocon Narmada Electronics Limited, Baroda
6	Potassium carbonate	ICP-AES and Flame AAS	PbO, Cr_2O_3 , Fe_2O_3	M/s. Videocon Narmada Electronics Limited, Baroda
7	Sodium antimonate	ICP-AES and Flame AAS	PbO, Cr_2O_3 , CuO, Fe_2O_3	M/s. Videocon Narmada Electronics Limited, Baroda
8	Sand	Spectrophotometry and ICP-AES	Cl, TiO_2 , Fe_2O_3	M/s. Videocon Narmada Electronics Limited, Baroda
9	Zircon	Spectrophotometry and ICP-AES	ZrO_2 , SiO_2 , TiO2 , Al_2O_3 , Cl, Fe_2O_3	M/s. Videocon Narmada Electronics Limited, Baroda
10	Cerium oxide powder	ICP-AES, Gravimetry	CeO_2, CeO_2/REO,Nd_2O_3, La_2O_3,Pr_6O_{11},SiO_2,CaO, BaO, SrO, SO_3 , Fe_2O_3, Cl, Na_2O and Loss on ignition	M/s. Videocon Narmada Electronics Limited, Baroda
11	Zinc Oxide	Spectrophotometry	Cl	M/s. Videocon Narmada Electronics

				Limited, Baroda
12	Feldspar	Spectrophotometry	Cl	M/s. Videocon Narmada Electronics Limited, Baroda
13	Lead metal	Flame AAS	Fe, Cu, Zn	M/s. Videocon Narmada Electronics Limited, Baroda
14	Strontium carbonate	Spectrophotometry	Cl	M/s. Videocon Narmada Electronics Limited, Baroda Electronics Limited
15	Soda ash	Spectrophotometry	Cl,	M/s. Videocon Narmada Electronics Limited, Baroda
16	Haynes 188 alloy	ICP-AES	C, S, Mn, Cr, Ni, W, Fe, Co and La	Bharat Forge, Bangalore
17	Tantalum	ICP-AES	Mo, W, Ni, Fe, Mn, Nb, Ti, Cr, Ca, Al, Na & K	Anabond, Chennai
18	Fe-Mo FeSiMg Fe-Mo	ICP-AES and Spectrophotometry	P and Mo Mg, Si, Ca & Al Fe, Mo	Brakes India, Chennai
19	FeMo, Mo_2O_3, Mo_2O_5	ICP-AES	Mo, Pb, Cr & Ni	Brakes India, Chennai
20	Pb-Ca	ICP-AES	Ca	Elpro Ltd., Hyd.
21	Rare Earth fluoride, and oxide	Titration, Gravimetry and ICP-AES	Total Rare Earth Oxide, CeO_2, F, LOI	Schutz carbon, Gujarat
22	Hepatitis-B vaccine	CV-AAS, ICP-QMS and Ion Chromatography	Hg and Cs	Shanta Biotechnic, Hyderabad
23	Insulin	Flame AAS	Zn	Virchow Biotech, Hyderabad
24	Ayurvedic bhasmas	ICP-AES	Cu, Hg, P, Si, Zn, Pb, Fe, Al, Na, K	Central Council Ayur. Siddha
25	Ore	ICP-AES	Th, La, Nd, Zr, Ti, Pr, Ce	Star Earth Pvt Ltd. Taloja, Maharashtra
26	Cubic BN (cBN)	PIGE	B, N	Industry
27	Cu-Cr Blocks	PIGE, PIXE	Impurities Mg, Al, K, Ca, Fe, Ni, Rb, Sr, Zr	Crompton Greaves
28	Metallic Multilayer films	RBS	Au, Cu, Ni thickness	Asta Microwave
29	Graphite clothes	PIGE	Na	Advanced Systems Laboratory,

				Hyderabad
30	Nitride coated SS rods	NRRA	Nitrogen	M/s. Kumud Engineering, Hyderabad
31	Graphite samples	XRD	Phase identification	M/s. Munisofteck
32	Electrodes used in batteries	XRD	Graphite, $CaCO_3$, $CaO.SiO_2$ & (Fe_2O_3).	M/s. Munisoftek
33	Fluorinated HDPE bottles	NRRA	Fluorine Depth profiling	M/s. Bloom Packaging Industries, Mumbai
34	Surgical blades	NRRA	Fluorine Depth profiling	M/s. Hindustan Surgicals Limited
35	Oxide and Carbonate materials	PIGE	Fluorine	M/s. Videocon Narmada Electronics Limited, Baroda
35	Refinery Wastewater	ICP-QMS	Multi-element	M/s. Honeywell Company—UOP India Pvt Ltd
36	Soil, Fly ash and sediment samples	ICP-QMS	Mn, Ni, As, Cd, Pb	Community Environmental Monitoring, Chennai
37	Bacterial pellets	GFAAS	Cd, Cu, Sr	K K Labs
38	Water	GFAAS	Na	KTPS

11. Specialized Analytical Services

11.1 Mapping of Ga, Ge, Li and REEs in Indian coal fly ash (CFA)

Mapping of strategic elements (Ga, Ge, Li and REEs) present in coal fly ash (CFA) was carried out. Approximately 2 kg each of 33 CFA samples from different thermal power plants across India (11 samples from NLC collected by Mineral Processing Division, Materials Group, BARC, Hyderabad and 22 samples were collected by NCCCM-BARC, Hyderabad) and BHEL gasification plant, Hyderabad were analysed at NCCCM-NARC.The analytical results show that CFA obtained from NLC (lignite coal) contains higher REEs, but low concentration of Ga, Ge and Li. JPL-JHARLI (Haryana) and Shakti Nagar, U.P (both are obtained from bituminous coal) show reverse trend (i.e., low REE and high Ga, Ge and Li). CFA obtained from KSTPS (Kota) contains all the elements of interest at higher concentration. It is important to mention that KSTPS receives coal from Indian coal mines. After the mapping, now NCCCM is in the process of screening of CFA based on elements of interest with respect to particle size of CFA and precipitating steps involved in thermal power plant. Since KSTPS containing high concentration of all the interest elements, NCCCM-BARC have collected samples from the series of six Electrostatic Precipitators (ESP) of KSTPS and observed that concentration of Ga, Ge and Li increases with number of ESPs. Particularly, the concentration of Ge reached up to 46 mg Kg^{-1} at ESP-6 of KSTPS plant. This distribution of Ge along with Ga and Li in the ESPs is given in Table 5. This analytical data is useful for the extraction of Ge from CFA. This work is in progress to select suitable CFA for the production of CRM and also for the recovery of Li, Ga and Ge from CFA.

Table 5: *Analysis result of Ga, Ge and Li in CFA samples obtained from the series of Electrostatic precipitators of KSTPS, Kota.*

S No.	Sample description	Values are in $mgKg^{-1}$		
		Ge	Ga	Li
1	Unit 6, KSTPS, Kota, 1st field	8	19	60
2	Unit 6, KSTPS, Kota, 2nd field	19	29	63
3	Unit 6, KSTPS, Kota, 3rd field	21	44	95
4	Unit 6, KSTPS, Kota, 4th field	27	53	65
5	Unit 6, KSTPS, Kota, 5th field	41	60	95
6	Unit 6, KSTPS, Kota, 6th field	47	62	73

11.2 Purification of raw quartz by chemical leaching

For the past three decades NCCCM-BARC analysed thousands of samples to Gimpex Ltd Chennai. As required by this industry, a chemical leaching procedure for the purification of raw quartz powder of Indian origin was developed at NCCCM-BARC. The procedure involves leaching of raw quartz by chemical leaching using a mixture of reagents at hot condition. Then quartz powder was rinsed with de-ionized water to remove residual reagents and then dried at 100°C in a hot air oven. By this procedure, quartz powder obtained from major mines gets purified from 3N to maximum 5 N with respect to common impurities analysed in quartz powder. It was observed that for elements like Al, Na, K and Ca the reduction in impurity level was 5-50 times. Whereas, Cu, Zn, Mg, Ni and Fe levels were reduced upto300 times of their initial values in raw quartz. There was no improvement with respect to purification of Li and Ti. Few sets of raw and purified quartz samples are given in Table 6.

Table 6: *Analysis result of raw and purified (developed at NCCCM-BARC) quartz powders*

CCCM Code	Na	K	Ca	Fe	Al	Li	Mg	Ti	Mn	Cu	Zr
B-459	14	2	17	47	26	0.08	5.0	3.4	0.58	0.44	0.011
PFQB-459	4	1	3	1	5	0.06	0.52	2.2	0.08	0.02	0.010
B-460	300	11	43	22	600	0.08	3.5	5.7	0.56	0.27	0.022
PFQB-460	4	1	3	1	6	0.06	0.43	2.3	0.07	0.01	0.005
B-442	20	7	7	8	33	0.07	3.0	4.0	0.16	3.1	0.056
PFQB-442	0.5	<0.5	<1	2	5	0.05	0.18	2.8	0.01	0.01	0.049
B-443	23	7	9	5	33	0.05	3.0	3.4	0.09	1.3	0.004
PFQB-443	1.5	<0.5	2	<1	5	0.03	0.13	2.7	0.01	0.03	0.003
B-444	51	48	64	25	94	0.17	9.0	5.2	0.51	2.1	0.048
*PFQB-444	36	36	35	9	66	0.10	7.0	0.4	0.22	0.96	0.007

All the values are in mg/kg (ppm). B- raw quartz, PFQ-Purified quartz.

12. Major Technology Developments and Transfer

12.1 Fluoride Detection Kit (FDK)WT07NCCCM – transferred to 11 companies

A visual colourimetric reagent was developed by NCCCM/BARC for the estimation of fluoride in ground water. It has been rated **1st among 15 fluoride kits available in India** in survey carried out by Sri Ram research Institute, Delhi for UNICEF in the year 2009. This figure shows distinct colour formation by addition of 1 mL of reagent into 4 mL of water.

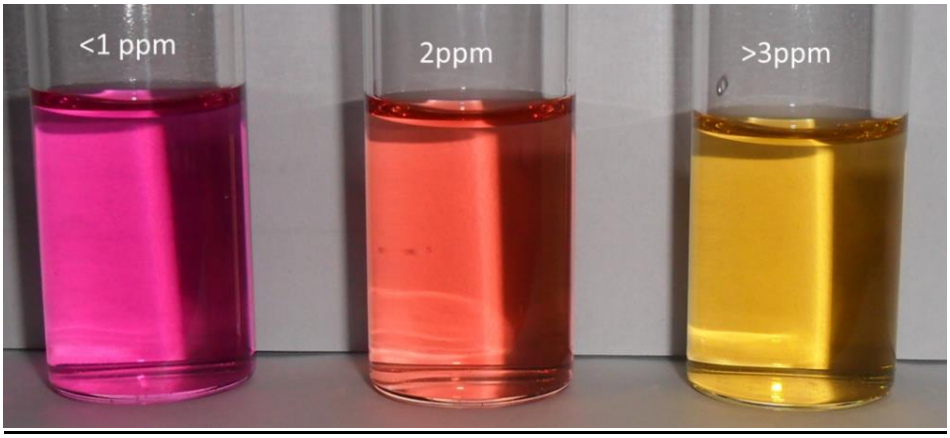

12.2 Fluoride Remediation from Water (TFRW) (WT20NCCCM) transferred to 8 firms

12.3 Visual detection kit for alcohol content in hand sanitizers (CH29NCCCM) transferred to 2 firms

12.4 SP-FeDK: Smartphone based Iron Detection Kit for boiler coolant water (WT25NCCCM)

12.5 Visual Detection Kit (VDK) for monitoring ethanol in petrol (CH34NCCCM)

12.6 A Field Detection Kit For Quick Determination Of Aluminium In Dialysis Fluids And Ground Waters (CH37NCCCM) - transferred to 1 firm

Aluminum functions as a neurotoxin due to its indiscriminate binding with various ligands (phosphate, citrate; proteins-transferrin, catecholamine). Of which, 85-90% is protein bound aluminum. It is significant to note that Al can cross blood brain barrier and accumulate in brain leading to memory impairment, cognitive dysfunction, neurodegenerative disorders (Parkinson's, Alzheimer's) etc.

The toxic effect of Al is of concern in chronic renal failure patients on dialysis and patients receiving long term parenteral nutrition. The dialysis process does not efficiently remove the excess aluminum from the body, so it may build up over time. If Al is present as a contaminant in these dialysis fluids, it is able to diffuse through the dialysis membranes and penetrate into the blood stream of the

patient. Therefore the detection of Al at trace levels is necessary to determine suitability of the test sample for medical applications as well as for human consumption. A simple and rapid visual colourimetric method is therefore developed by NCCCM/BARC for the detection of Al in peritoneal dialysis fluids and ground waters.

Since the developed visual colourimetric method is rapid and very simple, it can be easily applied to on-site testing of the samples; with very minimal instructions, the test kit can be easily used for the monitoring of Al in peritoneal dialysis fluids and ground waters. Using this kit the test samples can be immediately categorized as safe, permissible or toxic for their suitability with respect to aluminum.

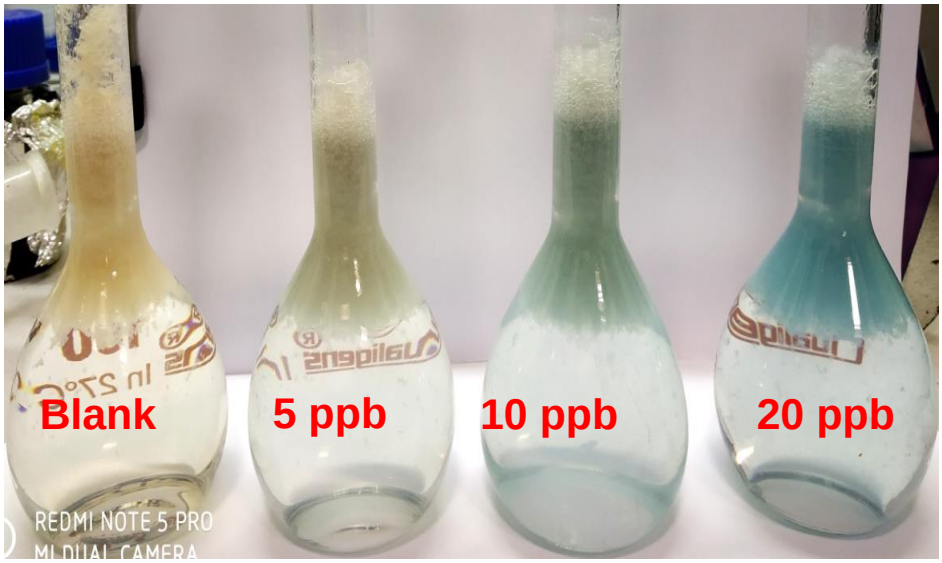

13. Facilities and Infrastructure at NCCCM

13.1 Bulk Analysis Section

i. Inductively Coupled Plasma – Atomic Emission Spectrometer (ICP-AES)
ii. Flame Atomic Absorption Spectrometer (FAAS)
iii. Ion – Chromatography (IC)
iv. Gas Chromatography – Mass Spectrometer (GC-MS)
v. Liquid Chromatography – Mass spectrometer (LC-MS)
vi. Carbon – Sulphur Analyser (CS Analyser)
vii. Moisture Analyser and Microwave digestion system

13.2 Surface and Profile Measurement Section

i. 3MV Tandem accelerator to carry out Ion Beam Analysis (IBA) of materials
ii. Scanning Electron Microscope for morphological and elemental characterisation
iii. X-ray Diffracto-meter for phase identification of thin films and powder samples
iv. X-ray Fluorescence Spectroscopy
v. Atomic Force Microscope for topographic measurements
vi. Thermal Evaporation system
vii. Magnetron sputtering system
viii. Furnaces for annealing & heat treatment
ix. Vicker's hardness tester
x. Four probe measurement system
xi. Solar cell tester

13.3 Environmental Analytical Section

i. Atomic Fluorescence Spectrometer
ii. Capillary Electrophoresis
iii. Closed Microwave Digestion system

13.4 Ultra Trace Analysis Section

i. Graphite Furnace Atomic Absorption Spectrometer
ii. Glow Discharge Mass Spectrometer
iii. Electrolyte Cathode Discharge Atomic Emission Spectrometer (ELCAD-AES)
iv. Tunable *cw*-ring lasers
v. Flame Atomic Absorption Spectrometer

14. Instrumentation support and related activities

14.1 Radiation Surveillance of 3MV Tandetron facility

There are many safety features related to radiation, utilities and various other operations incorporated for safe operation of the 3MV Tandem Accelerator by the manufacturer (HVEE). The sources of radiation are Bremsstrahlung due to charged particle acceleration inside the tank, X-ray and γ-ray radiations generated from the targets when bombarded with the ion beams, scattered ion beam interaction with walls of scattering chambers, and neutrons from any possible neutron generating reactions.

During the initial stages of installation in 1997, the radiation survey mapping of different locations in and around the facility was carried out for X-rays, γ-rays and neutron fields. The maximum doses generated by all possible radiations at the peak of the terminal voltage and maximum beam currents on SS target at 0° port, were measured. To minimise radiation levels in the occupancy areas, a high density (HD) concrete brick wall of 10″ thickness and 6′ high, with interlaced HD concrete bricks were installed at 1mt distance all around the accelerator tank. All user areas around the accelerator are made as restricted access zones. As the radiations were found to be at acceptable levels of <1mGy/hr in occupancy areas, AERB had sanctioned permission to run the accelerator up to 3 MV and proton currents up to 5 μA on target. As a safety measure, radiation interlocks were incorporated which in turn would trip the ion beam in case of high radiation field.

Until 2014, the Particle Accelerator Safety Committee (PASC) was overseeing the safety aspects for running the 3 MV Tandem Accelerator. Since the year 2015, RIT, Unit Level Safety Committee, Particle Accelerator (ULSC-PA) have been visiting the facility annually and making safety recommendations during their visits. These recommendations have been incorporated from time to time. Based on their recommendations, radiation survey was carried out in the years 2009, 2016 and 2022 in the presence of HPD, BARC, Mumbai to monitor and assess the radiation levels for X-ray, Gamma rays and neutrons. All the measurements showed that the values are well within the acceptable levels of <1mGy/hr in occupancy areas.

After obtaining the initial approval to operate the 3MV Tandetron facility from AERB, the facility is seeking renewal to operate the facility from regulatory bodies like AERB and BARC Safety Council (BSC) once every 5 years. The latest permission for renewal was obtained in the year 2022 to operate the facility up to June 30, 2026

.

14.2 Maintenance works on 3MV Tandem Accelerator

a) RF control unit pertaining to terminal voltage was malfunctioning. During troubleshooting, the fault was traced to a critical DC – DC converter. The faulty components were replaced with equivalent devices (24V to 5V DC-DC converter and 24V to +/-12V DC-DC converter). Necessary wiring modifications were carried out to install equivalent devices as there was no pin compatibility with faulty components.
b) Generating Volt Meter (GVM) of 3MV Tandem Accelerator failed to give feedback output of the terminal voltage. The faulty AC-DC converter (230Vac to +/- 15Vdc) of preamplifier power supply section of GVM was replaced with an equivalent device. The GVM was restored to operational condition.

c) During operation of Accelerator, low energy 90° bending magnet supply unit (40V/100A) failed. The fault was due to failure of one of the power transistor in the water cooled bank of 40 power transistors (2N3773) and a metal diode rectifier (70HF40). These critical components were replaced with equivalent ones and the sub-system was restored to its functionality.
d) The terminal voltage display unit of accelerator was upgraded with a 5½ digit DPM in place of old 4½ digit DPM, to obtain better display resolution for conducting ion beam experiments.
e) Various safety interlocks were implemented using programmable logic controller (PLC) as per safety committee recommendations.
f) Electrolytic capacitors of were in operation for 3 decades. Due to ageing of the electrolytic capacitors in the low energy (LE) and high energy (HE) magnet power supply unit, were not generating the specified power. After replacing all the 18 capacitors in capacitors bank, the units generated the requisite power as per the specifications.

14.3 Maintenance works on GDMS

a) During the analysis, the mass scan instability was identified due to mass shift in GDMS. This problem was due to the malfunctioning of the display unit of the RF control system. The faulty "display driver IC" and "local/remote switch" were replaced and the system was restored to its working condition.

14.4 GD-QMS

The Faraday cup detector should give about few hundred background counts per second when it is biased, but no counts were observed. Trouble shooting was performed to identify the source of the problem. The principal IC of the preamplifier for the Faraday cup is an electrometer operation amplifier with an ultra-low input bias current. The existing IC being used was AD 549J and its input bias current was ~ 250fA, for ultra-low current amplification. In typical GD mass spectrometers, few hundred background counts per second correspond to a current value which is much lower than 250fA. Since its input bias current was ~250fA, it cannot be utilized for amplifying currents at levels lower than 250fA Therefore; another IC (AD549L) whose input bias current was ~ 60fA was used. Background counts were not observed even after replacing the IC. Upon further analysing it was identified that 4^{th} pin of the IC was grounded instead of the 8^{th} pin. In principle, for any 8-Lead Metal Can [TO-99] IC, the 8^{th} pin is connected to casing, however in the replaced AD549L the 4^{th} pin was connected to casing. Therefore, another AD549L with its 8^{th} pin connected to the casing was procured and was utilized in the preamplifier, after which the significant background counts were observed.

In addition, there was no output from the power supply of the lens stack assembly, so all the sub systems were checked to identify the problem. The problem was resolved after replacing the controller IC-OP07 of 1kV DC power supply of the lens stack assembly. The corresponding trim-pots were tuned to adjust the slope of the mass scan to secure the complete mass scan range from 5 amu to 210 amu. The relay switches of vacuum gate valve were replaced for its optimum performance. After carrying out the above modifications the GD-QMS instrument started working with better stability.

14.5 Moisture Analyzer

The moisture analyzer (Make: Sartorius, Germany) is used to determine the moisture content of solid, powdered and liquid samples. The analyzer features the highest possible measuring accuracy that thermo-gravimetric moisture meter offers. This was not operational and on inspection it was observed that

two electronic circuit boards were stacked in a very compact assembly. The boards were inspected and it was identified that the protection circuit of the mains transformer was not working. On careful examination it was observed that the protecting TVS diode (which is a 'Transient voltage suppression' diode - P6KE200A) had short circuited due to power fluctuations. After replacing the faulty diode, all the outputs of the power supply (±15 V, ± 12V and ± 5V) were measured. Ensuring that all the power supply outputs were performing as per their certified specifications, all the PCBs and the mother board were reassembled. The moisture analyzer was restored to its normal functioning condition with proper temperature and weight calibration.

14.6 Ultra-sonic bath

The ultra-sonic bath (Germany make) uses cavitation triggered by low-frequency ultra sound. The frequencies are generated by using two pairs of IGBT (Insulated Gate Bipolar Transistors with ultrafast soft recovery diode) devices. It was found that the two ultrasonic transducers got dislodged from their home position and were in contact with the 'ultrasonic frequency generating circuit'. This led to a short circuit and consequently a couple of electronic components got damaged. On further examination of the circuit, it was observed that, two numbers of IGBTs and a feedback sensing resistor failed. As those components were not available, equivalent IGBTs were identified and procured from local market. After replacing the faulty components and reassembling the electronics circuit the functionality of ultrasonic generator was restored.

To circumvent the displacement of transducers from their preset position, an acrylic sheet of 5mm thick was mounted with proper ventilation between the electronic circuit PCB and the ultrasonic bath assembly. After carrying these modifications the ultrasonic bath started functioning satisfactorily.

14.7 Muffle Furnace

High performance Muffle furnace has a temperature controller, which monitors the temperature and also controls the power supplied to the heating elements. The unit has display of both set and measured temperature. The measured value reaches the set value in the display, but the actual temperature was totally different than that the displayed values. Upon careful examination, it was observed that the solid state relay (SSR) between controller and heating element was malfunctioning. After replacing with the new SSR, the furnace started working to the set high temperature, which was manually measured using a thermocouple.

14.8 GFAAS

Graphite furnace atomic absorption spectrometer (GFAAS) instrument has a HV power supply unit which had 16 core cables connected to the hallow cathode lamps. The insulation of these cables was worn out as it had deteriorated with time. As the exposed live wires are prone for short circuit, new 16 core cable was put in place and it was tested for the requisite voltages.

Also there was issue with leakage in the gas box. The gas box was opened and all the connections to the solenoid valves and Argon gas flow controller were reconnected by arresting all the leaks. With these changes, the instrument started functioning satisfactorily.

14.9 HV Pulse generator:

The resolution of the Time-of-flight mass spectrometer (TOF-MS) is limited by the initial kinetic energy (KE) distribution i.e., velocity distribution of the neutral atoms effusing from a high temperature

atom source. Due to this initial KE distribution, the resolution is limited to ~170 at the mass ^{85}Rb, when continuous extraction field is applied to the repeller grid. The resolution in the linear mode can be improved by a using pulsed extraction field. Hence pulsed high voltage power supply module with a very short rise time is required.

A commercial HV pulser's (DEI Model PVM 4140) input HV conditions were suitably modified for carrying out delayed pulsed extraction. The essential principle of delayed pulsed extraction necessitates that the voltages of the repeller grid and extraction grids are equal such that subsequent to the triggering of the laser pulse, the ionization region is maintained without any voltage gradient (dV/dx=0) for certain duration of time (~few hundred ns). Therefore, prior to applying pulsed voltage to the repeller grid, the offset voltage of the repeller grid should be identical to the voltage applied to the extraction grid. After certain time delay with respect to the laser pulse, the offset voltage of the repeller grid is increased by applying a pulsed voltage of about +700V. This HV pulser has two inputs viz., lower voltage (-HV or VLOW) and higher voltage (+HV or VHIGH). This HV pulser cannot be fed with voltages of the same polarity from two separate continuous HV DC sources. Positive power supplies sink (draw) electrons from ground, while negative power supplies source (push) electrons to ground. To operate with power supplies of common polarity, the lower voltage (-HV or VLOW) supply must be provided with an additional current flow path to the ground. If this path is not provided, the output voltage will not remain at (-HV In) when the pulse generator is not gated, but can be charged up to the potential of the VHIGH (+HV In) supply due to leakage current within the pulse generator. This is often observed if the load does not draw current, or as the pulse repetition frequency is increased. The path to ground must be accomplished with a shunt resistor (i.e. a resistor from the -HV In power supply input to ground) in low power applications, or with an active shunt regulator for high power applications. The value and size of the shunt resistance was optimized as per the requirement and the necessary modification was made to operate the HV pulser with same polarities at the two inputs. With the application of delayed (pulsed) extraction the resolution of the TOFMS could be improved to ~300.

15. Training and Outreach program

A large number of UG, PG, doctoral and postdoctoral students (475) from various UG colleges, PG colleges, state, central and deemed universities, NIT, IIIT, IIT, BITS etc., were trained in analytical chemistry, physics, biology and electronics at NCCCM, Hyderabad.

NCCCM-BARC carries out various outreach programs time to time to demonstrate, the technologies developed in centre, at schools, villages and to NGOs. The outreach program aims to educate the common people especially farmers and students about the practice to use the technology and its benefits. In this context, the colleagues from NCCCM have demonstrated:

- Visual Fluoride Detection Kit, which was developed by our centre at NIT, Raipur & CSIT, Durg.
- Visual detection kits of NCCCM like FDK, and available phosphorous in soil sample in Public Outreach program of Indian Nuclear Society at Bijlal Biyani Science college at Amaravati.
- On site Nitrogen and Phosphorus (available) determination in soil, demonstration carried out at Pantangi village of Rural Telangana
- On site Fluoride, Nitrogen and Phosphorus (available) determination in water at Gram Panchayat office, Kazipet – Yavapur, Telangana
- Onsite demonstration of Fluoride in Ground water & Phosphorus (available) in Soil samples to nearby villagers of HWB, Manuguru (under AKRUTI)
- On site Fluoride, Nitrogen and Phosphorus (available) determination in water and melamine in milk (Azaadi Ka Amrit Mahotsav) to the students of Zilla Parishad High School - Kolthur, Medchal – Malkajgiri Dist., Telangana

Scientists and farmers meet at Panthangi village, Nalgonda district, Telangana

Scientists and students meet at Kolthur village, Medchal district, Telangana

16. Publications

1. *Alpha induced gamma emission spectroscopy for the determination of nitrogen in materials; G. L. N. Reddy, A. A. Sukumar, Y. Sunitha, D. V. Lakshmipathy, J. V. Ramana, Sanjiv Kumar, Nuclear Instruments and Methods in Physics Research B 548 (2024) 165260.*
2. *Certified reference material (CRM) of tea powder (BARC - D3201) for K, Ca, P, Mg, Mn, Al, Fe, Ba, Zn, Cu, Sr, Pb, As, Cd, and Hg: Method validation and its production; Lori Rastogi, A. Durga Prasad, D. Sai Krishna, S. Yadlapalli, K. Dash, Food Control 158 (2024) 110241.*
3. *Development of an expeditious and sensitive microprecipitation approach using chrome azurol S and CTAB for visual detection of Fe(II) and Fe(III) in waters; Venkata Balarama Krishna Mullapudi, Aruna Jyothi Kora, K. Chandrasekaran, Journal of Analytical Chemistry 79(6) (2024) 773.*
4. *Renewable, natural, traditional dish wash cleaning materials used in India: An overview; Aruna Jyothi Kora, Bulletin of National Research Centre 48 (2024) 28.*
5. *Development of a simple and efficient two-step microwave-assisted digestion method for the determination of REEs, HFSEs and other elements in granite samples by ICP-AES; K. Chandrasekaran, M. V. Balarama Krishna, G. Venkateswarlu, Johnson George and Beena Sunilkumar, Journal of Analytical Atomic Spectrometry 39 (2024) 2116.*
6. *A simple and rapid copper-assisted microprecipitation method for the on-site separation of inorganic arsenic species in real water samples followed by hydride generation atomic fluorescence spectrometry (HG-AFS) determination; Venkata Balarama Krishna Mullapudi, Spectrochimica Acta Part B: Atomic Spectroscopy 211 (2024) 106833.*
7. *Interference-free ultratrace beryllium determination in alkaline effluents of beryllium processing plants by graphite furnace atomic absorption spectrometry after a novel graphene oxide-assisted dispersive micro solid phase extraction without using a chelating agent; D. Saikrishna, N. N. Meeravali and A. C. Sahayam, Journal of Analytical Atomic Spectrometry 39(5) (2024) 1322.*
8. *Improvement in the sensitivity of orthophosphate determination by controlling the self-reduction of excess ammonium molybdate followed by room temperature non-ionic mixed micelle cloud point extraction of anionic phosphomolybdenum blue for spectrophotometric determination; D. Saikrishna, G. Venkateshwarlu, N. N. Meeravali and A. C. Sahayam, Microchemical Journal 201 (2024) 110531.*
9. *Chemical characterisation of lithium based ceramics utilizing charged particle activation and ion beam techniques; S. Dasgupta, J. Datta, G. L. N. Reddy, M. Ghosh, K. K. Swain, Journal of Radioanalytical and Nuclear Chemistry (doi.org/10.1007/s10967-024-09639-8)*
10. *Hydrophobicity induced graphene oxide based dispersive solid phase microextraction of strontium from seawater and groundwater prior to GFAAS Determinatio; Maria Sebastian, D. Saikrishna, N. N. Meeravali, R. Shekhar and A. C. Sahayam, Journal of Analytical Atomic Spectrometry, (Revision submitted).*
11. *A single step acid assisted microwave digestion method for the complete dissolution of bauxite and quantitation of its composition (Al_2O_3, Fe_2O_3, SiO_2, TiO_2, Cr_2O_3, MgO, MnO and V_2O_5) by ICP-AES; A. Durga Prasad, L. Rastogi. S. Thangavel and K. Dash, Geostandards and Geoanalytical Research 47 (2023) 403.*
12. *Production of bauxite certified reference material (BARC- B1201) for nine (Al_2O_3, Fe_2O_3, SiO_2, TiO_2, V_2O_5, MnO, Cr_2O_3, MgO, and LOI) property values traceable to SI units; A.Durga Prasad, Lori Rastogi, V. K. Verma, V. Krishna Kumari, S. Yadlapalli and K. Dash, Geostandards and Geoanalytical Research 47 (2023) 629.*
13. *A domestic pressure cooker mediated, facile autoclaving method for the synthesis of silver nanoparticles; Aruna Jyothi Kora, MethodsX 11 (2023) 102438.*
14. *Gum tragacanth-mediated synthesis of metal nanoparticles, characterization, and their applications as bactericide, catalyst, antioxidant, and peroxidase mimic; Aruna Jyothi Kora, Green Processing and Synthesis 12 (2023) 20228138.*
15. *Ekavimsati patrani (21 leaves) used during Vinayaka Chaviti festival in India: Medicinal, ecological and cultural importance; Aruna Jyothi Kora, Advances in Traditional Medicine 23 (2023) 393.*
16. *Synthesis, characterization and in vitro antifungal action of gum ghatti capped copper oxide nanoparticles; Aruna Jyothi Kora, Biointerface Research in Applied Chemistry 3(2) (2023) 1.*
17. *Eutectic mixtures purity analysis by acid induced dispersive liquid liquid micro extraction and determination by HR-CS-ETAAS; K. Madhavi, G. Venkateswarlu, N. N. Meeravali, A. C. Sahayam, Journal of Analytical Atomic Spectrometry 38 (2023) 2332.*
18. *Determination of thallium in vegetative plant leaves near industrial areas by high resolution continuum source electrothermal atomic absorption spectrometry after salt induced cloud point extraction; N. N. Meeravali, K. Madhavi and A. C. Sahayam, Spectrochimica Acta Part B: Atomic Spectroscopy 200 (2023) 106613.*
19. *Growth and characterization of electron beam evaporated NiO thin films for room temperature formaldehyde sensing; K. Ganga Reddy, P. Nagaraju, G. L .N. Reddy, Partha Ghosal and M. V. Ramana Reddy; Sensors and Actuators A: Physical 346 (2022) 113876.*
20. *$^{28}Si(p,p'\gamma)^{28}Si$ nuclear reaction in the detection and depth profiling of Si in materials; Y. Sunitha , G. L. N. Reddy, Sanjiv Kumar; Nuclear Instruments and Methods in Physics Research B 527 (2022) 12.*
21. *Determination of impurities in graphite using Proton Induced Gamma ray Emission, Total Reflection X-ray Fluorescence and Instrumental Neutron Activation Analysis; M. Ghosh, T. A. Chavan, G. L. N Reddy, Remya Devi P. S, S. Kumar and K. K. Swain; Analytical Chemistry Letters 12 (2022) 437.*
22. *Inter-diffusion and stability studies in W/Cr and W/Fe films using ion beam analysis; G. L. N. Reddy, J. V. Ramana, A. A. Sukumar, Sanjiv Kumar, Nuclear Instruments and Methods in Physics Research B 518 (2022) 41.*

23. *Pseudo matrix-matched standards for the determination of iron in ferrocene and its derivatives by energy dispersive X-ray fluorescence spectrometry, Sunitha Yerroju, Thangavel Shanmugam, Lori Rastogi, Kishore Babu Neela, Yedukondalu Telugu, Sanjiv Kumar; X-Ray Spectrometry 51 (2022) 109.*
24. *Covellite (CuS) as a novel adsorbent for the direct removal of As (III) and As (V) simultaneously from groundwater; Thangavel Shanmugam, Venkata Balarama Krishna Mullapudi, Sunitha Yerroju, Aruna Jyothi Kora, Sanjiv Kumar, Separation Science and Technology 57(5) (2022) 683.*
25. *An in-house UV-photolysis setup for the rapid degradation of both cationic and anionic dyes in dynamic mode through UV/H_2O_2 based advanced oxidation process; Venkata Balarama Krishna Mullapudi, Arthi Salveru and Aruna Jyothi Kora, International Journal of Environmental Analytical Chemistry 102(17) (2022) 5567.*
26. *Blue arsenomolybdic acid-crystal violet ion-associate pair paving way for the field detection of arsenic in groundwater; M. V. Balarama Krishna, S. Thangavel, Y. Sunitha and Sanjiv Kumar, Analytical Methods 14 (2022) 3539.*
27. *ArsenazoIII functionalized gold nanoparticles: SPR based optical sensor for determination of uranyl ions (UO_2^{2+}) in groundwater; Nidhi Garg, Lori Rastogi, Santanu Bera, Anand Ballal, M. V. Balrama Krishna, Green Analytical Chemistry 3 (2022) 100032.*
28. *Direct determination of ultratrace sodium in reactor secondary coolant waters and other waters by electrolyte cathode discharge atomic emission spectrometry (ELCAD-AES); M. A. Reddy, R. Shekhar and A. C. Sahayam, Spectrochimica Acta Part B: Atomic Spectroscopy 198 (2022) 106551.*
29. *A sensitive vesicle mediated dispersive liquid-liquid microextraction of parts per quadrillion levels of beryllium from seawater samples prior to graphite furnace atomic absorption spectrometry determination; D. Sai Krishna, K. Madhavi, N.N. Meeravali, A.C. Sahayam, Analytica Chimica Acta 1191 (2022) 339313.*
30. *Effects of laser bandwidth and Autler-Townes doublet peaks of neighboring isotopes on the ionization lineshape of ^{168}Yb isotope; P.V. Kiran Kumar, G. Sridhar, Journal of Quantitative Spectroscopy & Radiative Transfer 277 (2022) 107995.*
31. *Development of a certified reference material (CRM) for seven trace elements (Al, Ca, Fe, K, Mg, Na and Ti) in high purity quartz; A. Durga Prasad, S. Thangvelu, Lori Rastogi, D. Soni and K. Dash and Sunil Jai Kumar, Microchemical Journal 172 (2022) 106926.*
32. *CW laser damage study in Ag/TiO_2 bilayer thin films: Role of interfacially diffused plasmonic silver nanoparticles; S. Maidul Haque, Rajnarayan De, C. Prathap, Sanjiv Kumar, G. L. N. Reddy, Shobhna Mishra and K. Divakar Ra,; Optical Materials 117 (2021) 111135.*
33. *An assessment of vitamin B12 through determination of cobalt by X-ray fluorescence spectrometry; Y. Sunitha, Sanjiv Kumar, Radiation Physics and Chemistry, 188 (2021) 109583.*
34. *Facile on-site quality monitoring of alcohol-based hand sanitizers by phase separation and color development with butyl acetate-crystal violet mixture; S. Thangavel, A. Durga Prasad, K. Dash, Sanjiv Kumar, Microchemical Journal 169 (2021) 106578.*
35. *Selective and sensitive detection of cholesterol using intrinsic peroxidase-like activity of biogenic palladium nanoparticles; Lori Rastogi, K. Dash, R. B. Sashidhar; Current Research in Biotechnology 3 (2021) 42.*
36. *Development of microwave assisted-UV digestion using diluted reagents for the determination of total nitrogen in cereals by ion chromatography; Lori Rastogi, Durga Prasad Ankam, S. Yadlapalli, K. Dash; Current Research in Food Science 4 (2021) 421.*
37. *Biogenic silver nanoparticles as an antibacterial agent against bacterial leaf blight causing rice phytopathogen Xanthomonas oryzae pv. Oryzae; Karunakar Reddy Namburi, Aruna Jyothi Kora, Anuradha Chetukuri, Vijaya Sree Meena Kumari Kota, Bioprocess and Biosystems Engineering 44 (2021) 1975.*
38. *Zirconium alginate beads: A renewable source for the biosorption of fluoride from contaminated ground water; Aruna Jyothi Kora, Current Trends in Biotechnology and Pharmacy 15(1) (2021) 70.*
39. *Development of a single-step microwave-assisted digestion method using dilute nitric acid for determination of bismuth in bismuth-containing pharmaceuticals by hydride generation-atomic fluorescence spectrometry; K. Chandrasekaran, M. V. Balarama Krishna, Nidhi Garg, Asian Journal of Pharmaceutical Analysis 11(2) (2021) 87.*
40. *Graphite furnace atomic absorption spectrometric studies for the quantification of trace and ultratrace impurities in the semiconductor grade organic chemicals such as triethylborate, tetraethylorthosilicate and trimethylphosphate; M .A. Reddy, R. Shekhar, A. C. Sahayam, Paritosh Jain, Spectrochimica Acta Part B: Atomic Spectroscopy 180 (2021) 106184.*
41. *Novel ionic reverse mixed micelle supramolecules in dispersive liquid-liquid microextraction for the successive/individual sensitive speciation analysis of iron in natural water by UV–Vis spectrophotometry; N. N. Meeravali, K. Madhavi and A. C. Sahayam, Microchemical Journal, 164 (2021) 105986.*
42. *A novel non-ionic nanoaggregate sensitized salt induced cloud point extraction of anionic beryllium-chrome azurol S for spectrophotometric determination of beryllium in environmental waters; D. Sai Krishna, N. N. Meeravali and A. C. Sahayam, Microchemical Journal, 160 (2021) 105651.*
43. *Frequency and amplitude modulation of a cw-dyelaser for measuring hyperfine frequency separations in optogalvanic spectra of ^{139}La I; P. V. Kiran Kumar and G. Srikanth, Applied Optics 60 (2021) 3430.*
44. *Synthesis of co-sputter deposited Ni–Ti thin alloy films and their compositional characterization using depth sensitive techniques; V. Karki , A. K. Debnath, S. Kumar, Debarati Bhattacharya, Thin Solid Films 697 (2020) 137800.*
45. *Exposure of Indian RAFM under variation of He+ flux and target temperature in the CIMPLE-PSI linear device; Trinayan Sarmah, Pubali Dihingia, Mizanur Rahman, J. Ghosh, P. Chaudhuri, Divesh N. Srivastava, B. Satpati, Sanjiv Kumar, M. Kakati, and G. De Temmerman; Nuclear Fusion 60 (2020) 106026.*
46. *Intrinsic peroxidase-like activity of 4-amino hippuric acid reduced/stabilized gold nanoparticles and its application in the selective determination of mercury and iron in ground water; Lori Rastogi, Durga Prasad Ankam, K. Dash, Spectrochimica Acta Part A: Molecular and Biomolecular Spectroscopy 228 (2020) 117805.*

47. *Synthesis and characterization of L-asparagine stabilised gold nanoparticles: Catalyst for degradation of organic dyes. Nidhi Garg, Santanu Bera, Lori Rastogi, Anand Ballal, M. V. Balaramakrishna, Spectrochimica Acta Part A: Molecular and Biomolecular Spectroscopy 232 (2020) 118126.*
48. *Antibacterial and antioxidant activities of aqueous extract of soapnuts (Sapindus mukorossi); Aruna Jyothi Kora, Current Trends in Biotechnology and Pharmacy 14(4) (2020) 388.*
49. *Traditional soapstone storage, serving, and cookware used in the Southern states of India and its culinary importance; Aruna Jyothi Kora, Bulletin of the National Research Centre 44 (2020) 83.*
50. *Nutritional and antioxidant significance of selenium-enriched mushrooms; Aruna Jyothi Kora, Bulletin of the National Research Centre 44 (2020) 34.*
51. *In situ synthesis and preconcentration of cetylpyridinium complexed hexaiodo platinum nanoparticles from spent automobile catalytic converter leachate using cloud point extraction; Aruna Jyothi Kora, K. Madhavi, N. N. Meeravali and Sunil Jai Kumar, Arabian Journal of Chemistry 13 (3) (2020) 4594.*
52. *Rice leaf extract synthesized silver nanoparticles: An in vitro fungicidal evaluation against Rhizoctonia solani, the causative agent of sheath blight disease in rice; Aruna Jyothi Kora, J. Mounika, R. Jagadeeshwar, Fungal Biology 124 (7) (2020) 671.*
53. *Characterisation of hafnium metal for its impurities by glow discharge quadrupole mass spectrometry using a non-matrix matched standard; R. Shekhar, M. A. Reddy, S. Thangavelu, Y. Sunitha, A. C. Sahayam and Sanjiv Kumar, Atomic Spectroscopy 41(3) (2020) 103.*
54. *A new sequential and simultaneous speciation analysis of thallium in coal effluents by graphite furnace atomic absorption spectrometry after a novel ligandless mixed micelle cloud point extraction; D. Saikrishna, N. N. Meeravali and S. J. Kumar, International Journal of Environmental Analytical Chemistry 100(10) (2020) 1079.*
55. *Effect of argon-nitrogen mixed ambient Ni sputtering on the interface diffusion of Ni/Ti periodic multilayers and supermirrors; N. Abharana, A. Biswas, P. Sarkar, S. Rai, S. Singh, S. Kumar, S. N. Jha, D. Bhattacharyya, Vacuum 169 (2019) 108864.*
56. *PESA in the analysis of hydrogen containing polymeric materials: Some basic considerations; Sanjiv Kumar, Y. Sunitha, A. A. Sukumar, J. V. Ramana, G. L. N. Reddy, Nuclear Instruments and Methods in Physics Research B 444 (2019) 1.*
57. *Composition dependent microstructure and optical properties of boroncarbide (BxC) thinfilms deposited by radio frequency-plasma enhanced chemical vapour deposition technique; A. Bute, S. Jena, D. Bhattacharya, S. Kumar, N. Chand, N. Keskar, S. Sinha, Materials Research Bulletin, 109 (2019) 175.*
58. *Tunable magnetic domains and depth resolved microstructure in Gd-Fe thinfilms; A. Talapatra, J. Arout Chelvane, B. Satpati, S. Kumar, J. Mohanty, Journal of Alloys and Compounds, 774 (2019) 1059.*
59. *Development of a Certified Reference Material for Lead in Noodles Powder; Lori Rastogi, K. Dash, R. Manjusha, A. Durga Prasad and Sunil Jai Kumar, Accreditation and Quality Assurance 24 (2019) 173.*
60. *Leaves as dining plates, food wraps and food packing material: Importance of renewable resources in Indian culture; Aruna Jyothi Kora, Bulletin of the National Research Centre 43 (2019) 205.*
61. *Applications of sand roasting and baking in the preparation of traditional Indian snacks: Nutritional and antioxidant status; Aruna Jyothi Kora, Bulletin of the National Research Centre 43 (2019) 158.*
62. *Plant arabinogalactan gum synthesized palladium nanoparticles: Characterization and properties; Aruna Jyothi Kora, Journal of Inorganic and Organometallic Polymers and Materials 29 (2019) 2054.*
63. *Multifaceted activities of plant gum synthesized platinum nanoparticles: Catalytic, peroxidase, PCR enhancing and antioxidant activities; Aruna Jyothi Kora, IET Nanobiotechnology 3(6) (2019) 602-608*
64. *Graphene oxide nanosheets in basic medium: A new potential adsorbent for microwave assisted cloud point extraction of beryllium from industrial effluents prior to ICP-OES determination; D. Sai Krishna, N. N. Meeravali and Sunil Jai Kumar, Analytical Methods 11 (2019) 2456.*
65. *Ultrasound-assisted extraction of Pb, Cd, Cr, Mn, Fe, Cu, Zn from edible oils with tetramethyl ammonium hydroxide and EDTA followed by determination using graphite furnace atomic absorption spectrometer; R. Manjusha, R. Shekhar and Sunil Jaikumar, Food Chemistry 294 (2019) 384.*
66. *Direct determination of impurities in high purity chemicals by electrolyte cathode discharge atomic emission spectrometry; R. Manjusha, R. Shekhar, Sunil Jai Kumar, Microchemical Journal 145 (2019) 301.*
67. *Characterization of Ultrapure Germanium (9N) Using a Wet Chemical Method for ICP-QMS and HR-CS-GFAAS Analysis; M. A. Reddy, R. Shekhar, Sunil Jai Kumar, Atomic Spectroscopy 40 (2019) 1.*
68. *Development of a simple and rapid microwave-assisted extraction method using very dilute solutions of perchloric acid and hydrogen peroxide for the multi-elemental analysis of food materials by ICP-OES: A green analytical method; M. V. Balarama Krishna, K. Chandrasekaran, G. Venkateswarlu and D. Karunasagar, Microchemical Journal 146 (2019) 807.*
69. *Hydrogen storage studies in Pd/Ti/Mg films; G.L.N. Reddy, Sanjiv Kumar, International Journal of Hydrogen Energy, 43 (2018) 2840.*
70. *Studies on synthesis of plasma fusion relevant tungsten dust particles and measurement of their hydrogen absorption properties; Trinayan Sarmah, N. Aomoa, Sidananda Sarma, U. Deshpande, B. Satpati, Divesh N. Srivastava, Sanjiv Kumar, M. Kakati, G. De Temmerman, Fusion Engineering and Design 127 (2018) 120.*
71. *A novel surfactant assisted dispersive liquid-liquid microextraction for the removal/recovery of beryllium from industrial effluents; N. N. Meeravali, K. Madhavi, Sunil Jai Kumar, Desalination and water treatment 101 (2018) 283.*
72. *A novel synergetic salt- and acid-induced ligandless mixed micelle cloud point extraction of ultratrace levels of Cd, Hg, Bi, and Tl From petrochemical effluents followed by ETAAS determination; K. Ravi Kumar, K. Madhavi, P. Shyamala, N. N. Meeravali, Sunil Jai Kumar, Atomic Spectroscopy 39 (2018) 119.*

73. *Development of a novel and robust microprecipitation approach using cetyltrimethyl ammonium bromide (CTAB) for preconcentration and speciation of mercury in waters prior to CVAAS determination; M.V. Balarama Krishna Mullapudi, Nidhi Garg, Dheram Karunasagar, International Journal of Environmental Analytical Chemistry 98 (2018) 811.*
74. *Determination of Thorium and Uranium in nickel based alloys by ICP-MS after matrix separation using novel co-polymer of ethylene glycol methacrylate and Bis[2-methacryloyloxyethyl] phosphate; M.V.Balarama Krishna, Sankararao Chappa, K. Chandrasekaran, D. Karunasagar, Ashok K. Pandey, Atomic Spectroscopy 39 (2018) 142.*
75. *A novel UV-photolysis approach with acetone and isopropyl alcohol for the rapid determination of fluoride in organofluorine-containing drugs by spectrophotometry; M. V. Balarama Krishna, D. Karunasagar, Journal of Food and Drug Analysis 26 (2018) 385.*
76. *Study of fluoride content in some commercial phosphate fertilizers; L. P. Ramteke, A. C. Sahayam, A. Ghosh, U. Rambabu, M. R. P. Reddy, K. M. Popat, B. Rebary, D. Kubavat, K. V. Marathe, P. K. Ghosh, Journal of Fluorine Chemistry 210 (2018) 149.*
77. *Bacillus cereus, selenite reducing bacterium from contaminated lake of an industrial area: A renewable nanofactory for the synthesis of selenium nanoparticle; Aruna Jyothi Kora, Bioresources and Bioprocessing 5 (2018) 1.*
78. *Gram +ve bacterium Staphylococcus aureus: A potential source for the green biosynthesis of monodispersed, smaller selenium nanoparticles; Aruna Jyothi Kora, Micro and Nano Letters 3 (2018) 1155.*
79. *Tree gum stabilized selenium nanoparticles: Characterization and antioxidant activity; Aruna Jyothi Kora, IET Nanobiotechnology 12 (2018) 658.*
80. *Peroxidase activity of biogenic platinum nanoparticles: A colorimetric probe towards selective detection of mercuric ions in water samples;, Aruna Jyothi Kora, Lori Rastogi, Sensors and Actuators B: Chemical 254 (2018) 690.*
81. *Biogenic silver nanoparticles synthesized with rhamnogalacturonan gum: Antibacterial activity, cytotoxicity and its mode of action; Aruna Jyothi Kora, R. B. Sashidhar, Arabian Journal of Chemistry 11 (2018) 313.*
82. *Growth and metabolic characteristics of hydrocarbon degrading bacteria isolated from an oil refinery soil; Aruna Jyothi Kora, Indian Journal of Geo-marine Sciences 47 (2018) 1029.*
83. *Green synthesis of palladium nanoparticles using gum ghatti (Anogeissus latifolia) and its application as an antioxidant and catalyst; Aruna Jyothi Kora, Lori Rastogi, Arabian Journal of Chemistry 11 (2018) 1097.*
84. *Speciation analysis of thallium in tobaccos using liquid chromatography inductively coupled plasma mass spectrometry W. –T. Chen, S. -J. Jiang, A. C. Sahayam, Microchemical Journal 141 (2018) 104.*
85. *Using electrothermal vaporization inductively coupled plasma mass spectrometry to determine S, As, Cd, Hg, and Pb in fuels; C. –H. Wu, S. –J. Jiang, A. C. Sahayam, Spectrochimica Acta Part B: Atomic Spectroscopy 147 (2018) 115.*
86. *Chemical vapor generation sample introduction for the determination of As, Cd, Sb, Hg, and Pb in nail polish by inductively coupled plasma mass spectrometry; F. –F. Huang, S. –J. Jiang, Y. –L. Chen, A. C. Sahayam, Spectrochimica Acta Part B: Atomic Spectroscopy 140 (2018) 84.*
87. *$^{18}O(p,p\gamma)^{18}O$ nuclear reaction in the determination of oxygen by proton induced gamma-ray emission; Y. Sunitha, Sanjiv Kumar, Journal of Radioanalytical and Nuclear Chemistry 314 (2017) 1803.*
88. *$^{10}B/^{11}B$ isotopic ratio and atomic composition of boron carbide: determination by proton induced γ-ray emission and proton elastic backscattering spectrometry; Y. Sunitha, Sanjiv Kumar, Applied radiation and Isotopes 128 (2017) 28.*
89. *Depth profiling Li in electrode materials of lithium ion battery by $^{7}Li(p,\gamma)^{8}Be$ and $^{7}Li(p,\alpha)^{4}He$ nuclear reactions; Y. Sunitha, Sanjiv Kumar, Nuclear Instruments and Methods in Physics Research B 400 (2017) 22.*
90. *Development of a simple and robust microwave-assisted decomposition method for the determination of rare earth elements in coal fly ash by ICP-OES; M. V. Balarama Krishna, G. Venkateswarlu, D. Karunasagar, Analytical Methods 9 (2017) 2031.*
91. *Development of on-line UV-induced volatile species generation for selenium speciation [Se(IV) and SeCN-] by ion chromatography-inductively coupled plasma mass spectrometry in petroleum refinery wastewater; K. Chandrasekaran, Nidhi Garg, D. Karunasagar, Journal of Analytical Atomic Spectrometry 32 (2017) 796.*
92. *Peroxidase-like activity of gum kondagogu reduced/stabilizedpalladium nanoparticles and its analytical application for colorimetricdetection of glucose in biological samples; Lori Rastogi, D. Karunasagar, R.B Sashidhar, Archana Giri, Sensors and Actuators B 240 (2017) 1182.*
93. *Selective colorimetric/visual detection of Al^{3+} using ascorbic acid capped gold nanoparticles in aqueous systems; Lori Rastogi, K. Dash, A. Ballal , Sensors and Actuators B, 248 (2017) 124.*
94. *Determination of antimony compounds in waters and juices using ion chromatography-inductively coupled plasma mass spectrometry; Y. –A. Lin, S. –J. Jiang, A. C. Sahayam, Food Chemistry 230 (2017) 76.*
95. *Speciation of mercury in fish oils using liquid chromatography inductively coupled plasma mass spectrometry; C. –H. Yao, S. –J. Jiang, A. C. Sahayam, Y. –L. Huang , Microchemical Journal 133 (2017) 556.*
96. *Electrothermal Vaporization Inductively Coupled Plasma Mass Spectrometry for the Determination of Cr, Cd, Hg, and Pb in Honeys; Y. –T. Li, S. –J. Jiang, A. C. Sahayam, Food Analytical Methods 10 (2017) 434.*
97. *Physico-chemical and bacteriological screening of Hussain Sagar lake: An urban wetland; Aruna Jyothi Kora, Lori Rastogi, Sunil Jai Kumar, B. N. Jagatap, Water Science 31 (2017) 24.*
98. *Bacteriogenic synthesis of selenium nanoparticles by Escherichia coli ATCC 35218 and its structural characterization; Aruna Jyothi Kora, Lori Rastogi, IET Nanobiotechnology 11 (2017) 179.*
99. *Determination of F, Na, Mg, Al and P in Indian tea powders by proton induced γ-ray emission technique; Y. Sunitha, A. Sarkar, Sanjiv Kumar, Analytical Methods 8 (2016) 7116.*
100. *Oxygen determination in materials by $^{18}O(p,\alpha\gamma)^{15}N$ nuclear reaction; Sanjiv Kumar, Y. Sunitha, G. L. N. Reddy, A. A. Sukumar, J. V. Ramana, A. Sarkar, Rakesh Verma, Nuclear Instruments and Methods in Physics Research B, 378 (2016) 38.*

101. *Synthesis of binary and multinary metal sulphides by precipitation and their characterization; Pritty Rao, Sanjiv Kumar, Naina Raje, R. B. Tokas, N. K. Sahoo, Materials Research Bulletin 79 (2016) 105.*
102. *A sensitive speciation analysis of chromium in natural and industrial effluents by electrothermal atomic absorption spectrometry after a novel ligandless mixed-micelle dispersive liquid–liquid microextraction; N. N. Meeravali, K. Madhavi, Sunil Jai Kumar, Journal of Analytical Atomic Spectrometry 31 (2016) 1582.*
103. *Green technology for monitoring the quality of water: Determination of toxic trace analyte concentrations using multi-elemental mixed micelle cloud point extraction; N. N. Meeravali, R. Manjusha, K. Madhavi, Sunil Jai Kumar, Desalination and Water Treatment, 57 (2016) 26880.*
104. *A new ion pair-based surfactant-assisted dispersive liquid-liquid microextraction of ultra trace levels of beryllium from natural and effluent samples followed by ETAAS determination;, N. N. Meeravali, K. Madhavi, Sunil Jai Kumar, Atomic Spectroscopy 37 (2016) 202.*
105. *Dispersive liquid-liquid microextraction for simultaneous preconcentration of platinum group elements (Pd, Os, Ir, and Pt) and selected transition elements (Ag, Cd, Ta, and Re) at parts per trillion levels in water and their determination by inductively coupled plasma-mass spectrometry; K. Chandrasekaran, D. Karunasagar, Journal of Analytical Atomic Spectrometry 31, 5 (2016) 1131.*
106. *Speciation of chromium in edible animal oils after microwave extraction and liquid chromatography inductively coupled plasma mass spectrometry; Y. -A. Lin, S. –J. Jiang, A. C. Sahayam, Y. –L., Huang , Microchemical Journal, 128 (2016) 274.*
107. *Determination of As, Hg and Pb in herbs using slurry sampling flow injection chemical vapor generation inductively coupled plasma mass spectrometry; C. -Y. Tai, S.-J.Jiang, A. C. Sahayam, Food Chemistry 192 (2016) 274.*
108. *Biomimetic synthesis of selenium nanoparticles by Pseudomonas aeruginosa ATCC 27853: An approach for detoxification of selenite; Aruna Jyothi Kora, Lori Rastogi, Journal of Environmental Management, 181 (2016) 231.*
109. *Exopolymer produced by Pseudomonas aeruginosa: A super sorbent for ruthenium; Aruna Jyothi Kora, Anupkumar Bhaskarapillai and Toleti Subba Rao, Separation Science and Technology 51 (2016) 1455.*
110. *Catalytic degradation of anthropogenic dye pollutants using palladium nanoparticles synthesized by gum olibanum, aglucuronoarabinogalactan biopolymer; Aruna Jyothi Kora, Lori Rastogi, Industrial Crops and Products 81 (2016) 1.*
111. *Traceable quantitation of cyanocobalamin (vitaminB12) via measurement of cobalt and phosphorus: a comparative assessment using inductively coupled plasma atomic emission spectrometry (ICP-AES) and ion chromatography (IC); K. Dash, Lori Rastogi, S. Thangavel, G. Venkateswarlu, RSC Advances 6 (2016) 111090.*
112. *An improved matrix separation method for characterization of ultrapure germanium (8N); M. A. Reddy, R. Shekhar, Sunil Jai Kumar, Talanta 159 (2016) 14.*
113. *Modified matrix volatilization setup for characterization of high purity germanium; Adisesharedy Meruva, Raparthi Shekhar, Sunil Jai Kumar, Talanta, 146 (2016) 259.*
114. *A probe into compositional and structural dependence of optical properties of lanthanum fluoride films prepared by resistive heating; Pritty Rao, Sanjiv Kumar, N. K. Sahoo, R. B. Tokas, Nuclear Instruments and Methods in Physics Research B, 342 (2015) 108.*
115. *Swift heavy ion beam mixing at V/Si interface; Reena Verma, Sanjiv Kumar, C. Lal, I.P. Jain, Current Applied Physics 15 (2015) 129.*
116. *Investigation on trace and major elements in anti-asthmatic medicinal plants by PIXE and PIGE techniques; R. K. Bhanisana Devi, H. Nandakumar Sarma, Sanjiv Kumar, Nuclear Instruments and Methods in Physics Research B, 343 (2015) 163.*
117. *Influence of boat material on the structure, stoichiometry and optical properties of gallium sulphide films prepared by thermal evaporation; Pritty Rao, Sanjiv Kumar, N. K. Sahoo, Materials Chemistry and Physics 164 (2015) 149.*
118. *Sol-gel synthesis of manganese oxide films and their predominant electrochemical propertie;, Abhimanyu Sarkar, Ashis Kumar Satpati, Vikram Kumar, Sanjiv Kumar, Electrochemica Acta 167 (2015) 126.*
119. *Electron beam deposition of amorphous manganese oxide thin film electrodes and their predominant electrochemical properties; Abhimanyu Sarkar, Ashis Kumar Satpati, Pritty Rao, Sanjiv Kumar, Journal of Power Sources, 284 (2015) 264.*
120. *Spectral tunability of cerium photoluminescence in nano sized LaF_3:Ce^{3+}; T. K. Srinivasan, N. Suriyamurthy, A. A. Sukumar, B. S. Panigrahi, B. Venkatraman, AIP Conf. Proc., 1665 (2015) 050024.*
121. *Development of a Method for the Microwave Assisted Digestion of Soils using Dilute Acids - Simultaneous Determination of 18 Trace Elements by Inductively Coupled Plasma-Mass Spectrometry; K. Chandrasekaran, P. R. Mamatha, D. Karunasagar, Atomic Spectroscopy 36 (2015) 202.*
122. *Robust ultrasound assisted extraction approach using dilute TMAH solutions for the speciation of mercury in fish and plant materials by cold vapour atomic absorption spectrometry (CVAAS); M. V. Balarama Krishna, D. Karunasagar, Analytical methods 7 (2015) 1997.*
123. *A novel Cu-BSA nanocomposite based vapour generation approach for the rapid determination of Hg in environmental and biological samples by CVAAS; M. V. Balarama Krishna, Lori Rastogi, D. Karunasagar, J. Nanoscience Letters, 5, (2015) 1.*
124. *An integrated approach based on oxidative pyrolysis and microwave-assisted digestion for the multi-elemental analysis of coal samples by ICP-based techniques; M. V. Balarama Krishna, K. Chandrasekaran, S. Chakravarthy, D. Karunasagar, Fuel 158 (2015) 770.*
125. *Antibacterial effects of gum kondagogu reduced/stabilized silver nanoparticles in combination with various antibiotics: A mechanistic approach; Lori Rastogi, Aruna Jyothi Kora, R. B. Sashidhar, Applied Nanoscience, 5 (2015) 535.*
126. *Bioprospecting of tree gums as a nanocomposite material for the synthesis of antibacterial silver nanoparticles; Aruna Jyothi Kora, R. B. Sashidhar, National Journal of Life Sciences 12 (2015) 127.*
127. *Antibacterial activity of biogenic silver nanoparticles synthesized with gum ghatti and gum olibanum: A comparative study; Aruna Jyothi Kora, R. B. Sashidhar, The Journal of antibiotics, 68 (2015) 88.*
128. *Isolation and characterization of an exopolymer producing pigmented Pseudomonas sp. from a nuclear desalination plan;, Aruna Jyothi Kora, T. S. Rao , Indian Journal of Geo-Marine Sciences, 44 (2015) 1358.*
129. *Determination of Pb in lipsticks by flow injection chemical vapor generation isotope dilution inductively coupled plasma mass spectrometry;, W. –N. Chen, S. –J. Jiang, Y. –L. Chen, A. C. Sahayam , Microchemical Journal 119 (2015) 128.*

130. *Determination of traces of As, B, Bi, Ga, Ge, P, Pb, Sb, Se, Si and Te in high-purity nickel using Inductively Coupled Plasma-Optical Emission Spectrometry (ICP-OES);, S.Thangavel, K. Dash, S.M.Dhavile, A.C.Sahayam, Talanta 131 (2015) 505.*
131. *Slurry sampling flow injection chemical vapor generation inductively coupled plasma mass spectrometry for the determination of trace Ge, As, Cd, Sb, Hg and Bi in cosmetic lotions; W. –N. Chen, S. –J. Jiang, Y. –L. Chen, A. C. Sahayam, Analytica Chimica Acta, 860 (2015) 8.*
132. *Synthesis of MgO nanoparticle loaded mesoporous Al_2O_3 and its defluoridation study; D. Dayananda, V. R. Sarva, S. V. Prasad, J. Arunachalam, P. Parameswaran, Narendra N. Ghosh, Applied Surface Science 329 (2015) 1.*
133. *A Simple Aqueous Solution Based Chemical Methodology for Preparation of Mesoporous Alumina: Efficient Adsorbent for Defluoridation of Water; D. Dayananda, V. R. Sarva, S. V. Prasad, J. Arunachalam, N. N. Ghosh, Particulate Science and Technology 33 (2015) 1.*
134. *Preparation of ZrO_2 nanoparticle loaded mesoporous Al_2O_3: A promising adsorbent for defluoridation of water; D. Dayananda, S. Gupta, V. R. Sarva, S. V. Prasad, J. Arunachalam, N. N. Ghosh , ScienceJet 4 (2015) 105.*
135. *Determination of trace elements in medicinal activated charcoal using slurry sampling electrothermal vaporization inductively coupled plasma mass spectrometry with low vaporization temperature; C. –C. Chen, S. –J. Jiang, A. C. Sahayam, Talanta 131 (2015) 585.*
136. *Determination of traces of As, B, Bi, Ga, Ge, P, Pb, Sb, Se, Si and Te in high-purity nickel using inductively coupled plasma-optical emission spectrometry (ICP-OES); S. Thangavel, K. Dash, S. M. Dhavile, A. C. Sahayam, Talanta 131 (2015) 505.*
137. *Dimensional dependence of voltage co-efficient of resistance (α_v) for PMNPT based varistors; K. V. N. S .V. P. L. Narasimham and K. Lal Kishore, Journal of The Institution of Engineers (India) 96 (2015) 349.*
138. *Tensile properties and fracture toughness of Zr–2.5Nb alloy pressure tubes of IPHWR220; H. K. Khandelwal, R. N. Singh, A. K. Bind, S. Sunil, J. K. Chakravartty, A. Ghosh, P. Dhandharia, D. Bhachawat, R. Shekhar, Sunil Jai Kumar, Nuclear Engineering and Design 293 (2015) 138.*
139. *Influence of post deposition annealing in air and vacuum on the properties of thermally evaporated gallium oxide films; Pritty Rao, Sanjiv Kumar, Superlattice and Microstructures 70 (2014) 117.*
140. *Depth profiling of titanium using a resonance in $^{48}Ti(p,\gamma)^{49}V$ nuclear reaction; G. L. N. Reddy, S. Vikram Kumar, J. V. Ramana, Sanjiv Kumar, Journal of Radioanalytical and Nuclear Chemistry 302 (2014) 1461.*
141. *Depth profiling Cr in surface layers by $^{52}Cr(p,\gamma)^{53}Mn$ nuclear resonance reaction analysis; Pritty Rao, S. Vikram Kumar, Sanjiv Kumar , Journal of Radioanalytical and Nuclear Chemistry 302 (2014) 1399.*
142. *Reversible hydrogen storage in vapour deposited Mg-5 at.% Pd powder composites; G. L. N. Reddy, Sanjiv Kumar, International Journal of Hydrogen Energy 328 (2014) 27.*
143. *Study of depth profile of hydrogen in hydrogenated diamond like carbon thin film using ion beam analysis technique; J. Datta, H. S. Biswas, P. Rao, G. L. N. Reddy, Sanjiv Kumar, N. R. Ray, D. P. Chowdhury, A. V. R. Reddy, Nuclear Instruments and Methods in Physics Research B 328 (2014) 27.*
144. *Study on the depth profile analysis of Fe/Co intermixing in [SmCo5/Fe]11 magnetic multilayers;, P. Saravanan, Jen-Hwa Hsu, A. Perumal, Anabil Gayen, G. L. N. Reddy, Sanjiv Kumar, S. V. Kamat, Physica B 448 (2014) 2.*
145. *Determination of boron concentration in borosilicate glass, boron carbide and graphite samples by conventional wet-chemical and nuclear analytical methods, K. Venkatesh, S. Chillar, G. S. Kamble, S. P. Pandey, M. Venkatesh, S. A. Kumar, Sanjiv Kumar, R. Acharya, P.K. Pujari, A.V.R. Reddy, J. Radioanal. Nucl. Chem., 302 (2014) 1425.*
146. *Precision two-photon spectroscopy of alkali elements , P. V. Kiran Kumar, M. V. Suryanarayana, Pramana - Journal of Physics, 83 (2014) 189.*
147. *Precision measurement of the hyperfine structure of $8d^2D_{3/2}$ state of ^{133}Cs by the radio frequency phase modulation technique, P.V. Kiran Kumar, B. Nisheeth, M. Sankari, M.V. Suryanarayana, Optics Communications, 320 (2014) 77.*
148. *Hyperfine structure and isotope shift measurements of the $4f^76s^2(^8S^o_{7/2})$–$4f^76s6p(^8P_{9/2})$ 601.8154nm transition in Eu I by laser induced atomic beam fluorescence spectroscopy; G. V. S. G. Acharyulu, M. Sankari, P.V. Kiran Kumar, M.V. Suryanarayana, Journal of Quantitative Spectroscopy and Radiative Transfer 133 (2014) 251.*
149. *A novel non-chromatographic strategy for the sequential/simultaneous extraction and analysis of chromium species by electrothermal atomic absorption spectrometry in effluents and different water source;, N. N. Meeravali, R. Manjusha, Sunil Jai Kumar, Journal of Analytical Atomic Spectrometry 29 (2014) 2168.*
150. *Sequential extraction of platinum, cisplatin and carboplatin from environmental samples and pre-concentration/separation using vesicular coacervative extraction and determination by continuum source ETAAS;, N. N. Meeravali, K. Madhavi, R. Manjusha, Sunil Jai Kumar, Talanta, 118 (2014) 37.*
151. *A novel Cu-BSA nanocomposite based vapour generation approach for the rapid determination of Hg in aqueous media by CVAAS and on-line flow injection ICP-MS; Lori Rastogi, M. V. Balarama Krishna, K. Chandrasekaran, D. Karunasagar, Journal of Analytical Atomic Spectrometry 29 (2014) 721.*
152. *Determination of trace elements in Pb-Bi-eutectic by ICP-QMS after sequential removal of matrix by precipitation; K. Chandrasekaran, D.Karunasagar, Journal of Analytical Atomic Spectrometry 29 (2014) 1720.*
153. *Development of microwave-assisted digestion method for the rapid determination of chloride and fluoride in nuclear-grade boron carbide powders; M. V. Balarama Krishna, S. V. Rao, Y. Balaji Rao, N. S. Shenoy, D. Karunasagar, Analytical methods 6 (2014) 261.*
154. *Development of oxidative pyrolysis procedure for the rapid determination of boron in nuclear-grade graphite powders; M. V. Balarama Krishna, K. Chandrasekaran, S. Thangavel, D. Karunasagar, Atomic Spectroscopy 35 (2014) 109.*
155. *Ultrasonic slurry sampling electrothermal vaporization inductively coupled plasma mass spectrometry for the determination of Cr, Fe, Cu, Zn and Se in cereals; S.-Y. Huang, S.-J. Jiang, A. C. Sahayam, Spectrochimica Acta Part B: Atomic Spectroscopy 101 (2014) 46.*

156. *Gum Kondagogu reduced/stabilized silver nanoparticles as direct colorimetric sensor for the sensitive detection of Hg^{2+} in aqueous system; Lori Rastogi, D. Karunasagar, B. Sashidhar Rao, J. Arunachalam, Talanta 118 (2014) 111.*
157. *Multi-element analysis of sunscreens using slurry sampling electrothermal vaporization inductively coupled plasma mass spectrometry; Y.-T. Li, S.-J. Jiang, Y.-L. Chen, A. C. Sahayam, Journal of Analytical Atomic Spectrometry 29 (2014) 2176.*
158. *Combined use of HPLC-ICP-MS and microwave assisted extraction for the determination of cobalt compounds in nutritive supplements; F. -Y. Yang, S. -J. Jiang, A. C. Sahayam, Food Chemistry 147 (2014) 215.*
159. *Preparation of CaO loaded mesoporous Al_2O_3: Efficient adsorbent for fluoride removal from water; Desagani Dayananda, Venkateswara R. Sarva, Sivankutty V. Prasad, Jayaraman Arunachalam, Narendra N. Ghosh, Chemical Engineering Journal 248 (2014) 430.*
160. *Traceable nucleic acid quantitation via phosphorus measurement by UV/visible spectrophotometry using crystal violet ion associate; K. Dash, S. Thangavel, Lori Rastogi, International Journal of Inorganic and Bioinorganic Chemistry 4 (2014) 16.*
161. *Microwave assisted extraction of Cr(III) and Cr(VI) from soil/sediments combined with ion exchange separation and inductively coupled plasma optical emission spectrometry detection; P. Mamatha, G. Venkateswarlu, A. V. N. Swamy, A. C. Sahayam, Analytical Methods 6 (2014) 9653.*
162. *Determination of cadmium in Zircaloys by electrolyte cathode discharge atomic emission spectrometry (ELCAD-AES); R. Manjusha, M. A. Reddy, R. Shekhar, Sunil Jai Kumar, Analytical methods 6 (2014) 9850.*
163. *Determination of thallium at trace levels by electrolyte cathode discharge atomic emission spectrometry with improved sensitivity; R. Shekhar, K. Madhavi, N. N. Meeravali, Sunil Jai Kumar, Analytical methods 6 (2014) 732.*
164. *A comparative study of conventionally sintered, microwave sintered and hot isostatic press sintered NZP and CZP structures interacted with fluoride; Ambarish Dey, Amit Das Gupta, Debrata Basu, Ritu D. Ambashta, Piaray Kishan Wattal, Sanjiv Kumar, Debasis Sen, S. Mazumder, Ceramic International 39 (2013) 9351.*
165. *Effect of Fe layer thickness and Fe/Co intermixing on the magnetic properties of Sm–Co/Fe bilayer exchange-spring magnets; P. Saravanan, J.H. Hsu, A. Gayen, A. K Singh, A. Perumal, G. L. N. Reddy, Sanjiv Kumar, S. V. Kamat, Journal of Physics D: Applied Physics 46 (2013) 155002.*
166. *Growth of copper indium sulphide films by thermal evaporation of mixtures of copper sulphide and indium sulphide powders; Pritty Rao, Sanjiv Kumar, N. K. Sahoo, Materials Research Bulletin 48 (2013) 2915.*
167. *Post analysis of an optical multilayer interference filter using numerical reverse synthesis and Rutherford backscattering spectrometry; N. K. Sahoo, Sanjiv Kumar, R. B. Tokas, S. Jena, S. Thakur, G. L. N. Reddy, Applied Optics 52 (2013) 2102.*
168. *Morphological variations of Mn-doped ZnO dilute magnetic semiconductors thin films grown by succesive ionic layer by adsorption reaction method; Subramanian Balamurali, Rathinam Chandramohan, Marimuthu Karunakaran, Thayan Mahalingam,Padmanaban Parameswaran, Nagamani Suryamurthy and Arcod Anandhakrishnan Sukumar, Microscopy Research and Technique 76 (2013) 751.*
169. *Hyperfine structure of the $7d\ ^2D_{3/2}$ level in cesium measured by Doppler-free two-photon spectroscopy; M. Sankari, P. V. Kiran Kumar, M.V. Suryanarayana, Physical Review A - Atomic, Molecular, and Optical Physics, 87 (2013) 012503.*
170. *Phase transfer catalyst assisted directly suspended droplet microextraction of platinum from geological and spent automobile converter samples prior to HR-CS-AAS determination; T. Revathi Reddy, N. N. Meeravali, A. V. R. Reddy, Analytical methods 5 (2013) 2343.*
171. *Novel reverse mixed micelle mediated transport of platinum and palladium through a bulk liquid membrane from real sample; T. Revathi Reddy, N. N. Meeravali, A. V. R. Reddy, Separation and Purification Technology 103 (2013) 71.*
172. *Reverse micelle mediated bulk liquid membrane separation of platinum, gold and silver from real samples; T. Revathi Reddy, N. N. Meeravali, A. V. R. Reddy, Separation Science and Technology 48 (2013) 1859.*
173. *A sensitive method for determination of phosphorous by continuum source graphite furnace atomic absorption spectrometry after a novel ionic liquid assisted CP; Sunil Jai Kumar, N. N. Meeravali, Manjusha Ranjit, Journal of Analytical Atomic Spectrometry 28 (2013) 585.*
174. *Microwave assisted aqua regia extraction of thallium from sediment and coal fly ash samples and interference free determination by continuum source ETAAS after CPE; N. N. Meeravali, K. Madhavi, Sunil Jai Kumar, Talanta, 104 (2013) 180.*
175. *Selenium Speciation by Liquid Chromatography-Particle Beam/Mass Spectrometry (LC-PB/MS): Application to a Yeast Reference Material and Synthetic Urine; J. Castro, M.V. Balarama Krishna, G. Ojeda, R. Kenneth Marcus, Analytical methods 5 (2013) 4053.*
176. *Oxidative pyrolysis combined with microwave-assisted extraction method for the multi-elemental analysis of boron carbide powders by inductively coupled plasma optical emission spectrometry (ICP-OES); M. V. Balarama Krishna, G. Venkateswarlu, S. Thangavel, D. Karunasagar, Analytical methods 5 (2013) 1515.*
177. *Dispersive liquid-liquid micro extraction of boron as tetrafluoroborate ion ($BF4^-$) from natural waters, wastewater and seawater samples and determination using a micro-flow nebulizer in inductively coupled plasma-quadrupole mass spectrometry; K. Chandrasekaran, D. Karunasagar, J. Arunachalam, Journal of Analytical Atomic Spectrometry 28 (2013) 142.*
178. *Determination of traces of boron in graphite powder by Inductively Coupled Plasma – Optical Emission Spectrometer (ICP-OES); S. Thangavel, K. Dash, S. M. Dhavile, A. C. Sahayam, Analytical Methods 5 (2013) 5799.*
179. *Enhancement of antibacterial activity of capped silver nanoparticles in combination with antibiotics, on model Gram-negative and Gram-positive bacteria; Aruna Jyothi Kora, Lori Rastogi, Bioinorganic Chemistry and Applications 2013 (2013) 871097.*
180. *Biosynthesis of silver nanoparticles by the seed extract of Strychnos potatorum: A natural phytocoagulant; Aruna Jyothi Kora, Jayaraman Arunachalam, IET Nanobiotechnology 7 (2013) 83.*
181. *Synthesis and characterization of bovine serum albumin-copper nanocomposites for antibacterial applications; Lori Rastogi, J. Arunachalam, Colloids and surfaces B: Biointerface 108 (2013) 134.*
182. *Green synthetic route for the size controlled synthesis of biocompatible gold nanoparticles using aqueous extract of garlic (Allium sativum); Lori Rastogi, J. Arunachalam, Advanced Materials Letters 4 (2013) 548.*

183. *Accurate quantitation standards of glutathione via traceable sulfur measurement by inductively coupled plasma optical emission spectrometry and ion chromatograph; Lori Rastogi, K. Dash, J. Arunachalam, Journal of Pharmaceutical Analysis 3 (2013) 180.*
184. *Determination of Cu, As, Hg and Pb in vegetable oils by electrothermal vaporization inductively coupled plasma mass spectrometry with palladium nano particles as modifier; W. -H. Hsu, S. -J. Jiang, A. C. Sahayam, Talanta 117 (2013) 268.*
185. *Determination of Pd, Rh, Pt, Au in road dust by electrothermal vaporization inductively coupled plasma mass spectrometry with slurry sampling; W. -H. Hsu, S. -J. Jiang, A. C. Sahayam, Analytica Chimica Acta 794 (2013) 15.*
186. *Cloud point extraction of Cr, Cu, Cd, and Pb from water samples and determination by electrothermal vaporization inductively coupled plasma mass spectrometry with isotope dilution; Y. –Z. Yi, S. –Y. Wu, S. –J. Jiang, A. C. Sahayam, Atomic Spectroscopy 34 (2013) 39.*
187. *Accurate quantification standards of DNA via phosphorus measurement through microwave induced combustion (MIC)-ion chromatography; Kulamani Dash, Lori Rastogi, Jayaraman Arunachalam, International Journal of Chromatographic Science 3 (2013) 10.*
188. *Microwave-assisted green chemistry approach for trace level chloride determination in high purity magnesium by suppressed ion chromatography, K. Dash, S. Thangavel, International Journal of Chromatographic Science 3 (2013) 24.*
189. *Determination of major to trace level elements in Zircaloys by electrolyte cathode discharge atomic emission spectrometry using formic acid; R. Manjusha, M. A. Reddy, R. Shekhar, Sunil Jaikumar, Jounal of Analytical Atomic Spectroscopy 28 (2013) 1932.*
190. *Determination of Impurities in High Purity Germanium by Inductively Coupled Plasma Quadrupole Mass Spectrometry (ICP-QMS) after Matrix Volatilization using Chlorine Gas; M. A. Reddy, R. Shekhar, Sunil Jai Kumar, Atomic Spectroscopy 34 (2013) 119.*
191. *Growth of stoichiometric indium sulphide films by thermal evaporation: influence of vacuum annealing on structural and physical properties, Pritty Rao, Sanjiv Kumar, Thin Solid Films 524 (2012) 93.*
192. *Simultaneous determination of ^{14}N and ^{15}N isotopes in opium by proton induced γ-ray emission technique; Pritty Rao, G. L. N. Reddy, S. Vikram Kumar, J. V. Ramana, N. Chattopadhyay, A. K. Basu, Seema Srivastava, R. K. Sarin, V. S. Raju, Sanjiv Kumar, Journal of Radioanalytical and Nuclear Chemistry 294 (2012) 127.*
193. *Depth profiling of oxygen in oxide films by $^{18}O(p,\alpha)^{15}N$ nuclear reaction analysis; G. L. N. Reddy, Pritty Rao, J. V. Ramana, S. Vikramkumar, V. S. Raju, Sanjiv Kumar , Journal of Radioanalytical and Nuclear Chemistry 294 (2012) 401.*
194. *Investigation of major and trace elements in some medicinal plants using PIXE , R. Kaur, A. Kuma, Navneet Kaur, B. P. Mohanty, M. Oswal, K. P. Singh, B. R. Behera, G. Singh, R. Puri, S. Sharma, Sanjiv Kumar, Pritty Rao, S. Vikramkumar, International Journal of PIXE 22 (2012) 113.*
195. *Indirect determination of Li via $^{74}Ge(n,\gamma)^{75m}Ge$ activation reaction induced by neutron from $^{7}Li(p,n)^{7}Be$ reaction; Sanjiv Kumar, G. L. N. Reddy, Pritty Rao, R. Verma, J. V. Ramana, S. Vikramkumar, V. S. Nuclear Instruments and Methods in Physics Research B 274 (2012) 154.*
196. *Measurement of the hyperfine splitting of the $9S_{1/2}$ level in Cesium by Doppler-free two-photon Spectroscopy; P.V. Kiran Kumar, M.V. Suryanarayana, Optics Communications 285 (2012) 1838.*
197. *Determination of Cd, Pb, Cu, Ni and Mn in effluents and natural waters by a novel salt induced mixed-micelle cloud point extraction using ETAAS; N. N. Meeravali, Sunil Jai Kumar, Analytical methods 4 (2012) 2435.*
198. *Dispersive liquid-liquid micro-extraction for simultaneous preconcentration of 14 lanthanides at parts per trillion levels from groundwater and determination using a micro-flow nebulizer in inductively coupled plasma quadrupole mass spectrometry; K. Chandrasekaran, D. Karunasagar, J. Arunachalam, Journal of Analytical Atomic Spectrometry 27 (2012) 1024.*
199. *A simple and rapid microwave-assisted extraction method using polypropylene tubes for the determination of total mercury in environmental samples by flow injection chemical vapour generation inductively coupled plasma mass spectrometry (FI-CVG-ICPMS); M. V. Balarama Krishna, K. Chandrasekaran, D. Karunasagar, Analytical methods 4 (2012) 1401.*
200. *A cost-effective and rapid microwave-assisted acid extraction method for the multi-elemental analysis of sediments by inductively coupled plasma atomic emission spectrometry (ICP-AES) and inductively coupled plasma mass spectrometry (ICP MS); M. V. Balarama Krishna, K. Chandrasekaran, G. Venkateswarlu, D. Karunasagar, Analytical methods 4 (2012) 3290.*
201. *Determination of trace elements in lead and lead based alloys by inductively coupled plasma optical emission spectrometry after separation of lead as lead fluoride precipitate; G. Venkateswarlu, A. C. Sahayam, S. C. Chaurasia, C. Das, Atomic Spectroscopy 33 (2012) 193.*
202. *Green fabrication of silver nanoparticles by gum tragacanth (Astragalus gummifer): A dual functional reductant and stabilizer; Aruna Jyothi Kora, J. Arunachalam, Journal of Nanomaterials 2012 (2012) 869765.*
203. *Size-controlled green synthesis of silver nanoparticles mediated by gum ghatti (Anogeissus latifolia) and its biological activit; Aruna Jyothi Kora, Sashidhar Rao Beedu, Arunachalam Jayaraman, Organic and Medicinal Chemistry Letters 2 (2012) 17.*
204. *Leaf extract of Dendrophthoe falcata: A renewable source for the green synthesis of antibacterial silver nanoparticles; Aruna Jyothi Kora, J. Arunachalam, Journal of Biobased Materials and Bioenergy 6 (2012) 158.*
205. *Aqueous extract of gum olibanum (Boswellia serrata): A reductant and stabilizer for the biosynthesis of antibacterial silver nanoparticles; Aruna Jyothi Kora, Sashidhar Rao Beedu, J. Arunachalam, Process Biochemistry 47 (2012) 1516.*
206. *Highly stable, protein capped gold nanoparticles as effective drug delivery vehicles for amino-glycosidic antibiotics; Lori Rastogi, Aruna Jyothi Kora, J. Arunachalam, Materials Science & Engineering C 32 (2012) 1571.*
207. *Microwave-assisted green synthesis of small gold nanoparticles using aqueous garlic (Allium sativum) extract: their application as antibiotic carriers; Lori Rastogi, J. Arunachalam, International Journal of Green Nanotechnology 4 (2012) 163.*
208. *Cloud point extraction combined with flow injection vapor generation inductively coupled plasma mass spectrometry for preconcentration and determination of ultra trace Cd, Sb and Hg in water samples; P. -H. Liao, S. -J. Jiang, A. C. Sahayam, Journal of Analytical Atomic Spectrometry 27 (2012) 1515.*

209. *Determination of trace elements in silicon powders by inductively coupled plasma quadrupole mass spectrometry with a membrane desolvation sample introduction system; P. -K. Hsiao, S. -J. Jiang, A. C. Sahayam, T. C. Hsiao, Atomic Spectroscopy 33 (2012) 1.*
210. *Palladium nanoparticles as the modifier for the determination of Zn As, Cd, Sb, Hg and Pb in biological samples by ultrasonic slurry sampling electrothermal vaporization inductively coupled plasma mass spectrometr;, Y. -Z. Yi, S. -J. Jiang, A. C. Sahayam, Journal of Analytical Atomic Spectrometry 27 (2012) 426.*
211. *Sample treatment approaches for trace level determination of cesium in hepatitis B vaccine by suppressed ion chromatograph; K. Dash, S. Thangavel, L. Rastogi, S. M. Dhavile, J. Arunachalam , Chromatographia 75 (2012) 17.*
212. *Determination of Boron in Uranium-Aluminum-Silicon and Aluminum-Silicon-Nickel (SILUMIN) Alloys by Inductively Coupled Plasma Atomic Emission (ICP-AES); S. Thangavel, K. Dash, S. M. Dhavile, S. C. Chaurasia, J. Arunachalam, Atomic Spectroscopy 33 (2012) 31.*
213. *DNA quantification via traceable phosphorus measurement through microwave-assisted UV digestion – ion chromatography; K. Dash, L. Rastogi, J. Arunachalam, Analyst 137 (2012) 668.*
214. *A simple in- house dry ashing chamber for the rapid determination of total mercury in organic- rich solid materials by oxidative pyrolysis followed by CVAAS and FI- ICPMS detection; M. V. Balarama Krishna, A. C. Sahayam, D. Karunasagar, Analytical Methods 4 (2012) 586.*
215. *Electrochemical characterization of oxide film formed at high temperature on Alloy 690; Geogy J. Abraham, Rajan Bhambroo, V. Kain, R. Shekhar, G. K. Dey, V. S. Raja, Nuclear Engineering and Design 243 (2012) 69.*
216. *Improvement of sensitivity of electrolyte cathode discharge atomic emission spectrometry (ELCAD-AES) for mercury using acetic acid medium; R. Shekhar, Talanta 93 (2012) 32.*
217. *Incorporation of transparent conducting oxide characteristics and oxygen analysis in vacuum annealed indium oxide films; Pritty Rao, Sanjiv Kumar, Santanu Bera, G. L .N. Reddy, J. V. Ramana, V. S. Raju, Nuclear Instruments and Methods in Physics Research B 269 (2011) 2549.*
218. *Measurement of differential cross-sections and widths of resonances in $^{32}S(p, p'\gamma)^{32}S$ reaction in the 3.0–4.0 MeV region; Pritty Rao, Sanjiv Kumar, S. Vikramkumar, V. S. Raju, Nuclear Instruments and Methods in Physics Research B 269 (2011) 2557.*
219. *Isotope shift and hyperfine structure measurements of $4s\ ^2S_{1/2} \rightarrow 6s\ ^2S_{1/2}$ two-photon transition of potassium isotope; P.V. Kiran Kumar, M.V. Suryanarayana, Journal of Physics B: Atomic, Molecular and Optical Physics 44 (2011) 055003.*
220. *Theoretical and Experimental Understanding of the Anomalous Odd-to-Even Isotope Ratios of Tin in a 1 + 1 Single-Colour Resonance Ionization Mass Spectrometry: Revisited; Manda Sankari, International Journal of Optics 2011 (2011) 473910.*
221. *A sensitive sequential non-chromatographic speciation analysis of chromium in natural/wastewaters by inductively coupled optical emission spectrometr; N. N. Meeravali, K. Madhavi, Sunil Jai Kumar, Journal of Analytical Atomic Spectrometry 26 (2011) 214.*
222. *Development of Low-Voltage Varistors using doped nano Zinc oxide Powder; K. V. N. S. V. P. L. Narasimham, Y. Sunita, J. Arunachalam and K. Lal Kishore, Technology Spectrum 5 (2011) 36.*
223. *Dispersive liquid-liquid micro extraction of uranium(vi) from groundwater and seawater samples and determination by inductively coupled plasma-optical emission spectrometry and flow injection-inductively coupled plasma mass spectrometry; K. Chandrasekaran, D. Karunasagar, J. Arunachalam, Analytical Methods 3 (2011) 2140.*
224. *Ultraviolet Photolysis assisted mineralization and determination of trace levels of Cr, Cd, Cu, Sn, and Pb in isosulfan blue by ICP-MS; K. Dash, G. Venkateswarlu, S. Thangavel, S. C. Chaurasia, Microchemical Journal 98 (2011) 312.*
225. *Determination of trace elements in silicon powder using slurry sampling electrothermal vaporization inductively coupled plasma mass spectrometry; P. -K. Hsiao, S. -J. Jiang, A. C. Sahayam, Journal of Analytical Atomic Spectrometry 26 (2011) 586.*
226. *Rapid green synthesis of highly stable silver nanoparticles using aqueous garlic extract under sunlight and their antibacterial potential; Lori Rastogi, J. Arunachalam, Materials Chemistry and Physics 129 (2011) 558.*
227. *Assessment of antibacterial activity of silver nanoparticles on Pseudomonas aeruginosa and its mechanism of action; Aruna Jyothi Kora, J. Arunachalam, World Journal of Microbiology and Biotechnology 27 (2011) 1209.*
228. *Incorporation of oxygen during oxidative annealing of thermally evaporated In films; Pritty Rao, Sanjiv Kumar, G. L. N. Reddy, S. Veena, S. Kalavathi, J. V. Ramana, V. S. Raju, Nuclear Instruments and Methods in Physics Research B, 268 (2010) 3395.*
229. *Coexistence of anion and cation vacancy defects in vacuum-annealed In_2O_3 thin films; C. Sudakar, A. Dixit, Sanjiv Kumar, M. B. Sahana, G. Lawes, R. Naik, V. M. Naik, Scripta Materialia 62 (2010) 63.*
230. *Competitive adsorption of toxic heavy metal contaminants by gum kondagogu (Cochlospermum gossypium): A natural hydrocolloid; V.T.P. Vinod, R. B Sashidhar, A. A. Sukumar, Colloids and Surfaces B: Biointerfaces 75 (2010) 490.*
231. *Mixed-micelle cloud point extraction combined with inductively coupled plasma mass spectrometry for pre-concentration and determination of platinum from geological matrices; N. N. Meeravali, Shiuh-Jen Jiang, Atomic Spectroscopy 31 (2010) 111.*
232. *In situ enhanced hydrophobic character induced clouding phenomenon in mixed micelle combined with CV-AAS for the determination of mercury in environmental matrices; N. N. Meeravali, Manjusha Ranjit, Sunil Jai Kumar, Atomic Spectroscopy 31 (2010) 143.*
233. *An acid induced mixed-micelle mediated cloud point extraction for the separation and pre-concentration of platinum from road dust and determination by inductively coupled plasma mass spectrometry; N. N. Meeravali, Sunil Jai Kumar, Shiuh-Jen Jiang, Analytical Methods 2 (2010) 1101.*
234. *On-Line Speciation of Inorganic Arsenic in Natural Waters using Polyaniline (PANI) with Determination by Flow Injection-Hydride Generation-Inductively Coupled Plasma Mass Spectrometry at Ultra-Trace Levels; K. Chandrasekaran, M. V. Balarama Krishna, D. Karunasagar, Journal of Analytical Atomic Spectrometry 25 (2010) 1348.*

235. *On-line speciation of inorganic and methyl mercury in waters and fish tissues using polyaniline micro-column and flow injection-chemical vapour generation-inductively coupled plasma mass spectrometry (FI-CVG-ICPMS); M.V. Balarama Krishna, K. Chandrasekaran, D. Karunasagar, Talanta 81 (2010) 462.*
236. *Gum kondagogu (Cochlospermum gossypium): A template for the green synthesis and stabilization of silver nanoparticles with antibacterial application; Aruna Jyothi Kora, R. B. Sashidhar, J. Arunachalam, Carbohydrate Polymers 82 (2010) 670.*
237. *Protection against radiation induced oxidative damage by an ethanolic extract of Nigella sativa L, Lori Rastogi, Feroz Shaikh, Badri Narain Pandey, Arti Jagtap, Kaushala Prasad Mishra, International Journal of Radiation Biology 86 (2010) 719.*
238. *Distribution of heavy metals in the vicinity of a nuclear power plant, east coast of India: With emphasis on copper concentration and primary productivity; R. Rajamohan, T. S. Rao, B. Anupkumar, A. C. Sahayam, M. V. Balarama Krishna, V. P. Venugopalan, S. V. Narasimhan, Indian Journal of Marine Sciences 39 (2010) 182.*
239. *Synergistic effect of methyl isobutyl ketone (MIBK) and tributyl butyl phosphate (TBP) on extraction of tellurium for the determination of trace impurities in tellurium; G. Venkateswarlu, A. C. Sahayam, S. C. Chaurasia, Atomic Spectroscopy 31 (2010) 187.*
240. *Dry ashing of organic rich matrices with palladium for the determination of arsenic using ICP-MS; A.C. Sahayam, S. C. Chaurasia, G. Venkateswarlu, Analytica Chimica Acta 661 (2010) 17.*
241. *Fluoride removal from ground water by sol-gel γ-alumina coated ceramic honeycomb; K. Dash, U. S. Hareesh, R. Johnson, J. Arunachalam , Water Practice &Technology 5 (2010) 61.*
242. *Study of Trace Metal Profile of Palm Wine (Elaeis guineensis) Using ICP-AES and ICP-MS; K. Dash, S. V. Rao, G. Venkateswarlu, S. Thangavel, S. C. Chaurasia, Atomic Spectroscopy 31 (2010) 182.*
243. *Determination of mercury in Hepatitis-B vaccine by electrolyte cathode glow discharge atomic emission spectrometry (ELCAD-AES); R. Shekhar, D. Karunasagar, K. Dash, Manjusha Ranjit, Journal of Analytical Atomic Spectrometry 25 (2010) 875.*
244. *Studies on interdiffusion in Pd/Mg/Si films: towards improved cyclic stability in hydrogen storage; Y. Sunitha, G. L. N. Reddy, Sanjiv Kumar, V.S. Raju, Applied Surface Science 256 (2009) 1553.*
245. *Intermixing and formation of Pd-Mg intermetallics in Pd/Mg/Si film; G. L. N. Reddy, Sanjiv Kumar, Y. Sunitha, S. Kalavathi, V. S. Raju, Journal of Alloys and Compounds 481 (2009) 714.*
246. *Hydrogen storage in Pd capped thermally grown Mg films: studies by nuclear resonance reaction analysis; Sanjiv Kumar, G. L. N. Reddy, V. S. Raju, Journal of Alloys and Compounds 476 (2009) 500.*
247. *Surface and interface reactions of sputtered TiNi/Si thin films; A. K. Nanda Kumar, S. Jayakumar, M. D. Kannan, S. Rajagopalan, A. K. Balamurugan, K. Tyagi, Sanjiv Kumar, G. L. N. Reddy, J. V. Ramana, V. S. Raju, Journal of Applied Physics 105 (2009) 063517.*
248. *Strong plasmon absorption in InN thin films; A. Dixit, C. Sudhakar, J. S. Thakur, K. Padmanabhan, Sanjiv Kumar, R. Naik, V. M. Naik, G. Lawes, Journal of Applied Physics 105 (2009) 053104.*
249. *Measurement of Ge escape peaks in PIXE spectra recorded using high purity Ge (HPGe) detector; Sanjiv Kumar, G. L. N. Reddy, V. S. Raju, International Journal of PIXE 19 (2009) 67.*
250. *Isotope shifts and hyperfine structure in the 555.8-nm $^1S_0$-$^3P_1$ line of Yb; KanhaiyaPandey, Alok K. Singh, P. V. Kiran Kumar, M. V. Suryanarayana, Vasant Natarajan, Physical Review A - Atomic, Molecular, and Optical Physics, 80 (2009) 022518.*
251. *Optical selectivity calculations of ^{90}Sr isotope indouble optical resonance photoionization schemes; M. Sankari, J. Opt. Soc. Am. B, 26 (2009) 400.*
252. *A novel cloud point extraction approach using cationic surfactant for the separation and preconcentration of chromium species in natural water prior to ICP-DRC-MS determination; N. N. Meeravali, Shiuh-Jen Jiang, Talanta 80 (2009) 173.*
253. *Comparison of cloud point extraction and matrix volatilization procedures for Cr, Cu, Fe, Ni and Pb in a germanium matrix by graphite furnace atomic absorption spectrometry; M. A. Reddy, N. N. Meeravali, Sunil Jai Kumar, Atomic Spectroscopy 30 (2009) 89.*
254. *On-line preconcentration and recovery of palladium from waters using polyaniline (PANI) loaded in mini-column and determination by ICP-MS; elimination of spectral interferences; M. V. Balarama Krishna, Manjusha Ranjit, K. Chandrasekaran, G. Venkateswarlu, D. Karunasagar, Talanta 79 (2009) 1454.*
255. *Determination of elemental constituents in different matrix materials and flow injection studies by the electrolyte cathode glow discharge technique with a new design; R. Shekhar, D. Karunasagar, M. Ranjit, J. Arunachalam, Analytical Chemistry 81 (2009) 8157.*
256. *Determination of inorganic selenium species [Se(IV) and Se(VI)] in tube well water samples in Punjab; India, K. Chandrasekaran, M. Ranjit, J. Arunachalam, Chemical Speciation and Bioavailability 29 (2009) 15.*
257. *Nano platinum catalysed dry ashing of flour samples for the determination of trace metals by Inductively coupled plasma optical emission spectrometry; A.C. Sahayam, G. Venkateswarlu, S.C.Chaurasia, Atomic Spectroscopy 30 (2009) 139.*
258. *Determination of mercury in hepatitis –B vaccine using colloidal palladium as modifier by electrothermal AAS; K. Dash, S. Thangavel, S. C. Chaurasia, J. Arunachalam, Atomic Spectroscopy 30 (2009) 26.*
259. *Superior bactericidal activity of SDS capped silver nanoparticles: Synthesis and characterization; Aruna Jyothi Kora, R Manjusha, J. Arunachalam, Materials Science and Engineering C 29 (2009) 2104.*
260. *Ferromagnetism in CuO-ZnO multilayers; C. Sudhakar, B. Kirby, Sanjiv Kumar, K.Padmanabhan, R. Naik, V.M.Naik, G. Lawes, Applied Physics Letters 93 (2008) 042502.*
261. *Depth profiling of Mg by ^{24}Mg(p,p'γ)^{24}Mg resonant nuclear reaction; G. L. N. Reddy, Sanjiv Kumar, J. V. Ramana, S. Vikram Kumar, V. S. Raju, Nuclear Instruments and Methods in Physics Research B 266 (2008) 3281.*
262. *Study of lineshapes in the selective ionization of ^{176}Yb isotope in two-step resonance three step ionization scheme; M. Sankari, P.V. Kiran Kumar, M.V. Suryanarayana, Journal of the Optical Society of America B: Optical Physics 25 (2008) 1820.*
263. *Absolute frequency determination of the $5P_{3/2} \rightarrow 7P_{1/2}$ transition in ^{87}Rb; Kanhaiya Pandey, P. V. Kiran Kumar, M. V. Suryanarayana, Vasant Natarajan, Optics Letters 33 (2008) 1675.*

264. *Isotope selective near-resonant two-photon ionizationof ^{41}Ca isotope via the 4s11s $^{1}S_0$ intermediate state; M. Sankari, Applied Optics 47 (2008) 3289.*
265. *Interference free ultra trace determination of Pt, Pd and Au in geological and environmental samples by inductively coupled plasma quadrupole mass spectrometry after a cloud point extraction; N. N. Meeravali, Shiuh-Jen Jiang, Journal of Analytical Atomic Spectrometry 23 (2008) 854.*
266. *Ultra-trace speciation analysis of thallium in environmental water samples by inductively coupled plasma mass spectrometry after a novel sequential mixed-micelle cloud point extraction; N. N. Meeravali, Shiuh-Jen Jiang,Journal of Analytical Atomic Spectrometry 23 (2008) 555.*
267. *Microwave assisted mixed micelle cloud point extraction of Au and Tl from environmental samples without using a chelating agent prior to ICP-MS determination; N.N. Meeravali, Shiuh-Jen Jiang, Journal of Analytical Atomic Spectrometry 23 (2008) 1365.*
268. *Determination of selenium (IV) at ultratrace levels in natural water samples by UV-assisted vapor generation -'collect and punch' -inductively coupled plasma mass spectrometry; K. Chandrasekaran, M. Ranjit, D. Karunasagar, J. Arunachalam, Atomic Spectroscopy 29 (2008) 129.*
269. *Determination of trace elements in Indian rice by ETAAS and ICP-AES; R. Manjusha, K. Dash, D. Karunasagar, J. Arunachalam, Atomic Spectroscopy 29 (2008) 51.*
270. *Antibacterial activity of silver nanoparticles on Pseudomonas aeruginosa; Aruna Jyothi Kora, R. Manjusha, J. Arunachalam, Nanotoxicology 2 (2008) S19.*
271. *Separation of trace impurities from boric acid using cloud point extraction for their determination by DRC-ICP-MS; A. C. Sahayam, Shiuh-Jen Jiang, F.-Y. Chen, Atomic Spectroscopy 29 (2008) 1.*
272. *UV photolysis –assisted digestion of tea (camellia Sinensis) and tulsi (Ocimum Sanctum) and their infusions: comparison of available trace elements; K. Dash, R. Manjusha, S. Thangavel, S. C. Chaurasia, J. Arunachalam, Atomic Spectroscopy 29 (2008) 56.*
273. *Determination of trace phosphorus in zirconium-niobium alloy and Zircaloy by UV-vis spectrophotometry; S. M. Dhavile, R. Shekhar, S. Thangavel, S. C. Chaurasia, J. Arunachalam, Talanta 76 (2008) 134.*
274. *Preparation of $BaTi_4O_9$ and $Ba_2Ti_9O_{20}$ ceramics by wet-chemical methods and their dielectric properties; Sanjiv Kumar, V. S. Raju, T. R. N. Kutty, Materials Science and Engineering B 142 (2007) 7.*
275. *Investigations on the oxidation of zirconium nitride films in air by nuclear reaction analysis and backscattering spectrometry; G. L. N. Reddy, J. V. Ramana, Sanjiv Kumar, S. Vikram Kumar, V. S. Raju, Applied Surface Science 253 (2007) 7230.*
276. *Investigations on the surface atomic composition and microstructure of sintered barium titanate; Sanjiv Kumar, V. S. Raju, T. R. N. Kutty, Journal of Materials Science 42 (2007) 3977.*
277. *Particle Induced X-ray Emission (PIXE) studies of some Indian medicinal plants; K. Nomita Devi, H. Nandakumar Sarma, Sanjiv Kumar, International Journal of PIXE 17 (2007) 169.*
278. *Elemental analysis of some antioxidant-rich medicinal plants of Manipur by Particle Induced X-ray Emission (PIXE); K. Nomita Devi, H. Nandakumar Sarma, Sanjiv Kumar, Indian Journal of Physics 81 (2007) 3.*
279. *Design and development of flame reactor unit for carbon nano rods (CNRs) production; Vivek Dhand, J. S. Prasad, M. Venkateswara Rao, K. Naga Mahesh, L. Anupama, V. Himabindu, Y. Anjaneyulu, V. S. Raju, A. A. Sukumar, Indian Journal of Engineering & Materials Sciences 14 (2007) 235.*
280. *Isotope selective near-resonant two-photon ionization of calcium isotopes; P. V. Kiran Kumar, M. Sankari and M. V. Suryanarayana, Journal of Physics D - Applied Physics 40 (2007) 288.*
281. *Studies on reduction of chloride matrix interferences on determination of germanium using zirconium–ruthenium and palladium–magnesium modifiers by electrothermal atomic absorption spectrometry; N. N. Meeravali M. A. Reddy, Sunil Jai Kumar, Spectrochimica Acta Part B: Atomic Spectroscopy 62 (2007) 504.*
282. *Cloud point extraction of trace metals from seawater and determination by Electrothermal Atomic Absorption Spectrometry (ETAAS) with Ir permanent modifier; N. N. Meeravali, M. A. Reddy, Sunil Jai Kumar, Analytical Science 23 (2007) 351.*
283. *The use of Horwitz Function in the Evaluation of Data in Proficiency Testing Exercises, MAPAN; K. Chandrasekaran, N. Mokhtar, J. Arunachalam, Journal of Metrology Society of India 22 (2007) 45.*
284. *Development of an in situ evaporation system for the preconcentration of anionic impurities in high purity water; S. M. Dhavile, S. Thangavel, K. Dash, S. V. Rao, S. C. Chaurasia, Chromatographia 66 (2007) 819.*
285. *Speciation analysis of mercury and lead in fish samples using LC-ICP-MS; L.-F. Chang, Shiuh-Jen Jiang, A. C. Sahayam, Journal of chromatography A 1176 (2007) 143.*
286. *Microwave assisted volatilization of silicon as fluoride for the trace impurity determination in silicon nitride by DRC-ICP-MS; A.C. Sahayam, Shiuh-Jen Jiang, Chia-Ching Wan, Analytica Chimica Acta 605 (2007) 130.*
287. *Volatilisation of in situ generated antimony trichloride using aqua regia vapors for the determination of ultra trace impurities in high purity antimony using ICP-MS; A. C. Sahayam, Shiuh-Jen Jiang, Chia-Ching Wan, Analytica Chimica Acta 598 (2007) 214.*
288. *Speciation of chromium and vanadium in environmental samples using HPLC-DRC-ICP-MS; C.-Y. Kuo, Shiuh-Jen Jiang, A. C. Sahayam, Journal of Analytical Atomic Spectrometry 22 (2007) 636.*
289. *Determination of traces of rubidium in high purity cesium chloride by electro thermal atomic absorption spectrometry (ETAAS) using boric acid as a modifier; K. Dash, S. Thangavel, S. C. Chaurasia, J. Arunachalam, Analytica Chimica Acta 584 (2007) 210.*
290. *UV-photolysis assisted digestion of food samples for the determination of selenium by electrothermal atomic absorption Spectrometry (ETAAS); R. Manjusha, K. Dash, D. Karunasagar, Food Chemistry 105 (2007) 260.*
291. *Sorption of mercury on chemically synthesized polyaniline; P .Ramya Devi, Sanjiv Kumar, R. Verma, M. Sudersnan, Journal of Radioanalytical and Nuclear Chemistry 269 (2006) 217.*
292. *Synthesis and characterization of methylbismuth(III) complexes containing dithio ligands: 2. Crystal and molecular structure of [MeBiCl(S2CNEt2)] and transformation of some [MeBi(S2CNR '(2))(2)] to Bi_2S_3; K. Jain, V. Sharma, R. Bohra, A. A. Sukumar, V. S. Raju, J. E. Drake, Journal of Organometallic Chemistry 691(2006) 4128.*

293. *Isotope-selective excitation of ^{41}Ca isotope in Doppler-free two-photon continuous-wave excitation: a case study; P. V. Kiran Kumar, M. Sankari, G. V. S. G. Acharyulu, M. V. Suryanarayana, Applied Optics 45 (2006) 8979.*
294. *Optimization of the conditions for simultaneous non-selective excitation of plutonium isotopes for isotope ratio measurements in resonance ionization mass spectrometry; M. Sankari, P.V. Kiran Kumar, M.V. Suryanarayana, International Journal of Mass Spectrometry 254 (2006) 94.*
295. *Wavelength dependent Stark compensation in isotope selective Doppler-free two photon ionization; M. Sankari, P.V. Kiran Kumar, M.V. Suryanarayana, Optics Communications 259 (2006) 612.*
296. *Studies of mercury pollution in a lake due to a thermometer factory situated in a tourist resort: Kodaikkanal, India; D.Karunasagar, M. V. Balarama Krishna, Y. Anjaneyulu, J. Arunachalam, Environmental Pollution 143 (2006) 153.*
297. *Speciation of Cr in natural and wastewaters using immobilized Aspergillus niger and its determination by GFAAS and FAAS; S. V. Rao, M. V. Balarama Krishna, J. Arunachalam, Atomic Spectroscopy 27 (2006) 86.*
298. *Speciation of Cr(III) and Cr(VI) in sea water after separation with sulphate form of Dowex-1 and ETAAS determination, A. Aparna, M. Sumithra, G. Venkateswarlu, A. C. Sahayam, S. C. Chaurasia, T.Mukherjee, Atomic Spectroscopy 27 (2006) 134.*
299. *A combined sub boiling and isopiestic distillation method for the purification of hydrofluoric acid used for ICP-MS elemental analysis;, S. C. Chaurasia, A. C. Sahayam, R. K. Mishra, G. Venkateswarlu, T. Mukherjee, Atomic Spectroscopy 27 (2006) 123.*
300. *Determination of indium in high purity antimony by electro thermal atomic absorption spectrometry (ETAAS) using boric acid as a modifier; K. Dash, S. Thangavel, S. C. Chaurasia, J. Arunachalam, Talanta 70 (2006) 602.*
301. *Determination of trace impurities in chromium matrices after separation as Cr(III) using oxalate form of anion exchanger; G. Venkateswarlu, A. C. Sahayam, S. C. Chaurasia, T. Mukherjee, Talanta 68 (2006) 748.*
302. *Preconcentration of total inorganic selenium (selenite and selenate) in natural waters using Zero -Valent Iron and determination by GFAAS; S. V. Rao, J.Arunachalam, Atomic spectroscopy 27 (2006) 165.*
303. *Chemical and Structural characterisation of Nickel based Superalloys doped with Minor and Trace elements; Raparthi Shekhar, J. Arunachalam, Niranjan Das, A. M. Srirama Murthy, Materials Science & Engineering A 435 (2006) 491.*
304. *Determination of thallium in nickel-based superalloys by ICP-QMS after multi-matrix separation; Raparthi Shekhar, J. Arunachalam, Niranjan Das, A. M. Srirama Murthy, Atomic Spectroscopy 27 (2006) 30.*
305. *Studies on surface composition and chemical states of calcium manganites; Sanjiv Kumar, V.S. Raju, S. Bera, S. Vijayanandhini, T. R. N. Kutty, Nuclear Instruments and Methods in Physics Research B 237 (2005) 623.*
306. *Depth profiling of nitrogen using 429 keV and 897 keV resonances in the $^{15}N(p,\alpha\gamma)^{12}C$ Reaction; Sanjiv Kumar, S. V. Kumar, G. L. N. Reddy, V. Kain, J. V. Ramana, V. S. Raju, Nuclear Instruments and Methods in Physics Research B, 240 (2005) 704.*
307. *Application of backscattering spectrometry for composition and thickness determination of zirconium oxide layers in autoclaved zircaloy; Sanjiv Kumar, J. V. Ramana, S. V. Kumar, V. S. Raju, J Journal of Radioanalytical and Nuclear Chemistry 265 (2005) 441.*
308. *Trace element analysis of some medicinal plants of Manipur using PIXE and PIGE Techniques;, R. K. Bhanisana Devi, H. K. N. Sarma, J. Arunachalam, Sanjiv Kumar, Indian Journal of Physics 79 (2005) 417.*
309. *Double metal-insulator transitions and magneto resistance: An intrinsic feature of Ru substituted La(0.67)Ca(0.33)MnO(3); L. Seetha Lakshmi, V. Sridharan, R. Rawat, A. A. Sukumar, M. Kamuddin, V. S. Sastry, V. S. Raju, Journal of Physics: Condensed Matter 18 (2005) 4427.*
310. *Ultrasonic probe extraction of tin from botanical and biological reference materials and determination using end capped electrothermal atomic absorption spectrometry (EC-ETAAS) with Zirconium-iridium permanent modifie; Sunil Jai Kumar, M. A. Reddy, N. N. Meeravali, Journal of Analytical Atomic Spectrometry 20 (2005) 124.*
311. *Fast furnace program with end-capped tubes for the determination of sub ppb-levels of Cd in food and biological SRMs using ETAAS after ultrasonic probe extraction; N. N. Meeravali, M. A. Reddy, Sunil Jai Kumar, Atomic Spectroscopy 26 (2005) 68.*
312. *Speciation of Cr(III) and Cr(VI) in waters using immobilized moss and determination by ICP-MS and FAAS; M. V. Balarama Krishna, K. Chandrasekaran, S. V. Rao, D. Karunasagar, J. Arunachalam, Talanta 65 (2005) 135.*
313. *Preconcentration and speciation of inorganic and methyl mercury in waters using polyaniline and gold trap-CVAAS; M. V. Balarama Krishna, D. Karunasagar, S. V. Rao, J. Arunachalam, Talanta 68 (2005) 329.*
314. *A rapid ultrasound-assisted thiourea extraction method for the determination of inorganic and methyl mercury in biological and environmental samples by CVAAS; M. V. Balarama Krishna, M. Ranjit, D. Karunasagar, J. Arunachalam,Talanta 67 (2005) 70.*
315. *Removal and preconcentration of inorganic and methyl mercury from aqueous media using a sorbent prepared from the plant Coriandrum sativu; D.Karunasagar, M. V. Balarama Krishna, S. V. Rao, J. Arunachalam, Journal of Hazardous Materials 118 (2005) 133.*
316. *Ultrasound-assisted analyte extraction for the determination of sulfate and elemental sulfur in zinc sulfide by different liquid chromatography techniques; K. Dash, S. Thangavel, N. V. Krishnamurthy, S. V. Rao, D. Karunasagar, J. Arunachalam, Analyst 130 (2005) 498.*
317. *Removal of ^{106}Ru from actual low-level radioactive waste solutions using Polyaniline as anion-exchanger; M. V. Balarama Krishna, J. Arunachalam, D. R. Prabhu, V. K. Manchanda, S. Kumar, Separation Science and Technology 40 (2005) 1313.*
318. *Microwave-assisted vapor phase dissolution of photoresist and silicon oxide based slurry samples for the determination of trace impurities by high resolution ICP-MS; Chia-Ching Wan, Shiuh-Jen Jiang, Min-Ta You and A. C. Sahayam, Journal of Analytical Atomic Spectrometry 11 (2005) 1290.*
319. *Determination of Cr(VI) in potable water samples after selective Preconcentration on oxalate form of Dowex-1 and electro thermal atomic absorption spectrometric determination; A.C. Sahayam, G. Venkateswarlu, S. C. Chaurasia, Analytica Chimica Acta 537 (2005) 267.*
320. *Microwave- assisted volatilization of silicon fluorides for the determination of trace impurities in high purity silicon powder and quartz by ICP-MS; Ruey-Lin Ueng, Shiuh-Jen Jiang, Chia-Ching Wan, A. C. Sahayam, Analytica Chimica Acta 536 (2005) 295.*

321. *Vapor phase matrix extraction of high purity di-boron trioxide and trace analysis using electro thermal AAS; K. Dash, S. Thangavel, S. M. Dhavile, S. V. Rao, S. C. Chaurasia, J. Arunachalam, Analytica Chimica Acta 546 (2005) 229.*
322. *Determination of traces of chloride and fluoride in H_2SO_4, H_3PO_4 and H_3BO_3 by in situ analyte distillation - Ion chromatography; S. Thangavel, K. Dash, S. M. Dhavile , S. C. Chaurasia, T. Mukherjee, Journal of Chromatography A 1047 (2005) 229.*
323. *Determination of Cu, Zn, As, Cd, In, Sn, Pb, Bi in nickel-based superalloys after multi-matrix separation; Raparthi Shekhar, J. Arunachalam, Niranjan Das, A.M. Srirama Murthy, Atomic Spectroscopy 26 (2005) 191.*
324. *Multielemental characterisation of a Cobalt by Glow Discharge Quadrupole Mass Spectrometry; Raparthi Shekhar, J. Arunachalam, Niranjan Das, A.M. Srirama Murthy, Talanta 65 (2005) 1270.*
325. *Determination of Boron in Zr-Nb alloys using Glow Discharge Quadrupole Mass Spectrometry; Raparthi Shekhar, J. Arunachalam, G. Radha Krishna, H .R. Ravindra, B. Gopalan, Journal of Nuclear Materials 340 (2005) 284.*
326. *Compositional analysis of silicon nitride films on Si and GaAs by backscattering spectrometry and nuclear resonance reaction analysis;, Sanjiv Kumar, V.S. Raju, Nuclear Instruments and Methods in Physics Research B 226 (2004) 631.*
327. *Structure, composition and microhardness of (Ti,Zr)N and (Ti,Al)N coatings prepared by DC magnetron sputtering; J.V. Ramana, Sanjiv Kumar, C. David, V. S. Raju, Materials Letters 58 (2004) 2553.*
328. *Studies of some elements in urinary stones by PIXE technique; N. K. Sharatchandra, H. K. N. Sarma, Sanjiv Kumar, J. Arunachalam, Indian Journal of Physics 78 (2004) 511.*
329. *The effect of conditioning by permanganate on the dissolution behavior of stellite particles in organic complexing acid medium; V. Subramaninan, P. Chandramohan, M. P. Srinivasan, A. A. Sukumar, V. S. Raju, S. V. Narasimhan, Journal of Nuclear Materials 334 (2004) 169.*
330. *Investigations on the $^1S_0 - ^1P_1 - ^1S_0$ nonresonant photoionization pathway for selective ionization of rare calcium and strontium isotopes; Manda Sankari, Pragada V. Kiran Kumar, Manda V. Suryanarayana, Journal of the Optical Society of America B: Optical Physics 21 (2004) 1369.*
331. *A Simple method for Synthesis of organotin species for the investigation of extraction procedures in sediments by Isotope Dilution-Gas Chromatography- Inductively Coupled Plasma Mass Spectrometry Part 2 phenyl tins; Sunil Jai Kumar, Solomon Tesfalidet, James P.Snell, Dong Nguyen Van, Wolfgang Frech, Journal of Analytical Atomic Spectrometry 19 (2004) 368.*
332. *Determination of Trace Impurities in High Purity Te (7N) using ICP-MS and transverse heated electrothermal AAS; M. A. Reddy, N. N. Meeravali, Sunil Jai Kumar, Atomic Spectroscopy 25 (2004) 267.*
333. *Preconcentration and determination of mercury in natural waters using immobilized biosorbent of Aspergillus niger; D. Karunasagar, M. V. Balarama Krishna, P. Maruthi Mohan, J.Arunachalam, Current Science 87 (2004) 1.*
334. *Sorption characteristics of inorganic, methyl and elemental mercury on lichens and mosses: implication in biogeochemical cycling of mercury; M. V. Balarama Krishna, D. Karunasagar, J. Arunachalam, Journal of Atmospheric Chemistry 49 (2004) 317.*
335. *Performance of immobilized moss on the removal of ^{137}Cs and ^{90}Sr from actual low level radioactive waste solutions; M. V. Balarama Krishna, J. Arunachalam, M. S. Mural, Surendra Kumar, V. K. Manchanda, Journal of Radioanalytical and Nuclear Chemistry 261 (2004) 551.*
336. *Removal of ^{137}Cs and ^{90}Sr from actual low level radioactive waste solutions using moss as a phyto-sorbent; M. V. Balarama Krishna, S. V. Rao, J. Arunachalam, M. S. Murali, Surendra Kumar, V. K. Manchanda, Separation and Purification Technology 38 (2004) 149.*
337. *Ultrasound-assisted extraction procedure for the determination of major, minor and trace elements in lichen and mussel samples by ICP-MS and ICP-AES; M. V. Balarama Krishna, J. Arunachalam, Analytica Chimica Acta 522 (2004) 179.*
338. *In-situ matrix evaporation by isothermal distillation of high-purity reagents for the determination of trace impurities by ion-chromatography; S. M. Dhavile, S. Thangavel, K. Chandrasekaran, K. Dash, S. V. Rao, S.C. Chaurasia, Journal of Chromatography A 1050 (2004) 223.*
339. *Ion-chromatographic determination of trace level phosphorus in purified quartz; K. Dash, S. Thangavel, S. V. Rao, K. Chandrasekaran, S. C. Chaurasia, J. Arunachalam, J Journal of Chromatography A 1036 (2004) 223.*
340. *Determination of trace metallic impurities in high purity quartz by ion-chromatography; K. Dash, K. Chandrasekaran, S. Thangavel, S. M. Dhavile and J. Arunachalam, Journal of Chromatography A 1022 (2004) 25.*
341. *Isopiestic distillation of arsenious chloride for the determination of trace impurities in high purity arsenic by ICP-AES; A.C. Sahayam, R. K. Mishra, G.Venkateswarlu, S. C. Chaurasia, Atomic Spectroscopy 25 (2004) 263.*
342. *In situ matrix evaporation by isothermal distillation of high-purity reagents for the determination of trace impurities by ion chromatography; S. M. Dhavile, S. Thangavel, K. Chandrasekaran, K. Dash, S. V. Rao, S. C. Chaurasia, Journal of Chromatography A, 1050 (2004) 223.*
343. *Ultrasound-assisted acid extraction of trace impurities from quartz samples followed by ICP-OES analysis; S. V. Rao, G. Venkateswarlu, K. Dash, S. M. Dhavile, S. C. Chaurasia , J. Arunachalam, Atomic Spectroscopy 25 (2004) 251.*
344. *Microwave-assisted volatilization of chlorides of Ge and Se for the determination of trace impurities in high purity Ge and Se by ICP-MS; Ruey-Lin Ueng, A. C. Sahayam, Shiuh-Jen Jiang, Chia-Ching Wan, Journal of Analytical Atomic Spectrometry 19 (2004) 681.*
345. *Determination of ultra trace impurities in high purity gallium arsenide by inductively coupled plasma mass spectrometry after volatilization of matrix; A.C. Sahayam, Shiuh-Jen Jiang, Chia-Ching Wan, Journal of Analytical Atomic Spectrometry 19 (2004) 407.*
346. *Spectrophotometric determination of boron in complex matrices by isothermal distillation of borate ester into curcumin; S. Thangavel, S. M. Dhavile, K. Dash, S. C. Chaurasia, Analytica Chimica Acta 502 (2004) 265.*
347. *Multielemental characterisation of a Nickel by Glow Discharge Quadrupole Mass Spectrometry; Raparthi Shekhar, J. Arunachalam, Niranjan Das, A. M. Srirama Murthy, Atomic Spectroscopy 25 (2004) 203.*
348. *Determination of Elemental Composition of Zr-Nb alloys by Glow Discharge Quadrupole Mass Spectrometry; Raparthi Shekhar, J. Arunachalam, G. Radha Krishna, H. R. Ravindra and B. Gopalan, Atomic Spectroscopy 25 (2004) 166.*
349. *Calculation of ^{91}Zr optical selectivities in two-color resonant three-photon ionization schemes; Pragada V. Kiran Kumar, Manda Sankari, Manda V. Suryanarayana Journal of the Optical Society of America B: Optical Physics 20 (2003) 1807.*

350. *A Simple method for Synthesis of organotin species for the investigation of extraction procedures in sediments by Isotope Dilution-Gas Chromatography-Inductively Coupled Plasma Mass Spectrometry Part 1 butyl tins; Sunil Jai Kumar, Solomon Tesfalidet, James P. Snell, Wolfgang Frech, Journal of Analytical Atomic Spectrometry 18 (2003) 714.*
351. *Study of mercury pollution using lichens and mosses as bio-monitors: Possible conversion of elemental mercury into inorganic forms; M. V. Balarama Krishna, D. Karunasagar, J. Arunachalam, Environmental Pollution 124 (2003) 357.*
352. *Biosorption of inorganic and methyl mercury by a biosorbent from Aspergillus niger; D. Karunasagar, J. Arunachalam, K. Rashmi, J. Naveena Lavanya Latha, P. Maruthi Mohan, World Journal of Microbiology and Biotechnology 19 (2003) 291.*
353. *Trace element analysis of high purity As through vapour phase dissolution and ICP-QMS; M. V. Balarama Krishna, J. Arunachalam, Talanta 59 (2003) 485.*
354. *Multichannel Vapour Phase Digestion (MCVPD) of high purity quartz powder and the determination of trace impurities by ICPAES and ICPMS; K. Dash, S. Thangavel, S. M. Dhavile, K. Chandrasekaran, S. C. Chaurasia, Atomic Spectroscopy 24 (2003) 143.*
355. *Trace element characterisation of high purity gallium: Matrix removal as gallium fluoride precipitate, A.C. Sahayam, S. Thangavel, S. C. Chaurasia, Atomic Spectroscopy, 24 (2003) 11.*
356. *Procedure for determination of trace ions in boric acid by matrix volatilization–ion chromatography; K. Dash, D. Karunasagar, S. C. Chaurasia, Journal of Chromatography A 1002 (2003) 137.*
357. *Quantitative determination of chlorine by glow discharge quadrupole mass spectrometry in Zr-2.5Nb alloys; R. Shekhar, J. Arunachalam, H. R. Ravindra, B. Gopalan, Journal of Analytical Atomic Spectroscopy 18 (2003) 381.*
358. *Investigations on the chemical states of sintered barium titanate by X-ray photoelectron spectroscopy; Sanjiv Kumar, V.S. Raju, T. R. N. Kutty, Applied Surface Science 250 (2002) 2003.*
359. *Calculation of single-color optical selectivities of the ^{91}Zr isotope for transitions in the 570 – 620 nm region; Pragada V. Kiran Kumar, Manda Sankari, Manda V. Suryanarayana, Journal of the Optical Society of America B: Optical Physics 19 (2002) 2833.*
360. *Effect of ^{87}Sr hyperfine structure on the isotopeselective excitation of ^{89}Sr and ^{90}Sr isotopes in collinear resonance ionization spectroscopy; M. Sankari, M. V.Suryanarayana, Journal of Physics B: Atomic, Molecular and Optical Physics 35 (2002) 9835.*
361. *Zirconium-iridium coating as a permanent modifier for determination of tin in stream sediment, oyster tissue and total diet slurries by electro thermal atomic absorption spectrometry; N. N. Meeravali, Sunil Jai Kumar, Journal of Analytical Atomic Spectrometry 17 (2002) 704.*
362. *Room temperature isopiestic distillation of in situ generated arsenious chloride and its application for the determination of trace level impurities in arsenious oxide; S. C. Chaurasia, A. C. Sahayam, R. K. Mishra, Analytical Chemistry 74 (2002) 6102.*
363. *Speciation of Cr(III) and Cr(VI) in potable waters by using activated neutral alumina as collector and ET- AAS for determination; A. C. Sahayam, Analytical and Bioanalytical Chemistry 372 (2002) 840.*
364. *Ion beam analysis of porous silicon layers; Sanjiv Kumar, J. V. Ramana, C. David, V. S. Raju, Nuclear Instruments and Methods in Physics Research B 179 (2001) 113.*
365. *Compositional characterization of chromium nitride films deposited by IBAD process on stainless steel; Sanjiv Kumar, V. S. Raju, R. Shekhar, J. Arunachalam, A. S. Khanna, K. G. Prasad, Thin Solid Films 388 (2001) 195.*
366. *Preparation and characterization of TiN films by electron cyclotron resonance sputtering for diffusion barrier applications; K. D. Vergheese, M. Rao, T. V. Balasubramanian, Sanjiv Kumar, Materials Science and Engineering B 83 (2001) 242.*
367. *The utility of W-Ir permanent chemical modifier for the determination of Ni and V in emulsified residual oil, fuel oil and naphtha by transverse heated electrothermal atomic absorption spectrometry; N. N. Meeravali, Sunil Jai Kumar, Journal of Analytical Atomic Spectrometry 16 (2001) 527.*
368. *A combined treatment approach using Fenton's reagent and zero-valent iron for the removal of As from drinking water; M. V. Balarama Krishna, K. Chandrasekharan, D. Karunasagar, J. Arunachalam, Journal of Hazard. Materials 84 (2001) 229.*
369. *A Simple vapour phase decomposition (VPD) of quartz powder in a polypropylene vessel and determination of phosphorus by Spectrophotometry; S. Thangavel, K. Dash, S. C. Chaurasia, Talanta 55 (2001) 501.*
370. *Characterisation of Zirconium nitride films prepared by DC magnetron sputtering; J. V. Ramana, Sanjiv Kumar, C. David, A. K. Ray, V. S. Raju, Materials Letters 43 (2000) 73.*
371. *Optical selectivity calculations of calcium isotopes in a double-resonance ionization schemes; M. Sankari, P.V. Kiran Kumar, M.V. Suryanarayana, Journal of Physics B: Atomic, Molecular and Optical Physics 33 (2000) 4927.*
372. *Selective excitation of odd gadolinium isotopes using two-colourphotoionisation schemes; P.V. Kiran Kumar, M.V. Suryanarayana, S. Gangadharan, Journal of Nuclear Materials 282 (2000) 255.*
373. *Comparison of density matrix and spectral simulation approaches for the calculation of isotopic selectivities; M. V. Suryanarayana, M. Sankari, Journal of Quantitative Spectroscopy and Radiative Transfer 67 (2000) 65.*
374. *Slurry sampling with rapid atomization microwave digestion versus Conventional atomization for the determination of copper, manganese and nickel in Algae matrix using transverse heated electrothermal atomic absorption spectrometry; N. N. Meeravali, Sunil Jai Kumar, Analytica Chimica Acta 404 (2000) 295.*
375. *Comparison of Open Microwave digestion and digestion by Conventional heating for the determination of Cd, Cr, Cu and Pb in Algae using transverse heated electrothermal atomic absorption spectrometry; N. N. Meeravali, Sunil Jai Kumar, Fresenius Journal of Analytical Chemistry 366 (2000) 313.*
376. *ICPMS determination of trace amounts of boron in high purity quartz; D. Karunasagar, K. Dash, K. Chandrasekaran, J. Arunachalam, Atomic Spectroscopy 21 (2000) 216.*
377. *Multi-element characterization of high purity Cd using ICP-MS and GD-MS; M. V. Balarama Krishna, R. Shekhar, D. Karunasagar, J. Arunachalam, Analytica Chimica Acta 408 (2000) 197.*

378. *Application of a Longer Path Length of Infrared cell for the determination of $TiOCl_2$ in$TiCl_4$; Sarala Raoot, N. Rukmani Desikan, R. Shekhar, J. Arunachalam, Applied Spectroscopy 54 (2000) 1412.*
379. *Multielement characterisation of high purity Cadmium using Inductively Coupled Plasma Quadrupole Mass Spectrometry (ICP-QMS) and Glow Discharge Quadrupole Mass Spectrometry (GD-QMS); M.V. Balarama Krishna, R. Shekhar, D. Karunasagar, J. Arunachalam, Analytica Chimica Acta 408 (2000) 199.*
380. *Isotope selective excitation of ^{155}Gd and ^{157}Gd isotopes from $^9D^\circ_{2-6}$ states using broadband lasers; M. Sankari, M.V. Suryanarayana, S. Gangadharan, Journal of Nuclear Materials 264 (1999) 122*
381. *Chromium speciation in water by Electrothermal Atomic Absorption Spectrometry (ET-AAS) after simultaneous adsorption of Cr (III) and Cr (VI) on an activated Alumina mini column; Sunil Jai Kumar, Peter Ostapczuk, Hendrik Emons; Atomic Spectroscopy 20 (1999) 194.*
382. *Determination of Trace metals in Naphtha using ICP-MS after emulsification with triton-X 100; Sunil Jai Kumar, S. Gangadharan, Journal of Analytical Atomic Spectrometry 14 (1999) 967.*
383. *Studies on the determination of trace elements in high purity Sb using GFAAS and ICP-QMS; M. V. Balarama Krishna, D. Karunasagar, J. Arunachalam, Fresenius' Journal of Analytical Chemistry 363 (1999) 353.*
384. *Analysis of high purity Antimony by Glow Discharge Quadrupole Mass Spectrometry; R. Shekhar, M. V. Balarama Krishna, J. Arunachalam, S. Gangadharan, Atomic Spectroscopy 20 (1999) 25.*
385. *Polyaniline, a conducting polymer, as a standard for hydrogen profiling on material surfaces; Sanjiv Kumar, J. V. Ramana, C. David, V. S. Raju, S. Gangadharan, Nuclear Instruments and Methods in Physics Research B, 142 (1998) 549.*
386. *Determination of $^6Li/^7Li$ isotope ratio using two photon resonance three photon resonance ionization mass spectrometry; M. V. Suryanarayana, M. Sankari, S. Gangadharan, International Journal of Mass Spectrometry and Ion Processes 173 (1998) 177.*
387. *Studies on the isotope selective photoionization of the low-abundant ^{168}Yb isotope; M. Sankari, M. V. Suryanarayana, Journal of Physics B: Atomic, Molecular and Optical Physics 31 (1998) 261.*
388. *Rapid Slurry atomization using transverse heated electrothermal atomic absorption spectrometry for the determination of cadmium, copper, manganese and lead in biological reference materials; N. N. Meeravali, Sunil Jai Kumar, Journal of Analytical Atomic Spectrometry 13 (1998) 647.*
389. *Determination of trace impurities in high purity gallium by inductively coupled plasma mass spectrometry and cross validation of results by transverse heated graphite furnace atomic absorption spectrometry; Sunil Jai Kumar, N. N. Meeravali, Jayaraman Arunachalam, Analytica Chimica Acta 371 (1998) 305.*
390. *Development of a 'collect and punch' cold vapor inductively coupled plasma mass spectrometric method for the direct determination of mercury at nanograms per litre levels; D.Karunasagar, J. Arunachalam, S.Gangadharan, Journal of Analytical Atomic Spectrometry13 (1998) 679.*
391. *Determination of Cr(VI) in potable water after selective separation of Cr(III) on ZnO; A. C. Sahayam, J. Arunachalam, S. Gangadharan , Canadian Journal of Analytical Sciences and Spectroscopy 43 (1998) 4.*
392. *Determination of Cd, Cu, Pb and Sb in environmental samples using polyaniline for separation; A.C. Sahayam, Fresenius' Journal of Analytical Chemistry 362 (1998) 285.*
393. *Application of polyaniline as anion exchanger for the separation of Bi and its determination by GFAAS; A.C. Sahayam, Atomic Spectroscopy 19 (1998) 107.*
394. *Thin film characterization using backscattering spectrometry; J. V. Ramana, V. S. Raju, S. Gangadharan, Journal of Radioanalytical and Nuclear Chemistry 217 (1997) 293.*
395. *A theoretical study of the isotope selective excitation of ^{138} La from $^2D_{3/2,5/2}$ states, M. Sankari, M. V. Suryanarayana, Spectrochimica Acta Part B: Atomic Spectroscopy 52 (1997) 735.*
396. *Simulation of isotopic selectivities and isotope ratio enhancement factors for gadolinium and lanthanum using narrow band laser excitation; M. V. Suryanarayana, M. Sankari, Zeitschrift für Physik D Atoms, Molecules and Clusters 39 (1997) 35.*
397. *In situ trapping of mercury vapors on Au, Pd-Au alloy or Pt-Rh alloy in the graphite furnace for the determination of Hg in environmental samples after microwave digestion; Sunil Jai Kumar, N. N. Meeravali, Atomic Spectroscopy 18 (1997) 166.*
398. *Graphite furnace atomic absorption spectrometric (GFAAS) determination of Cu, Cd, Cr, Mn, Ni and Pb in tellurium metal using precipitation, ion-exchange procedures; N. N. Meeravali, J. Arunachalam, Fresenius Journal of Analytical Chemistry 358 (1997) 484.*
399. *Determination of Total Chromium in terrestrial and marine samples by electrothermal atomic absorption spectrometry after pressure digestion; Sunil Jai Kumar, Peter Ostapczuk, Hendrik Emon, Fresenius J. Anal Chemistry 359 (1997) 171.*
400. *Optimization of design parameters of a reflectron geometry time of flight mass spectrometer; M. Sankari, M. V. Suryanarayana, Instrumentation Science & Technology 24 (1996) 23.*
401. *Comparison of NaOH fusion and microwave oven digestion for the determination of As and Se in coal fly ash reference material using hydride generation; Sunil Jai Kumar, N. N. Meeravali, Atomic Spectroscopy 17 (1996) 27.*
402. *Sorption of platinum, palladium, iridium and gold complexes on polyaniline;, Sanjiv Kumar, Rakesh Verma, B. Venkataramani, V. S. Raju, S. Gangadharan, Solvent extraction and ion exchange 13 (1995) 1097.*
403. *X-ray photoelectron spectroscopic study of Si(111) and Si(100) surfaces with chemically absorbed bromine, K. Sekar, G. Kuri, D. P. Mahapatra, B. N. Dev, J. V. Ramana, Sanjiv Kumar, V. S. Raju, Surface Science 302 (1994) 25.*
404. *Influence of chemical modifiers on the atomisation of tin in graphite furnace atomic absorption spectrometry (GFAAS); A.C. Sahayam, S. Gangadharan, Canadian Journal of Applied Spectroscopy 39 (1994) 61.*
405. *Accurate Determination of Selenium in the presence of Iron by Deuterium Arc Electrothermal Atomic Absorption Spectrometry; Sunil Jai Kumar, S. Gangadharan, Journal of Analytical Atomic Spectrometry 8 (1993) 127.*

Dr. R. Chidambaram (Former Chairman, AEC) and Dr. Sunil Jai Kumar (Former Head, NCCCM), during the Silver jubilee celebrations of NCCCM-BARC, Hyderabad.(30-11-2018)

Dr. Ajit Kumar Mohanty (the then Director, BARC), present Chairman, AEC along with Dr. A. K. Tyagi (the then Director, Chemistry Group, BARC) reviewing the activities of NCCCM-BARC, Hyderabad.(1-11-2021)

Mahua Tree *(Madhuca longifolia)*

National Centre for Compositional Characterisation of Materials (NCCCM)
Bhabha Atomic Research Centre (BARC)
Email: admncccm@barc.gov.in | Web:www.cccm.gov.in
Telephone: **040 - 2712 1365, 2712 5462**